Cosmic Ray Energy Spectrum and Anisotropy with ARGO-YBJ

G. Di Sciascio on behalf of the ARGO-YBJ Collaboration
INFN - Roma Tor Vergata
disciascio@roma2.infn.it

CRA2017
4th Cosmic Ray Anisotropy Workshop
10 - 13 October, 2017
Guadalajara, Jalisco, México

The ARGO-YBJ experiment

ARGO-YBJ is a telescope optimized for the detection of small size air showers

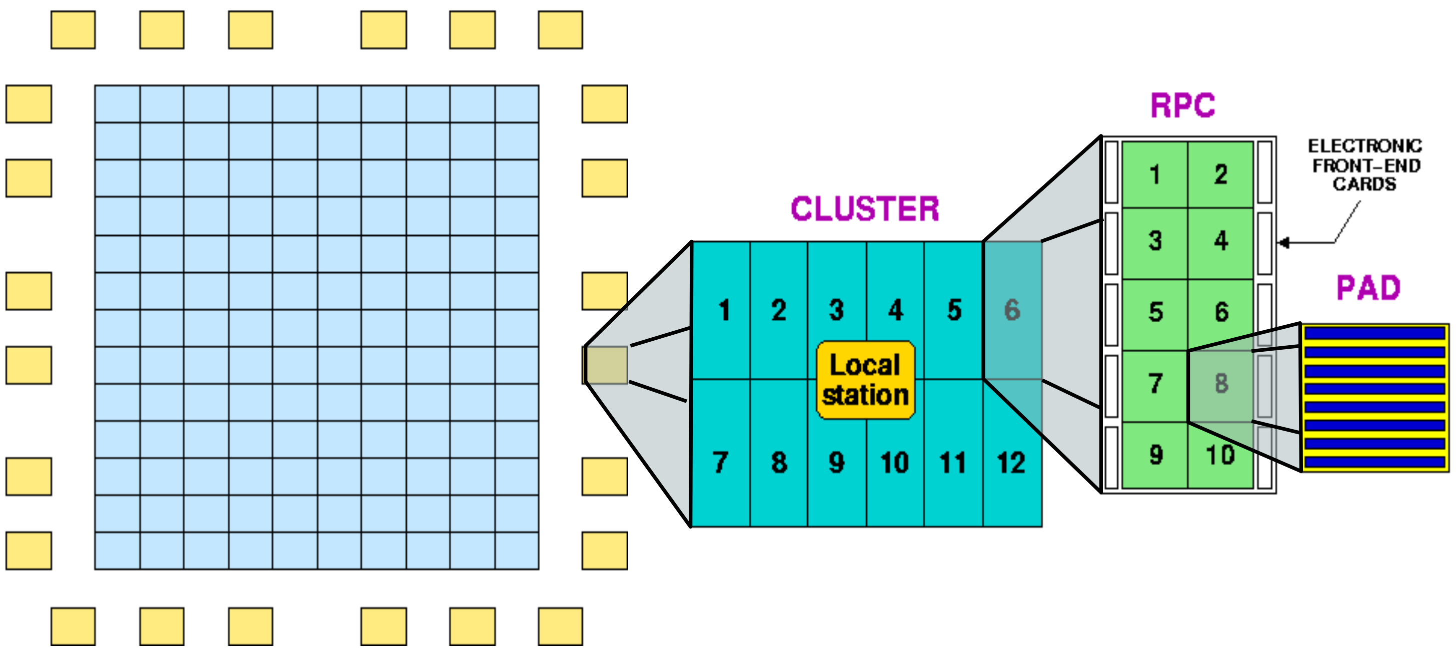

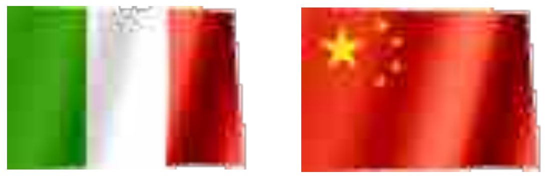

INFN IHEP/CAS

Longitude: 90° 31’ 50” East
Latitude: 30° 06’ 38” North

90 km North from Lhasa (Tibet)

4300 m above sea level
$\sim$ 600 g/cm^2

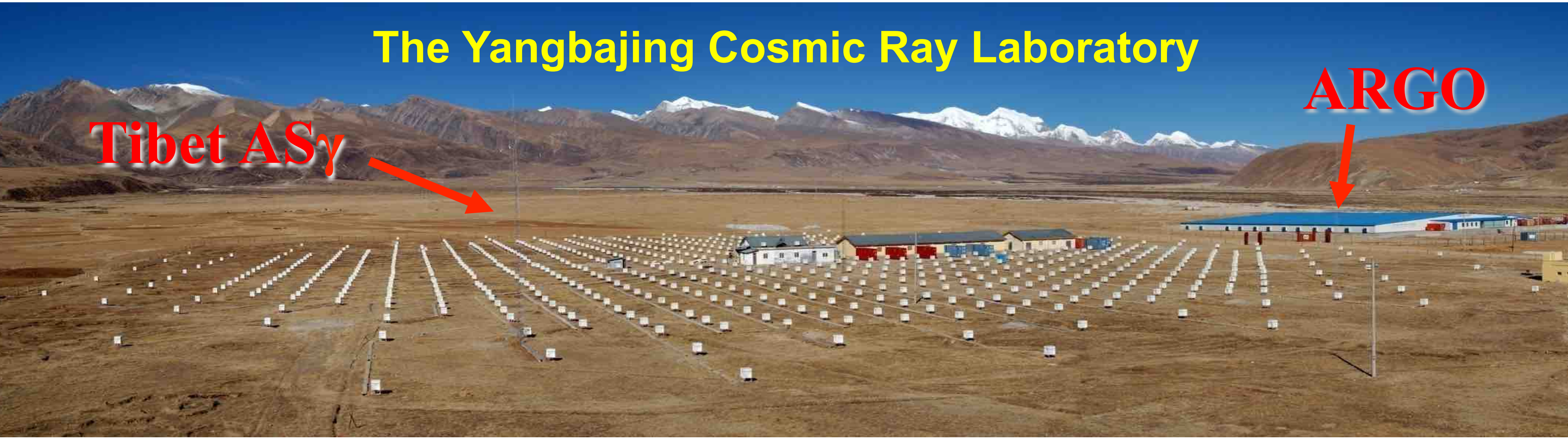

The ARGO-YBJ layout

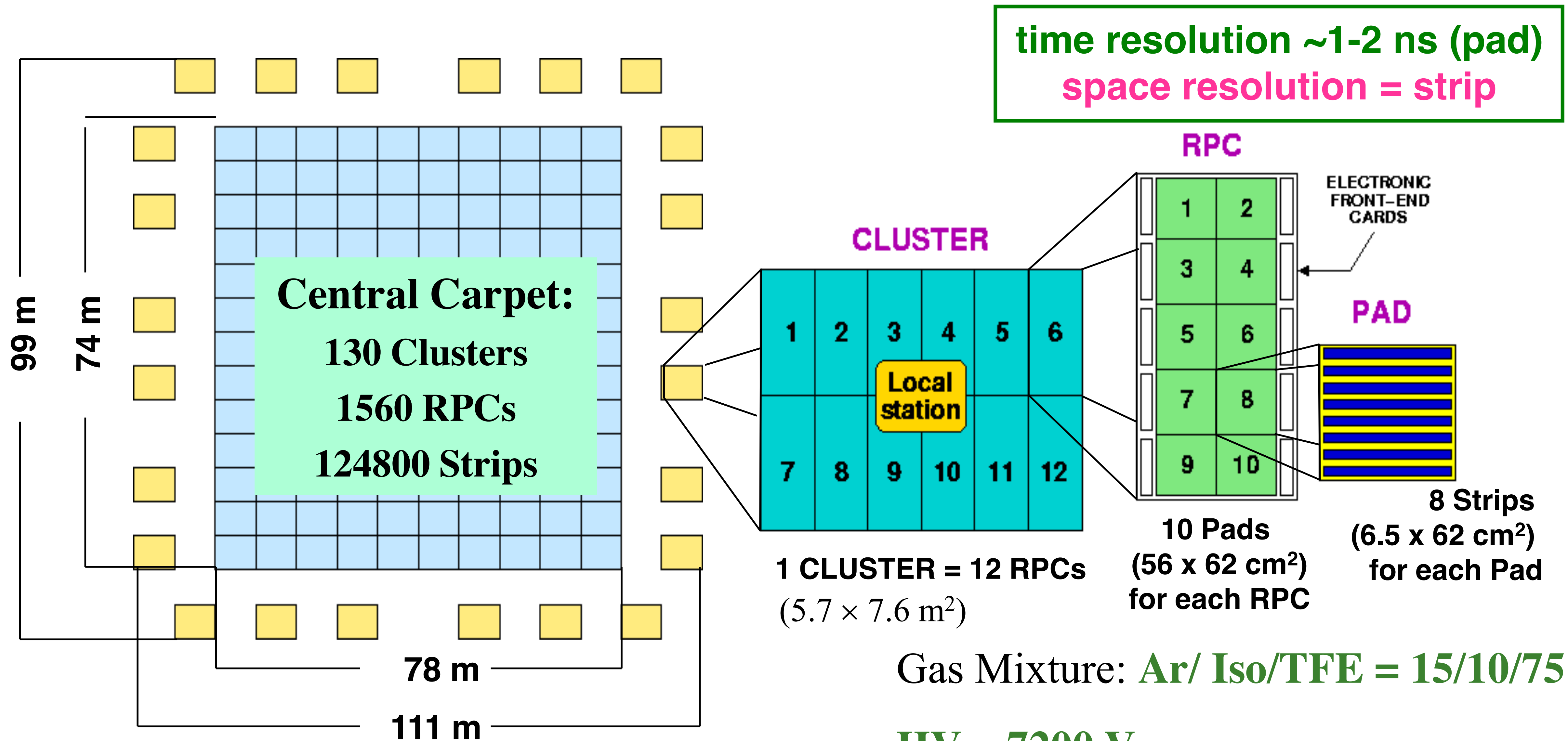

Gas Mixture: **Ar/ Iso/TFE = 15/10/75**

HV = 7200 V

Single layer of Resistive Plate Chambers (RPCs)
with a full coverage (92% active surface) of a large area (5600 m^2)
+ sampling guard ring (6700 m^2 in total)

The experimental hall

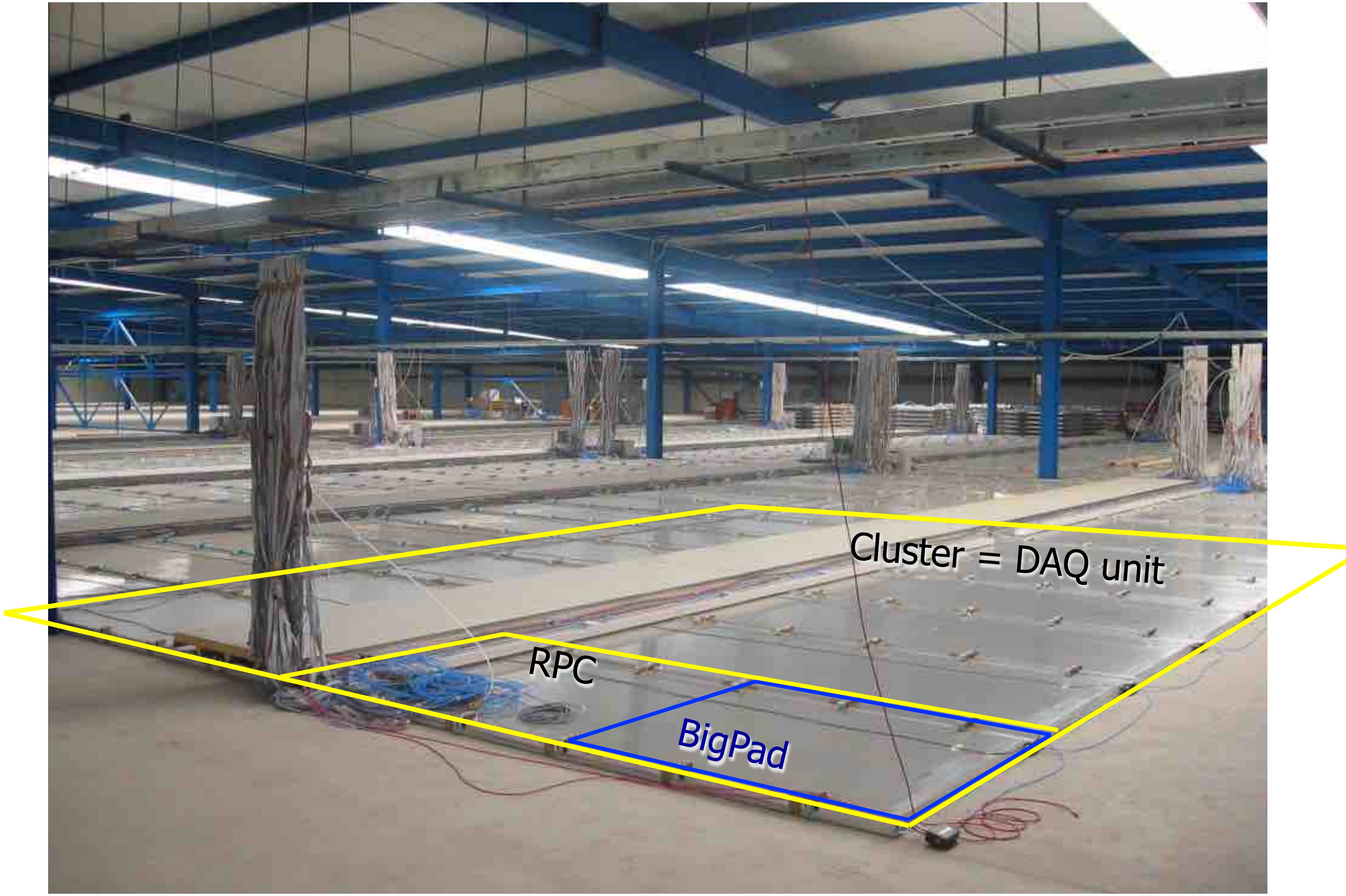

The basic concepts

…for an unconventional air shower detector

❖ HIGH ALTITUDE SITE
(YBJ - Tibet 4300 m asl - 600 g/cm2)

❖ FULL COVERAGE
(RPC technology, 92% covering factor)

❖ HIGH SEGMENTATION OF THE READOUT
(small space-time pixels)

Space pixels: 146,880 strips (7×62 cm^2)
Time pixels: 18,360 pads (56×62 cm^2)

… in order to

- image the shower front with unprecedented details
- get an energy threshold of a few hundreds of GeV

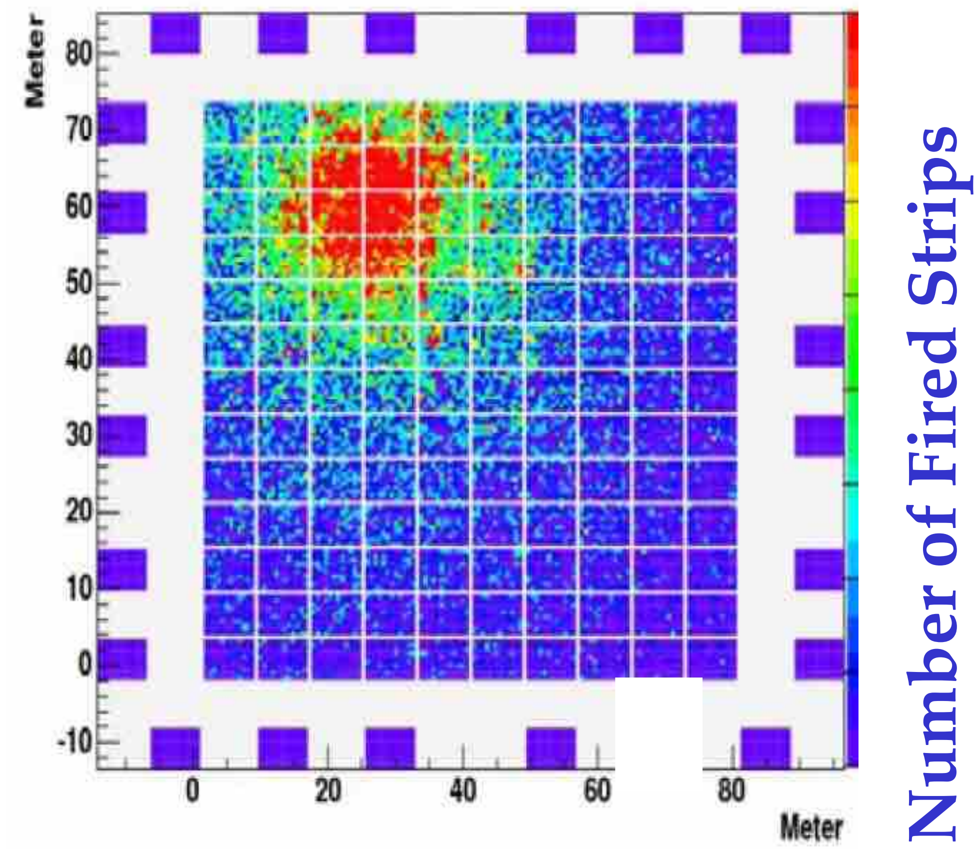

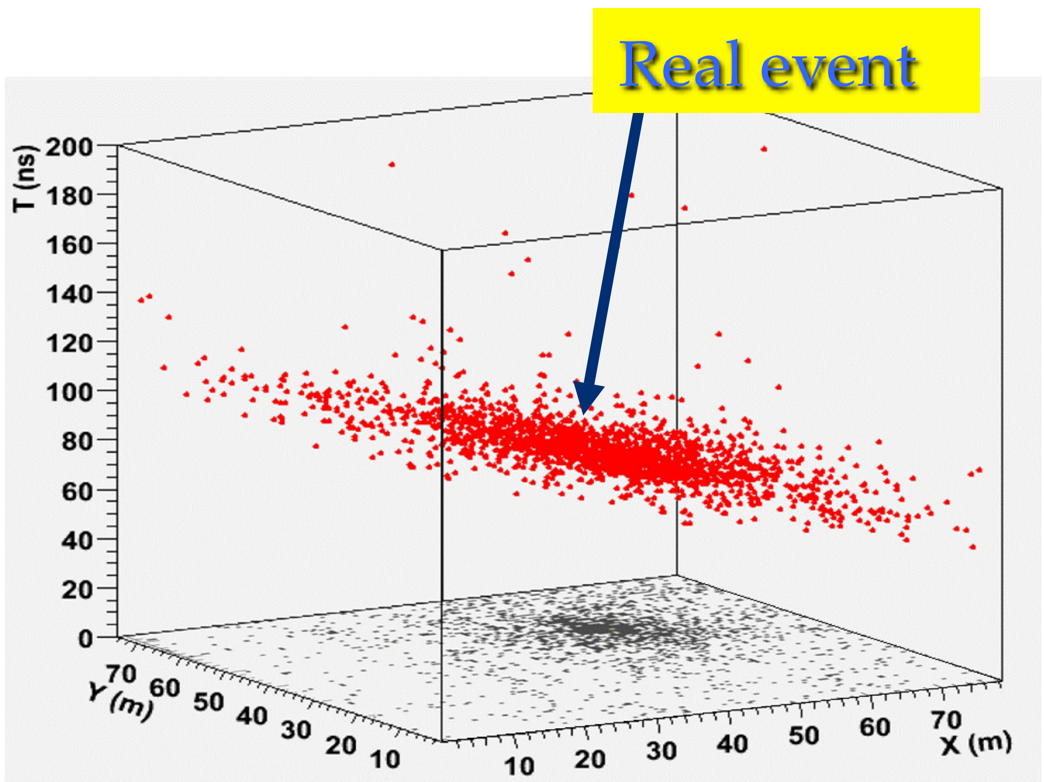

Shower detection

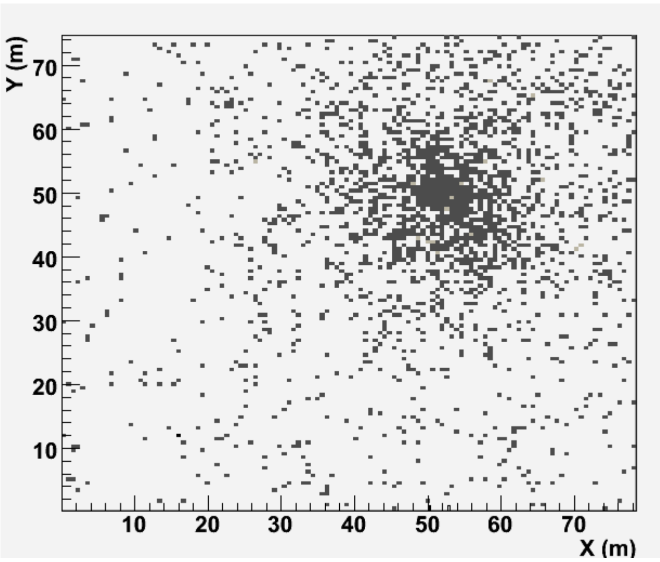

Fired pads on the carpet

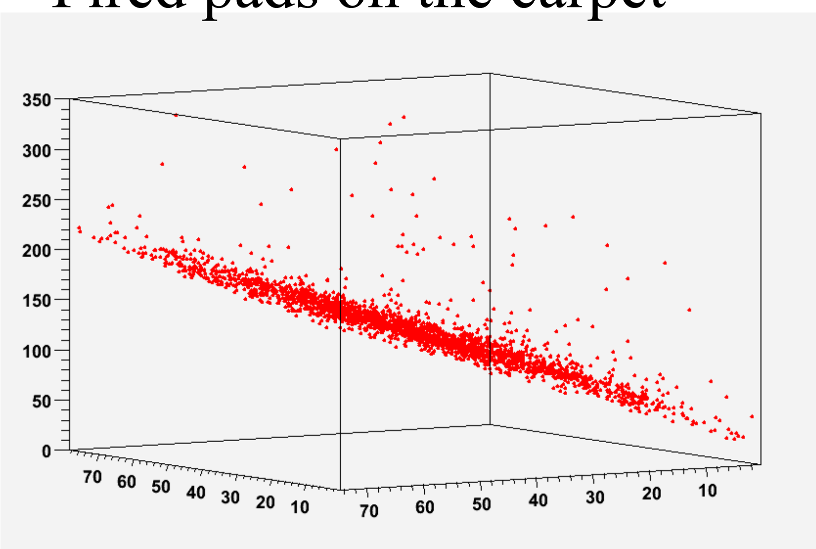

Arrival time vs position

Small and compact events

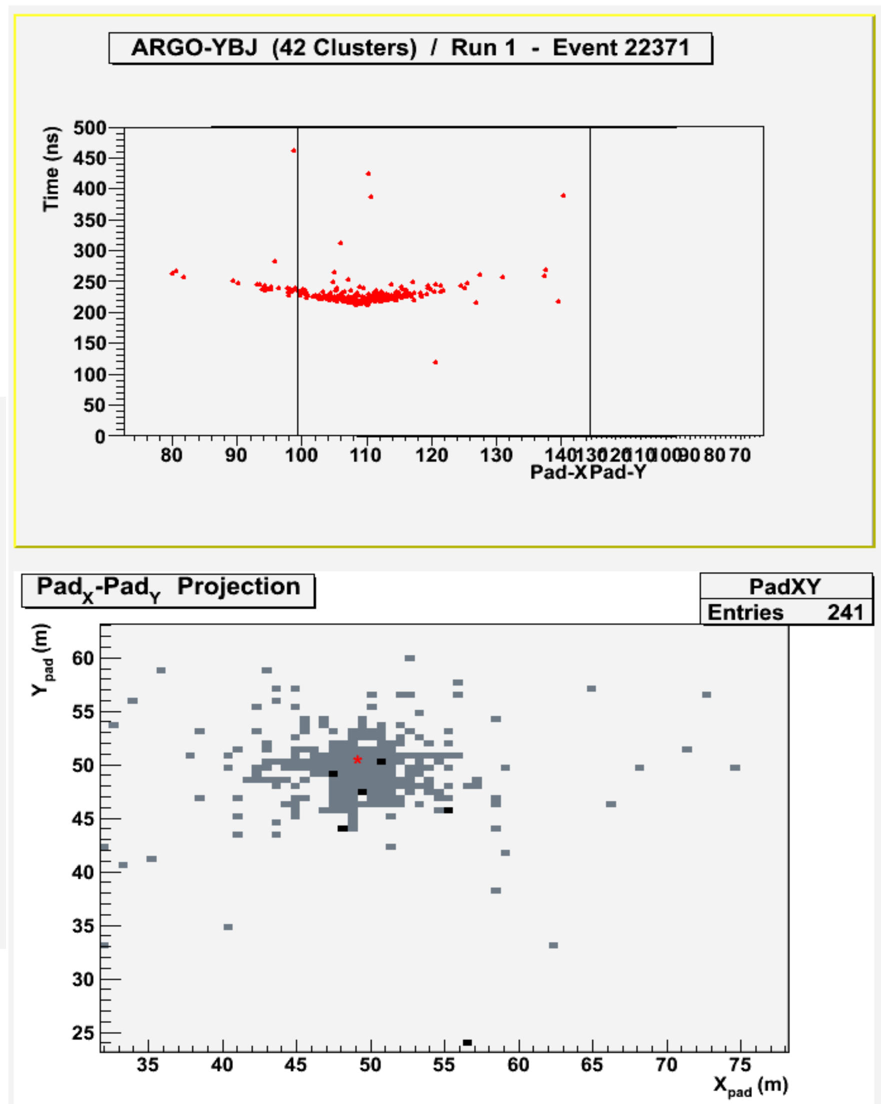

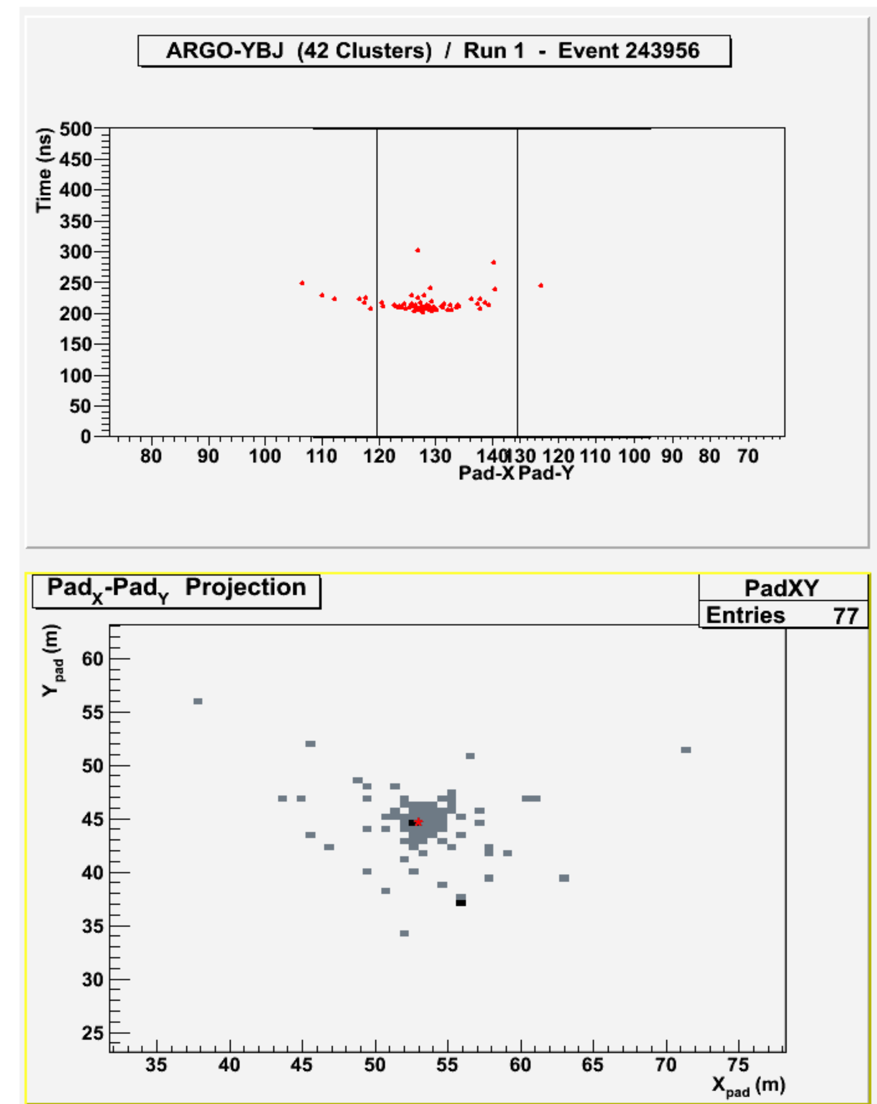

ARGO-YBJ energy distributions

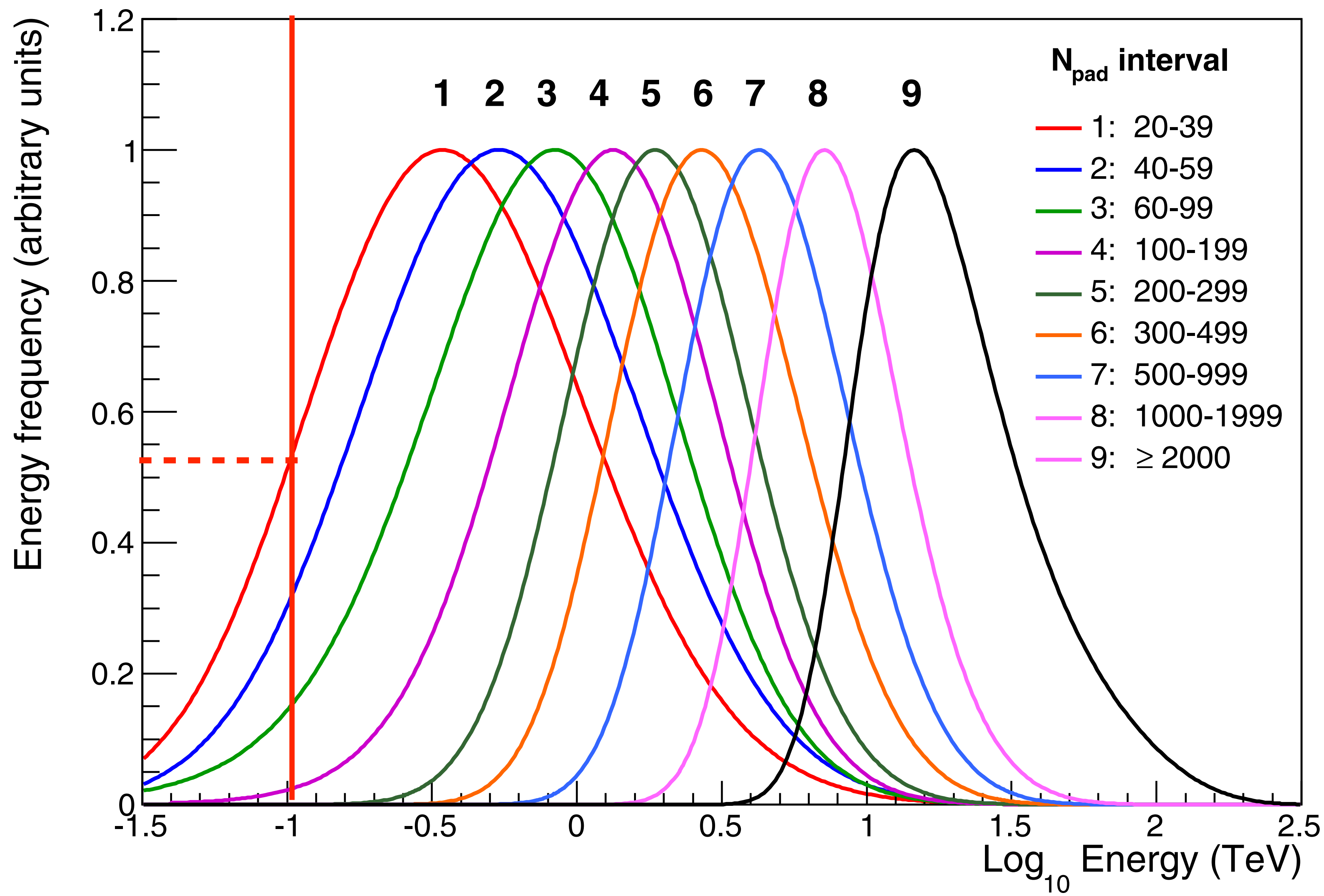

Figure 3. Normalized distribution of the primary gamma-ray energy for different $N_{\rm pad}$ intervals, for a Crab-like source.

Median energy first bin = 360 GeV

Topology-based Trigger logic:
>20 pads out of 15,000 bkg free !

The RPC charge readout

…extending the dynamical range up to 10 PeV

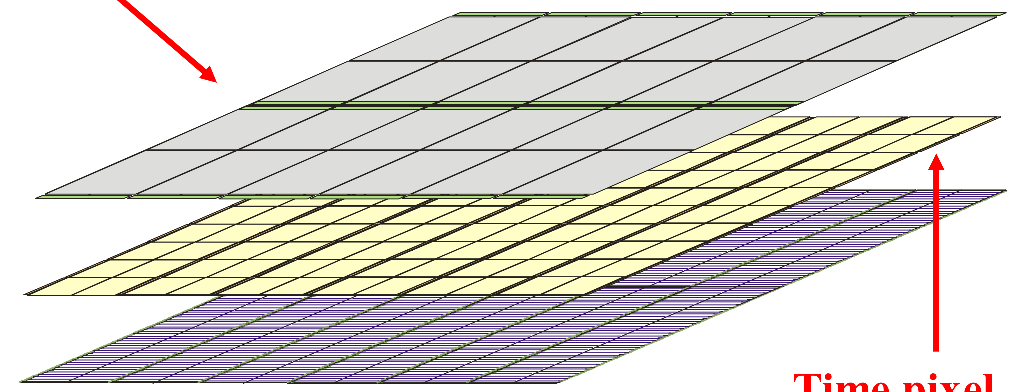

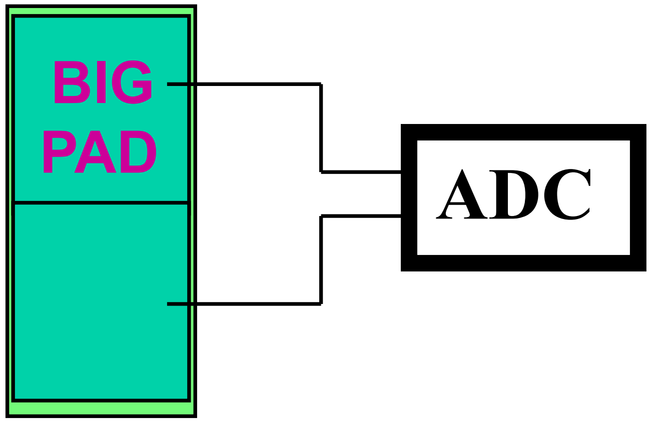

4 different gain scales used to cover a wide range in particle density:

$\rho_{max-strip} \approx 20$ particles/m^2

$\rho_{max-analog} \approx 10^4$ particles/m^2

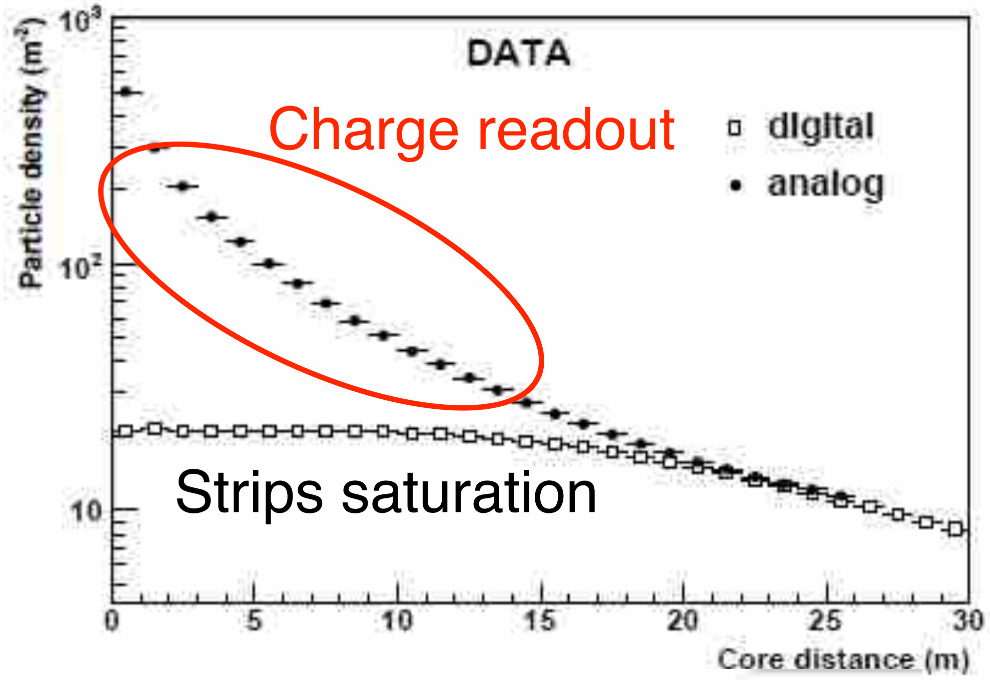

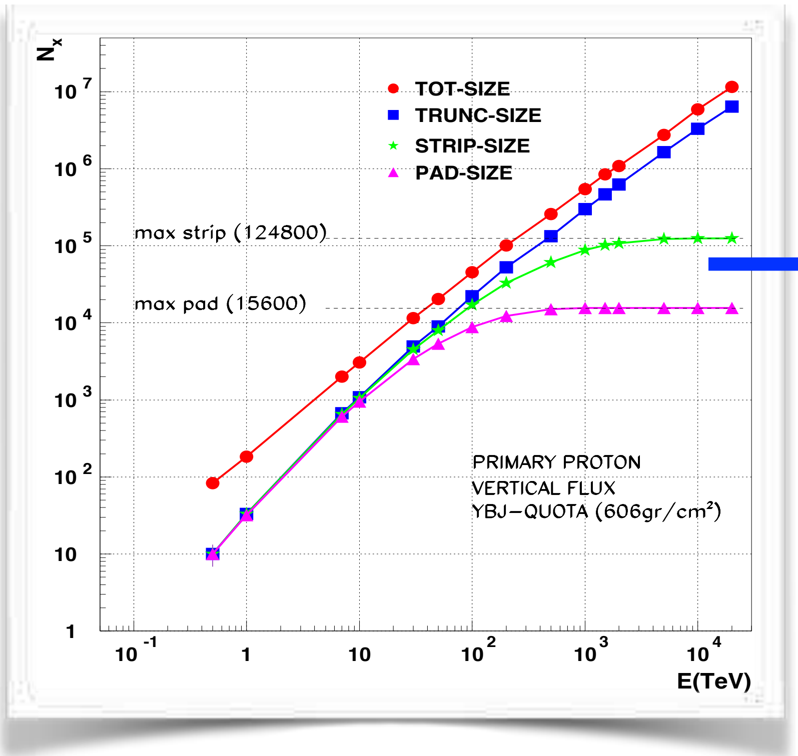

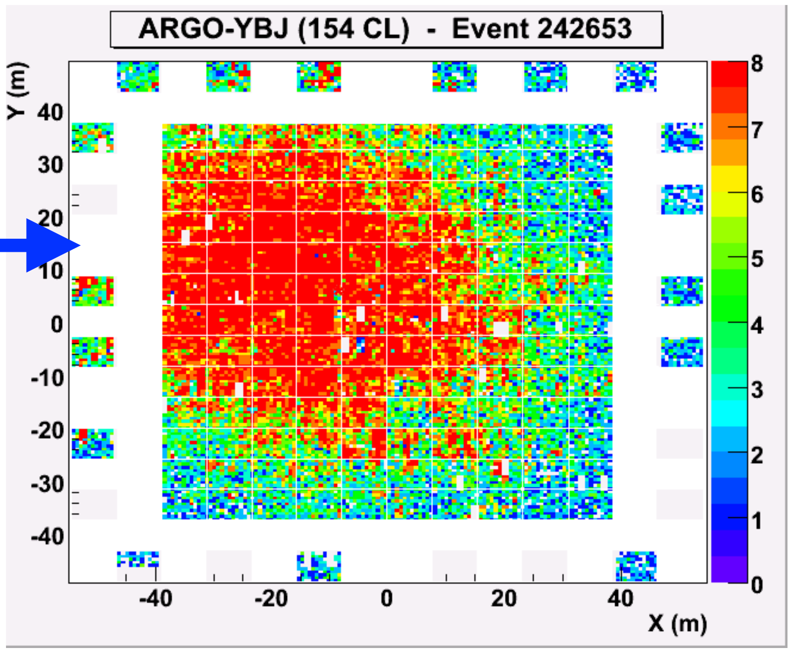

The RPC charge readout: the core region

MC: 100 TeV

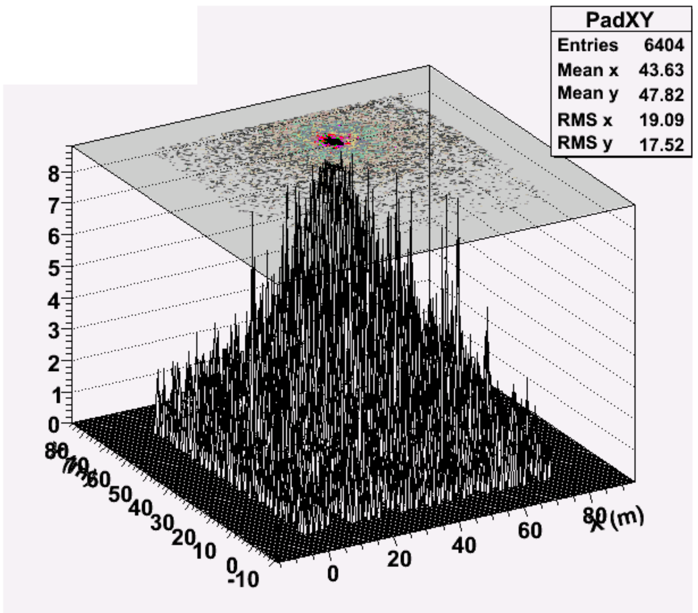

Strip read-out

MC: 1000 TeV

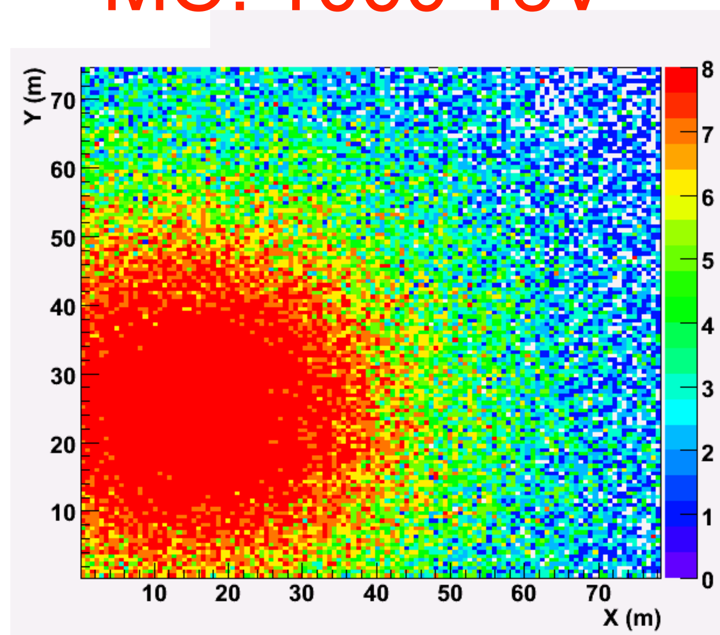

Strip read-out

Data

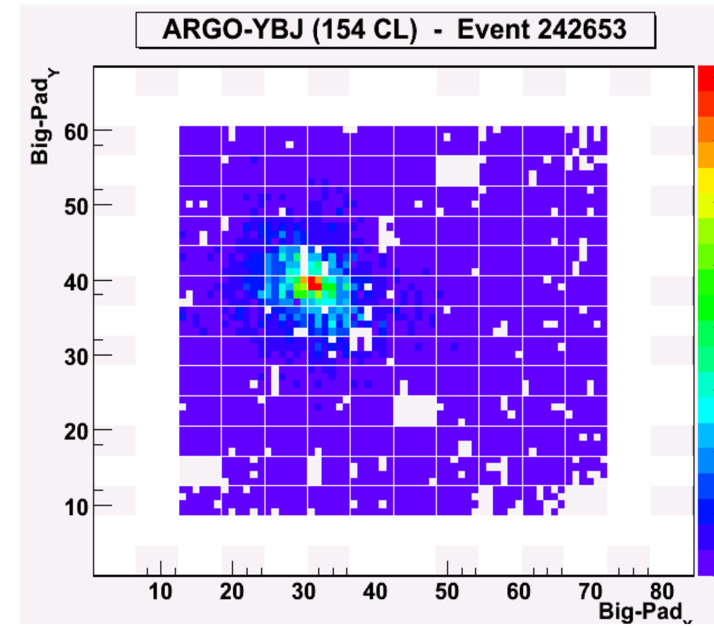

Strip read-out

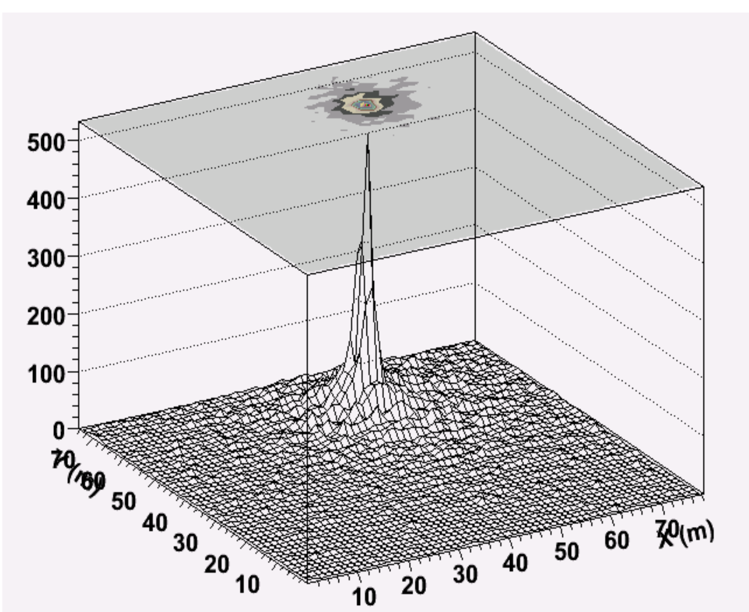

Charge read-out

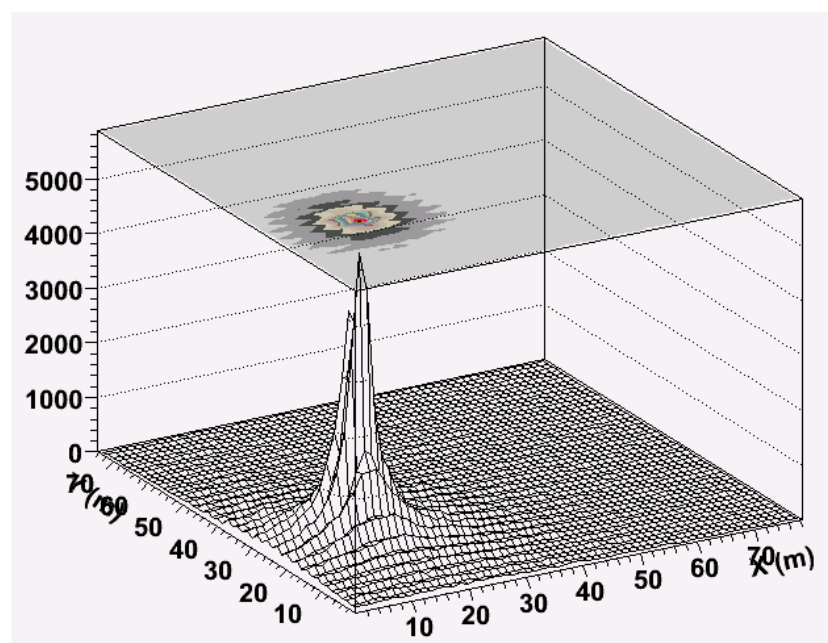

Charge read-out

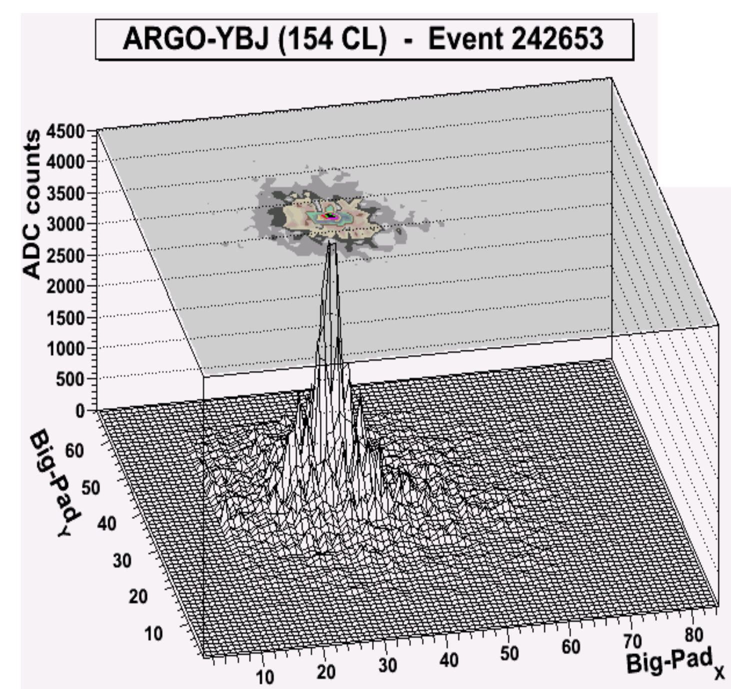

Charge read-out

ARGO-YBJ milestones

- In data taking since July 2004 (with increasing portions of the detector)
- Commissioning of the central carpet in June 2006
- Stable data taking full apparatus since November 2007
- End/Stop data taking: February 2013

- Average duty cycle ~87%
- Trigger rate ~3.5 kHz @ 20 pad threshold
- N. recorded events: ≈ $5 \cdot 10^{11}$ from 100 GeV to 10 PeV
- 100 TB/year data

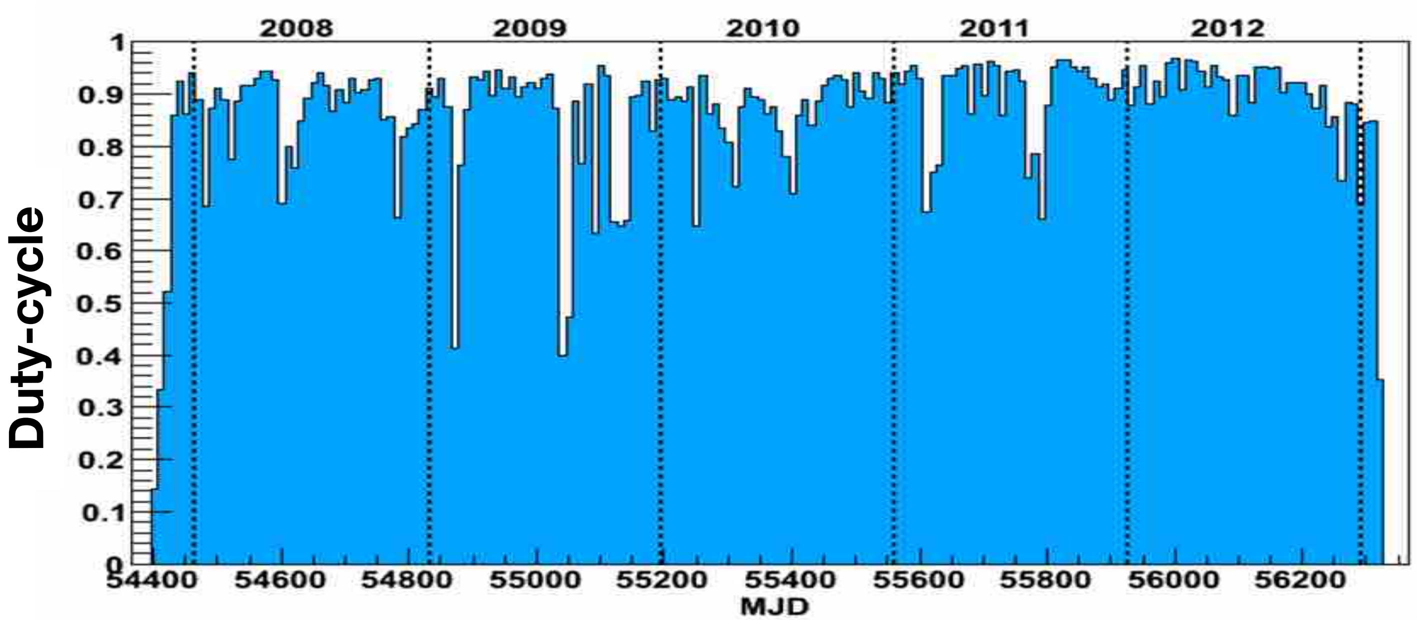

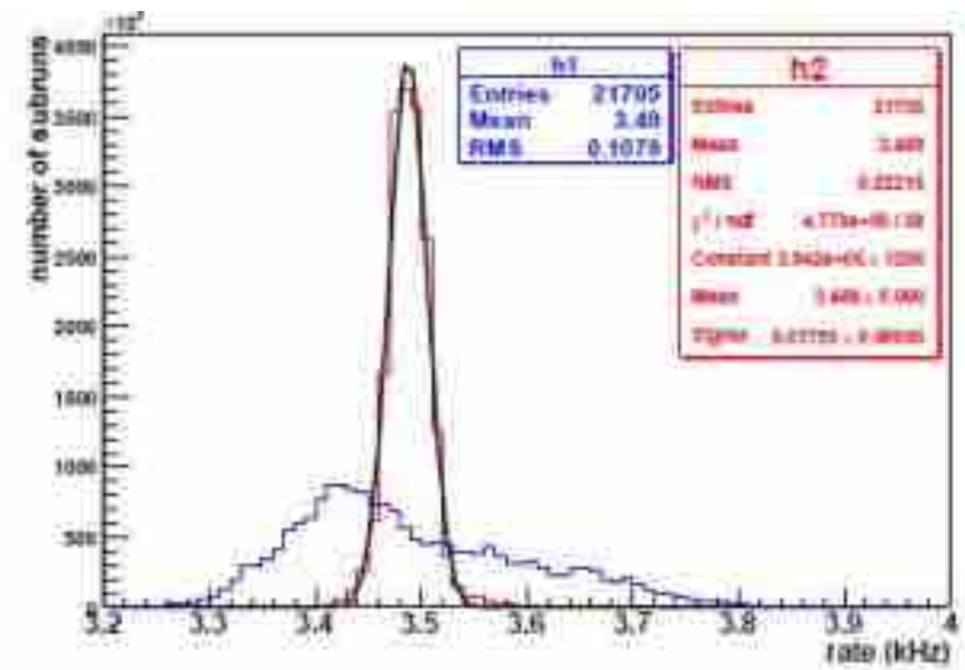

Intrinsic Trigger Rate stability 0.5%
(after corrections for T/p effects)

Detector stability at different energies

Stability of angular resolution and pointing accuracy (TeV)

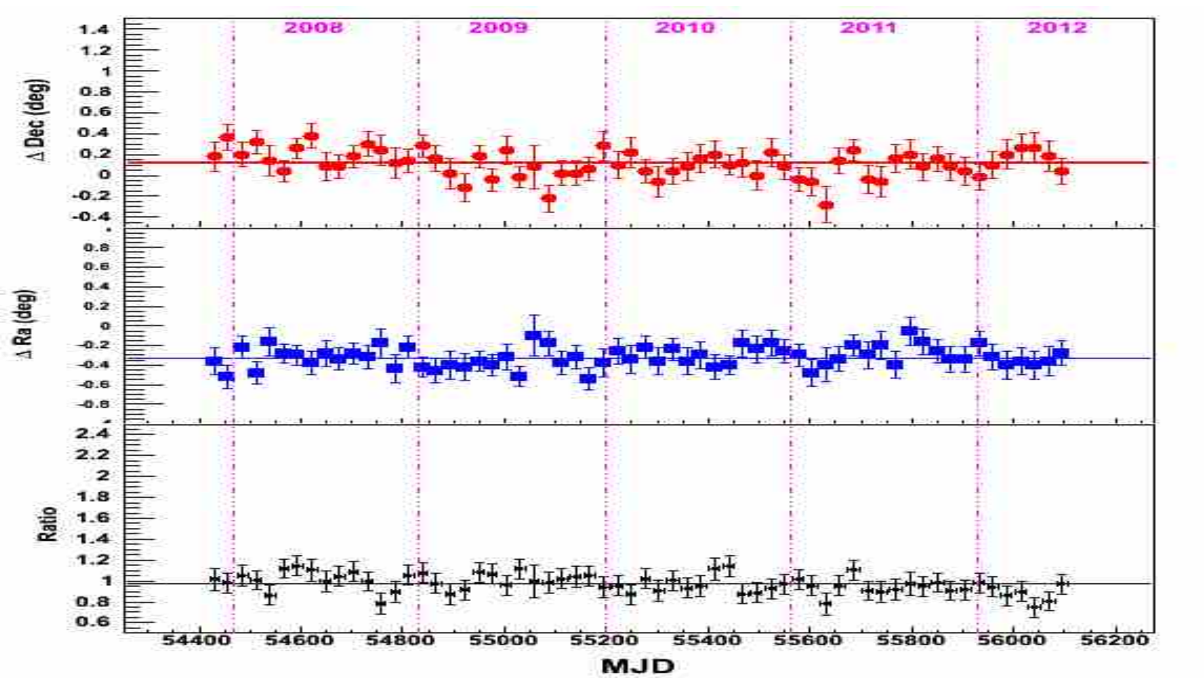

Distribution of particles hitting a cluster (GeV)

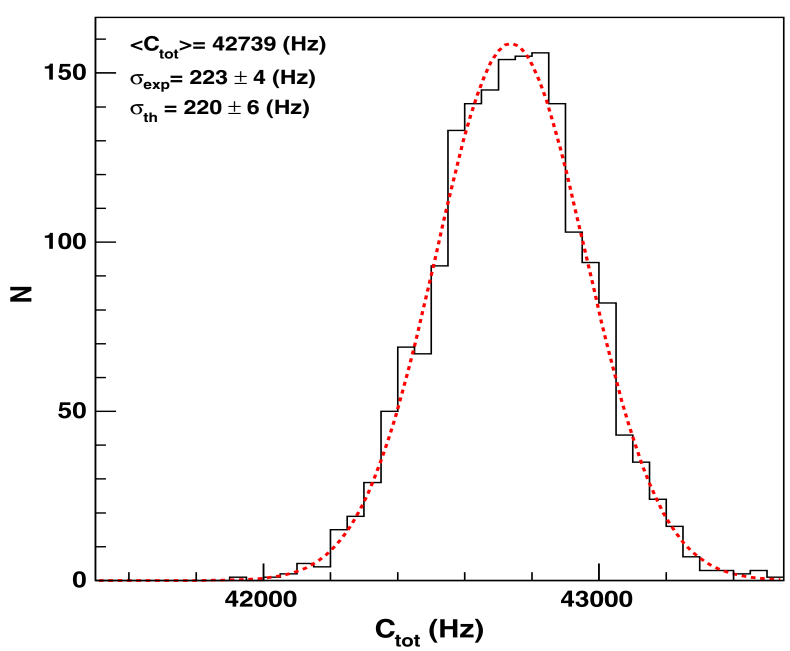

Stability of CR flux measurement
p+He spectrum (3 - 300 TeV)

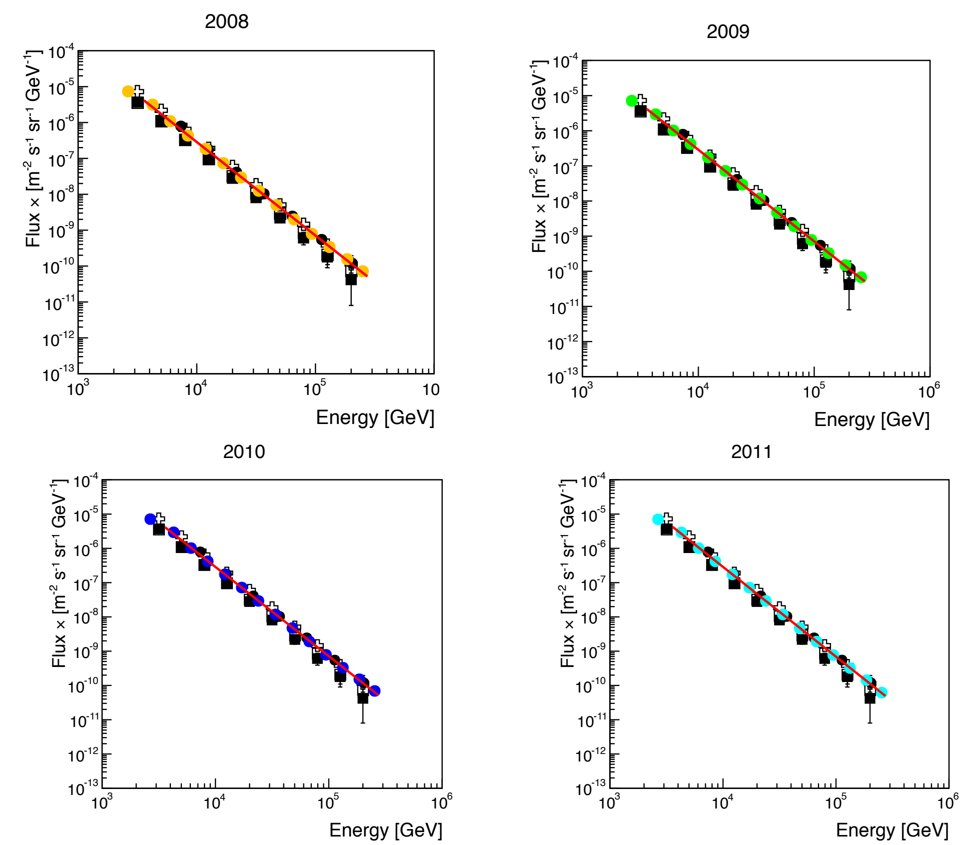

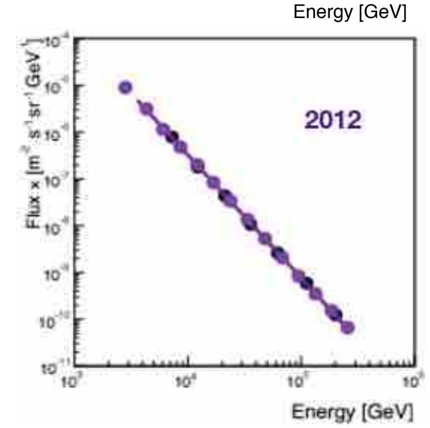

year	Gamma
2008	2.61±0.02
2009	2.61±0.02
2010	2.61±0.02
2011	2.62±0.02
2012	2.63±0.02

flux difference at 5% level

Calibration of the energy scale

(p+He) spectrum (2 - 700) TeV

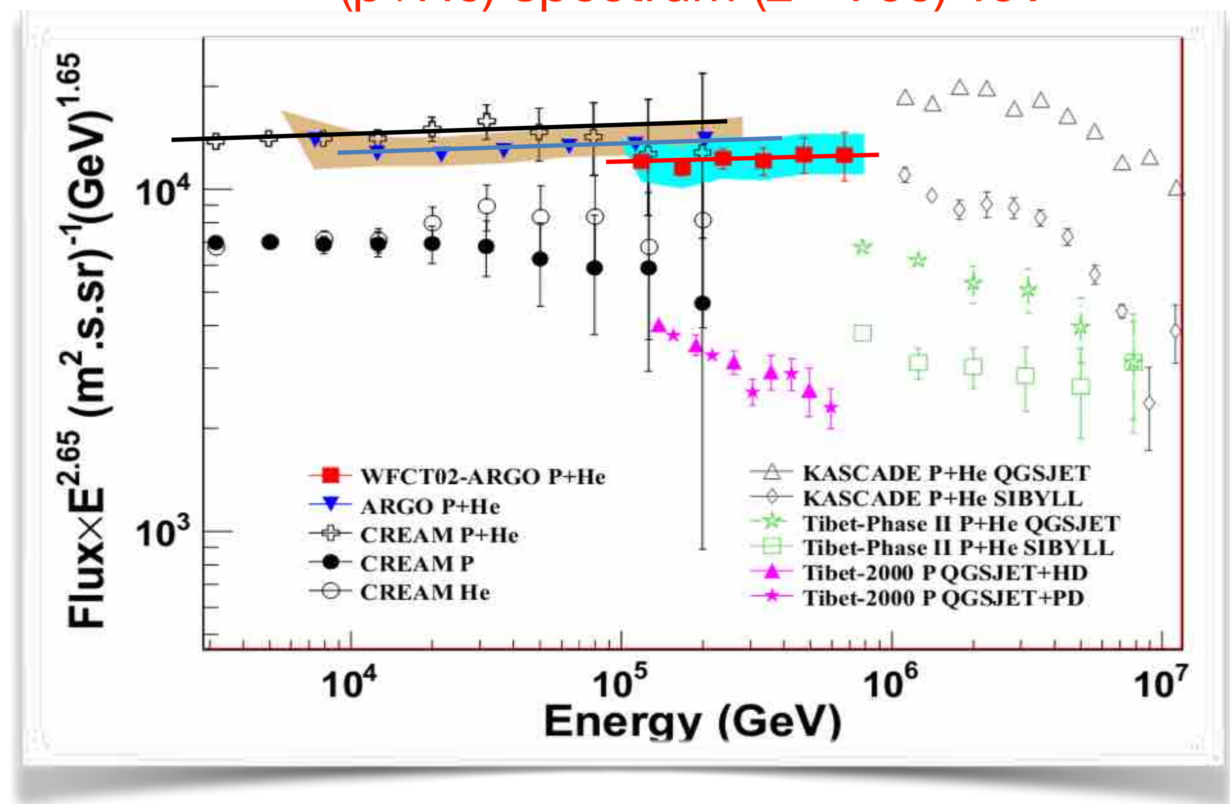

Chin. Phys. C 38, 045001 (2014)

ARGO-YBJ: *Moon shadow* tool

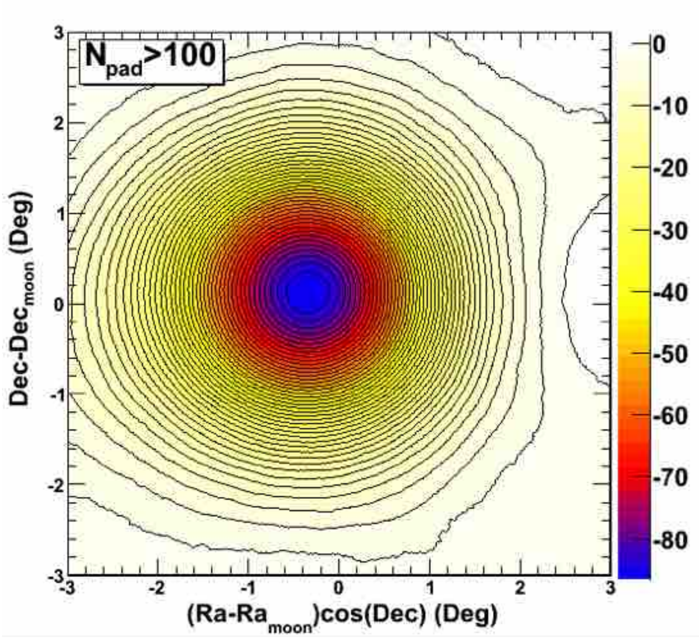

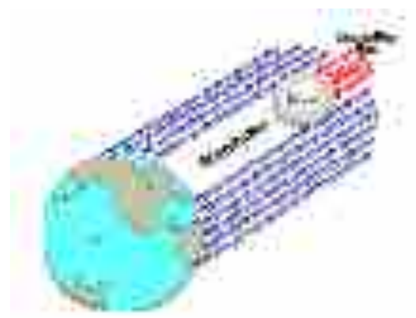

PRD 84 (2011) 022003

The energy scale uncertainty is estimated at 10% level in the energy range 1 – 30 (TeV/Z).

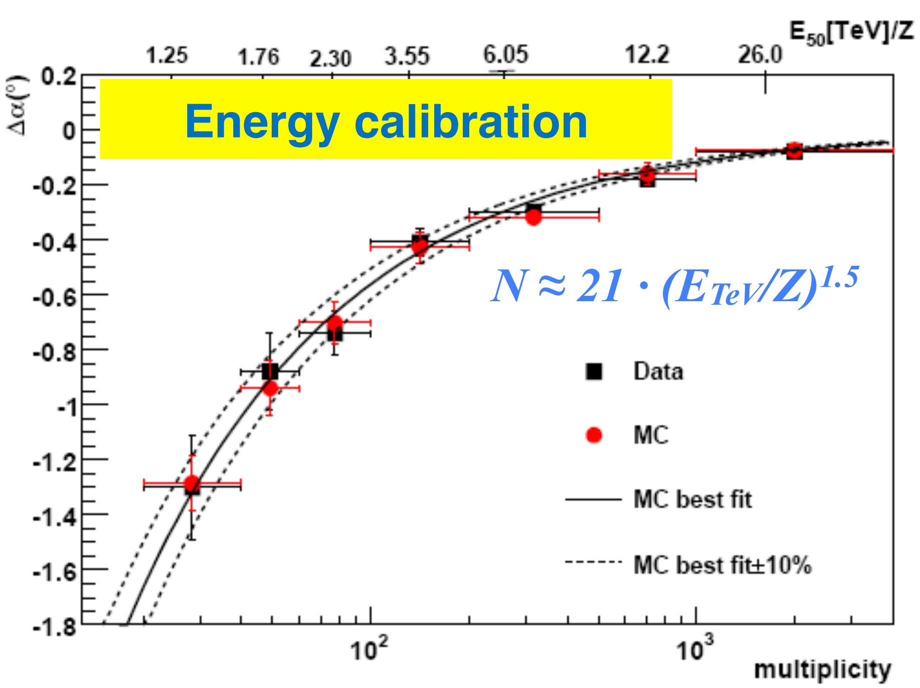

- CREAM: 1.09 × 1.95 × 10^{-11} (E/400 TeV)$^{-2.62}$
- ARGO-YBJ: 1.95 × 10^{-11} (E/400 TeV)$^{-2.61}$
- Hybrid: 0.92 × 1.95 × 10^{-11} (E/400 TeV)$^{-2.63}$

Single power-law: 2.62 ± 0.01

Flux at 400 TeV:

1.95 × 10^{-11}± 9% (GeV^{-1} m^{-2} sr^{-1} s^{-1})

The 9% difference in flux corresponds to a difference of ± 4% in energy scale between different experiments.

Azimuthal distribution EAS > 80 deg

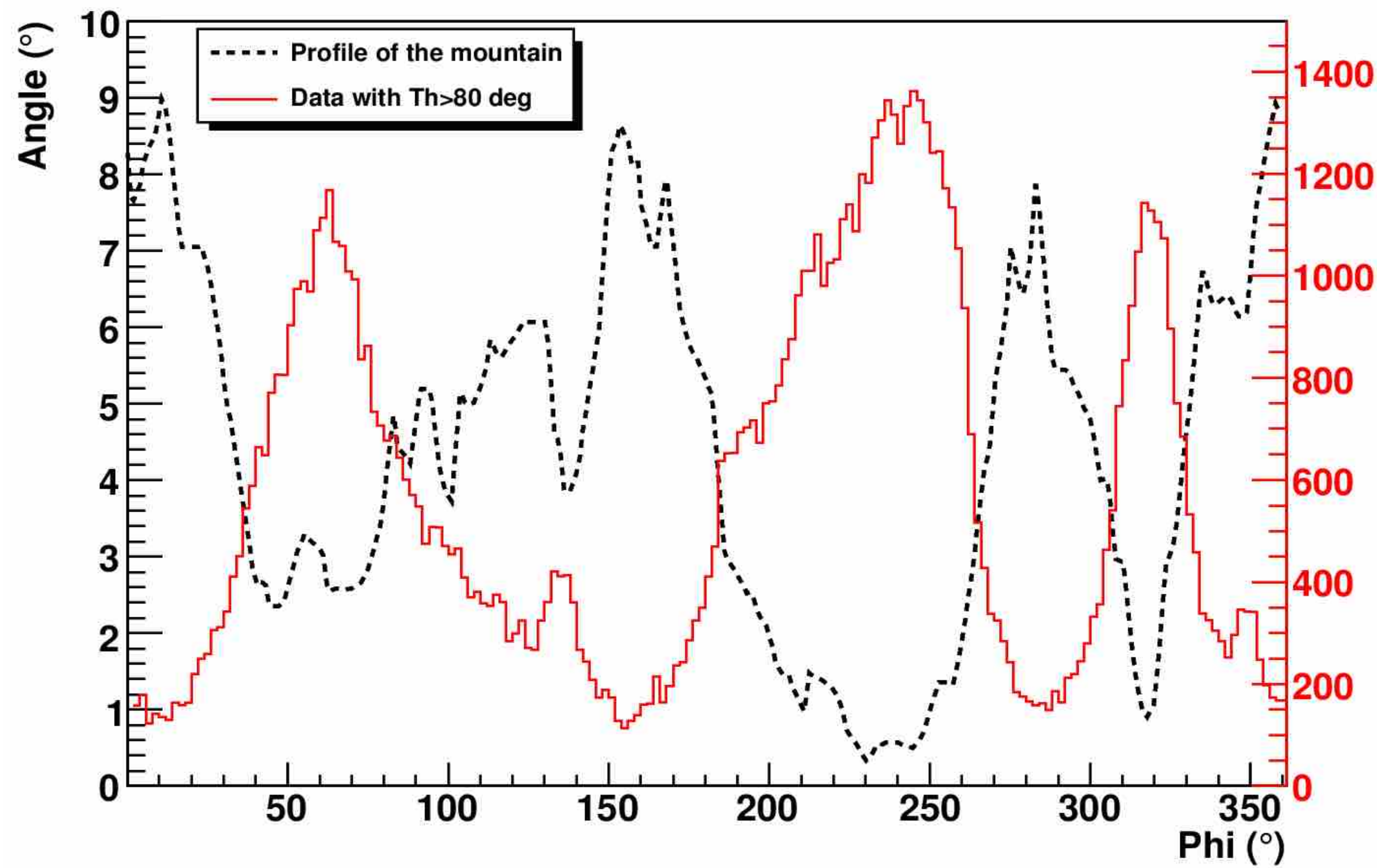

ARGO-YBJ: a multi-purpose experiment

A *multi-purpose experiment* capable of acting simultaneously as a Cosmic Ray detector and a Gamma Ray Telescope to face the open problems in Galactic CR Physics

- Sky survey -10% $\leq \delta \leq$ 70% (γ-sources, diffuse emission)
- High exposure for flaring activity (γ-sources, GRBs, solar flares)
- CR 1 TeV ➜ 10^4 TeV
  - p + He energy spectrum
  - Proton *"knee"*
  - Composition at the *knee*
  - Anisotropies
- Antip/p at TeV energies
- Solar and heliospheric physics
- Hadronic interactions, cross sections

"Main physics results of the ARGO-YBJ experiment", Int. J. of Mod. Phys. D23 (2014) 1430019

Approaching the knee

The origin of the *knee* in the all-particle spectrum is connected with the issue of the end of the Galactic CR spectrum and the transition to extragalactic CRs.

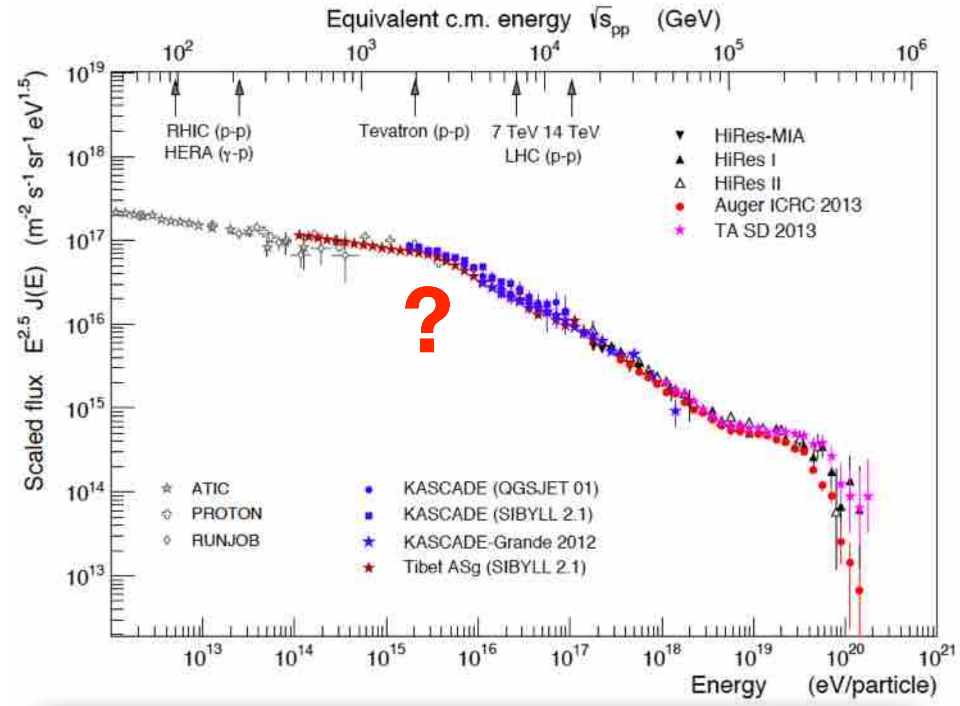

The standard model:

- Knee attributed to light (proton, helium) component
- Rigidity-dependent structure (Peters cycle): cut-offs at energies proportional to the nuclear charge $E_Z = Z \times 4.5$ PeV
- The sum of the flux of all elements with their individual cut-offs makes up the all-particle spectrum.

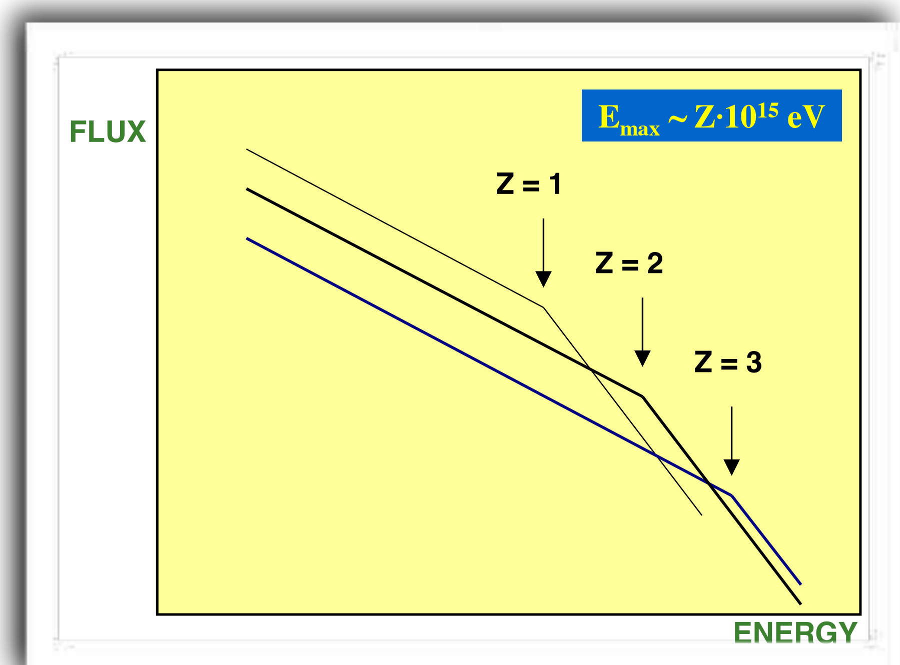

"The description of how particles escape from a SNR shock has not been completely understood yet, the reason being the uncertainties related to *how particles reach the maximum energies.*"

Morlino arXiv:1706.08275

$E_{max}(\text{iron}) = 26 \cdot E_{max}(\text{proton})$

But "acceleration up to PeV energies is problematic in all scenarios considered. This implies that either a different (more efficient) mechanism of magnetic field amplification operates at SNR shocks, or that the sources of GCR in the PeV energy range should be searched somewhere else."

Gabici arXiv:1610.07638

Experimental results still conflicting !

Composition at the knee - 1

KASCADE

Astroparticle Physics 24 (2005) 1
Astroparticle Physics 31 (2009) 86

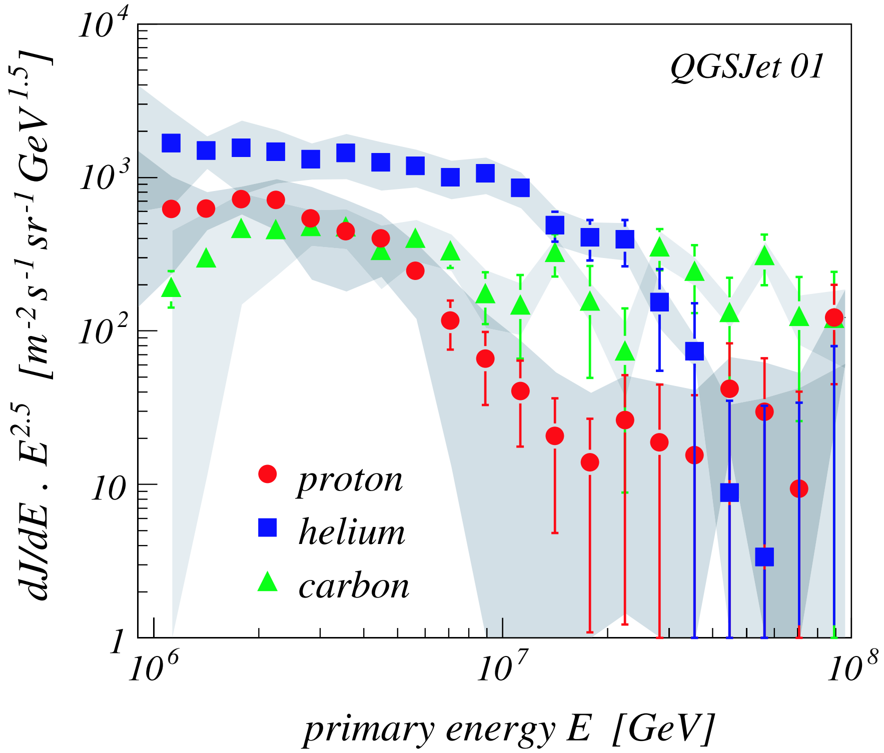

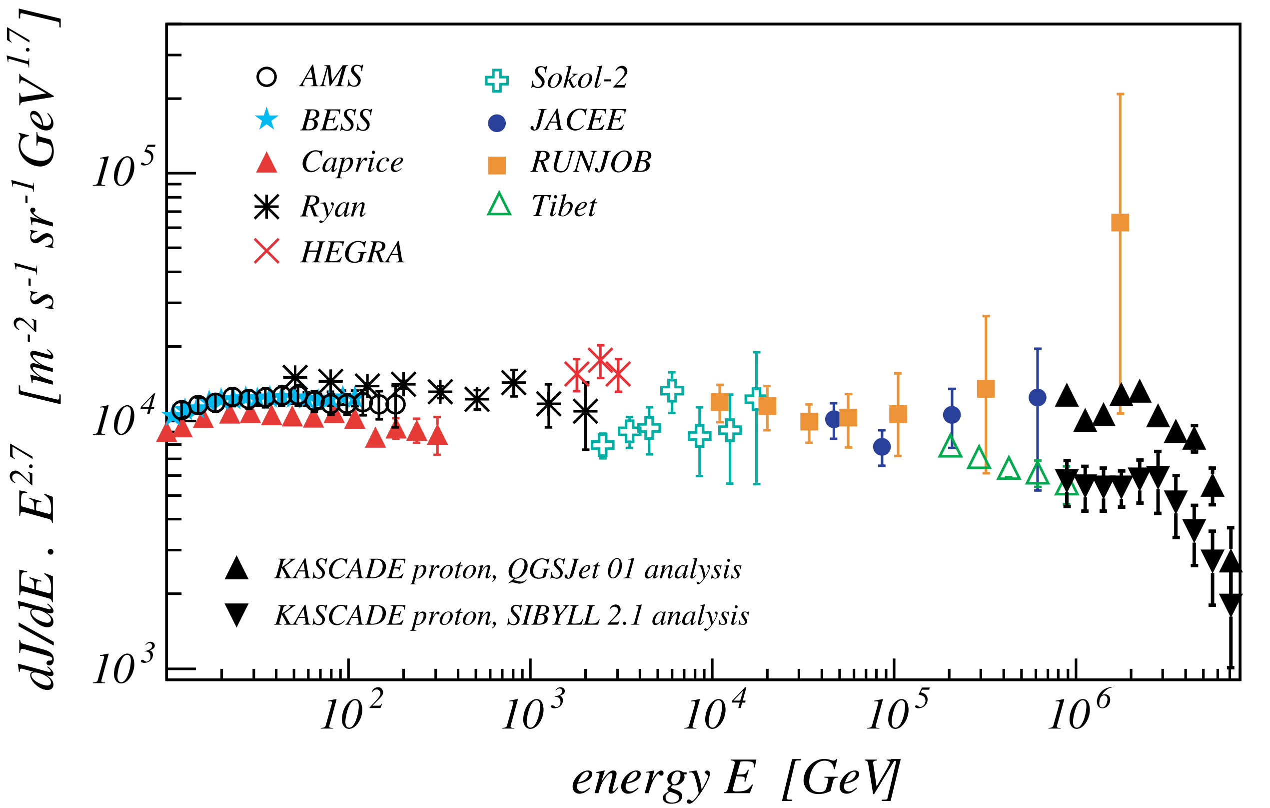

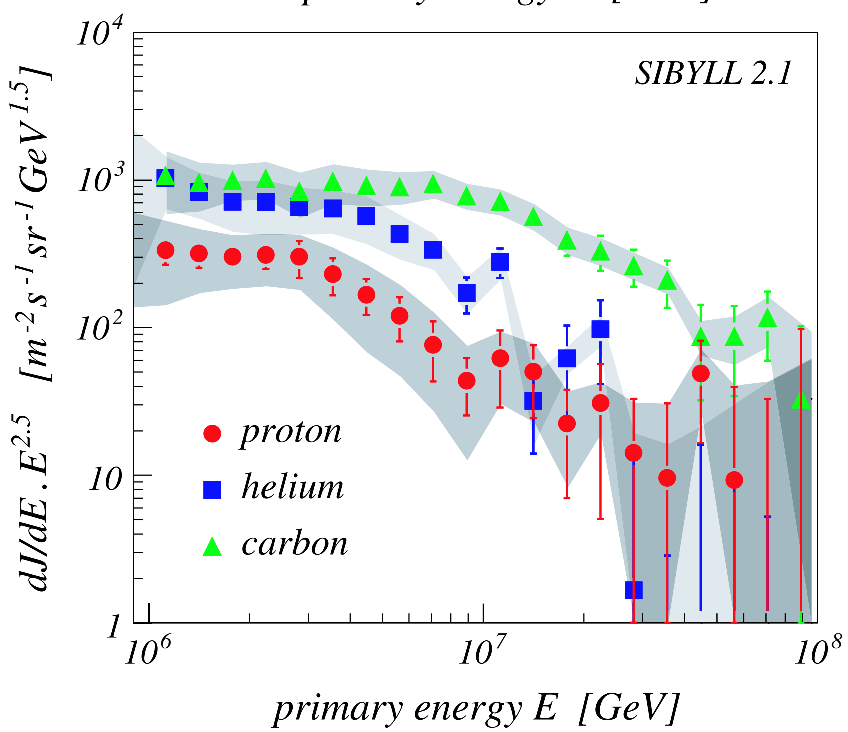

from the analysis of the nearly vertical shower set: The knee is observed at an energy around ≈5 PeV with a change of the index $\Delta\gamma \approx 0.4$. Considering the results of the mass group spectra, in all analyses an appearance of knee-like features in the spectra of the light elements is ascertained. In all solutions the positions of the knees in these spectra is shifted to higher energy with increasing element number.

Composition at the knee - 2

CASA-MIA

Astroparticle Physics 12 (1999) 1–17

The cosmic ray composition between 10^{14} and 10^{16} eV

M.A.K. Glasmacher[a], M.A. Catanese[a,1], M.C. Chantell[b], C.E. Covault[b], J.W. Cronin[b], B.E. Fick[b], L.F. Fortson[b,2], J.W. Fowler[b], K.D Green[b,3], D.B. Kieda[c], J. Matthews[a,4], B.J. Newport[b,5], D.F. Nitz[a,6], R.A. Ong[b], S. Oser[b], D. Sinclair[a], J.C. van der Velde[a]

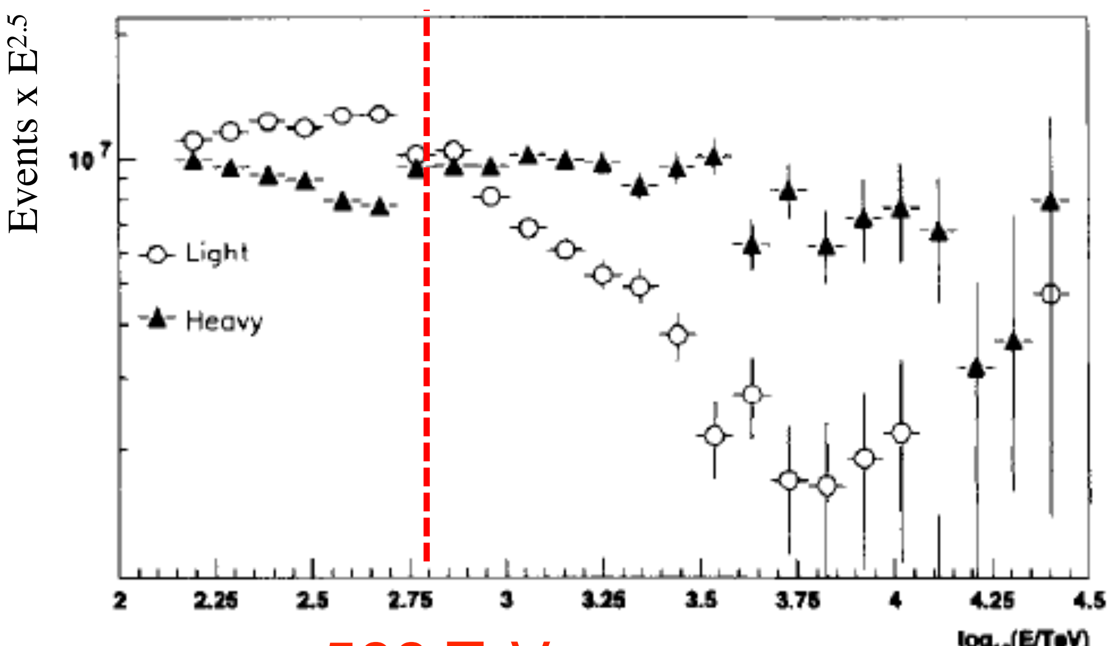

≈ 500 TeV

The spectra of the heavy and light components appear similar below 500 TeV, at which point the lighter component's spectral index steepens. The heavier component shows no such "knee" at that energy.

Tibet ASγ

Physics Letters B 632 (2006) 58–64

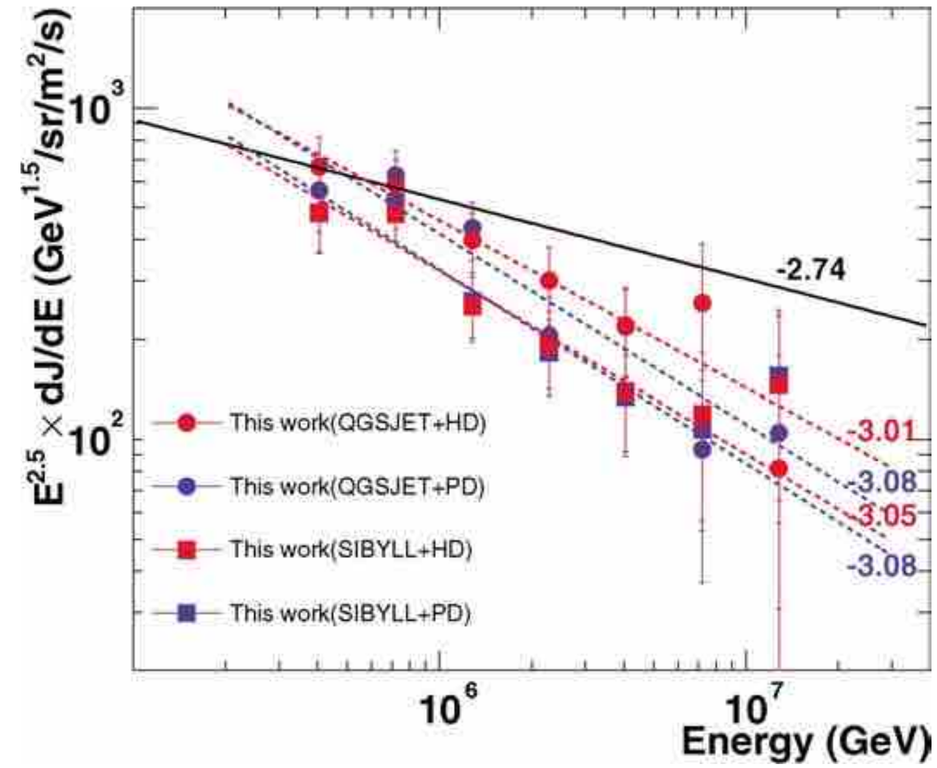

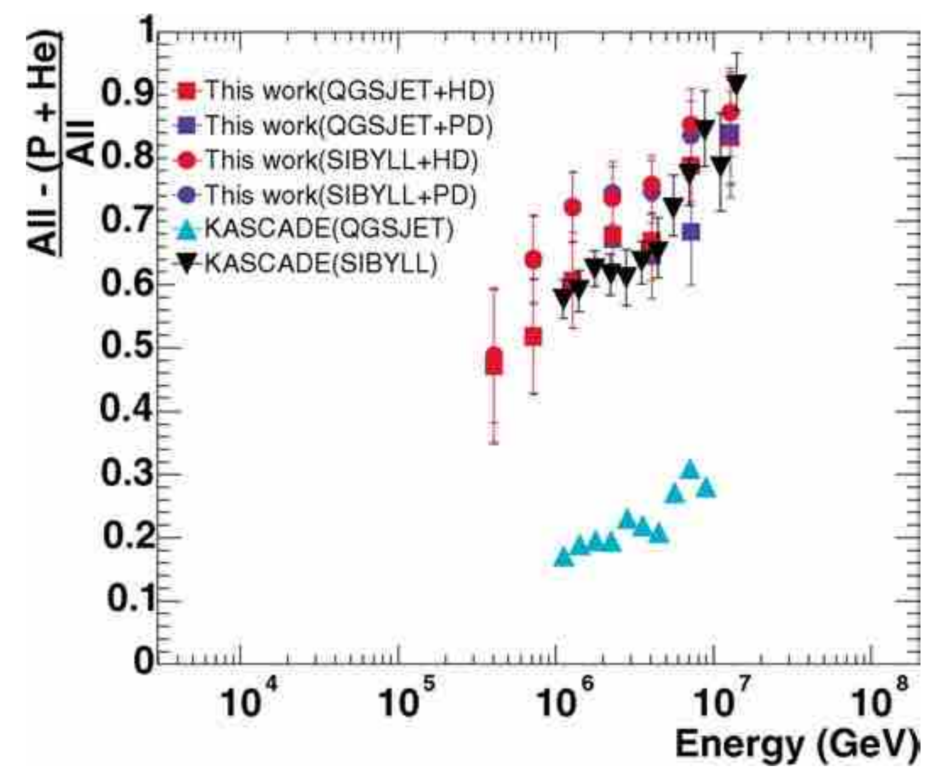

Strong dependence from hadronic models !

Composition at the knee - 3

BASJE-MAS *ApJ 612 (2004) 268*

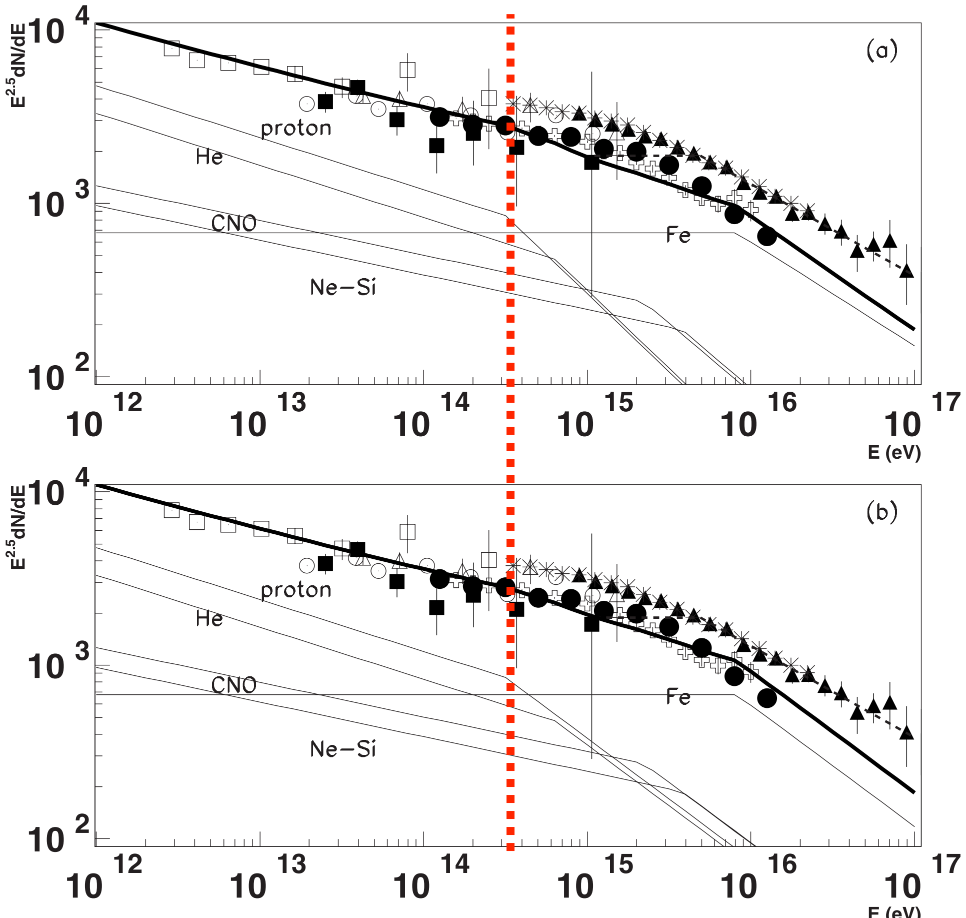

≈ 400 TeV

The measured $\langle \ln A \rangle$ increases with energy over the energy range of $10^{14.5}-10^{16}$ eV. This is consistent with our former Cerenkov light observations and the measurements by some other groups. The observed $\langle \ln A \rangle$ is consistent with the expected features of a model in which the energy spectrum of each component is steepened at a fixed rigidity of $10^{14.5}$ V.

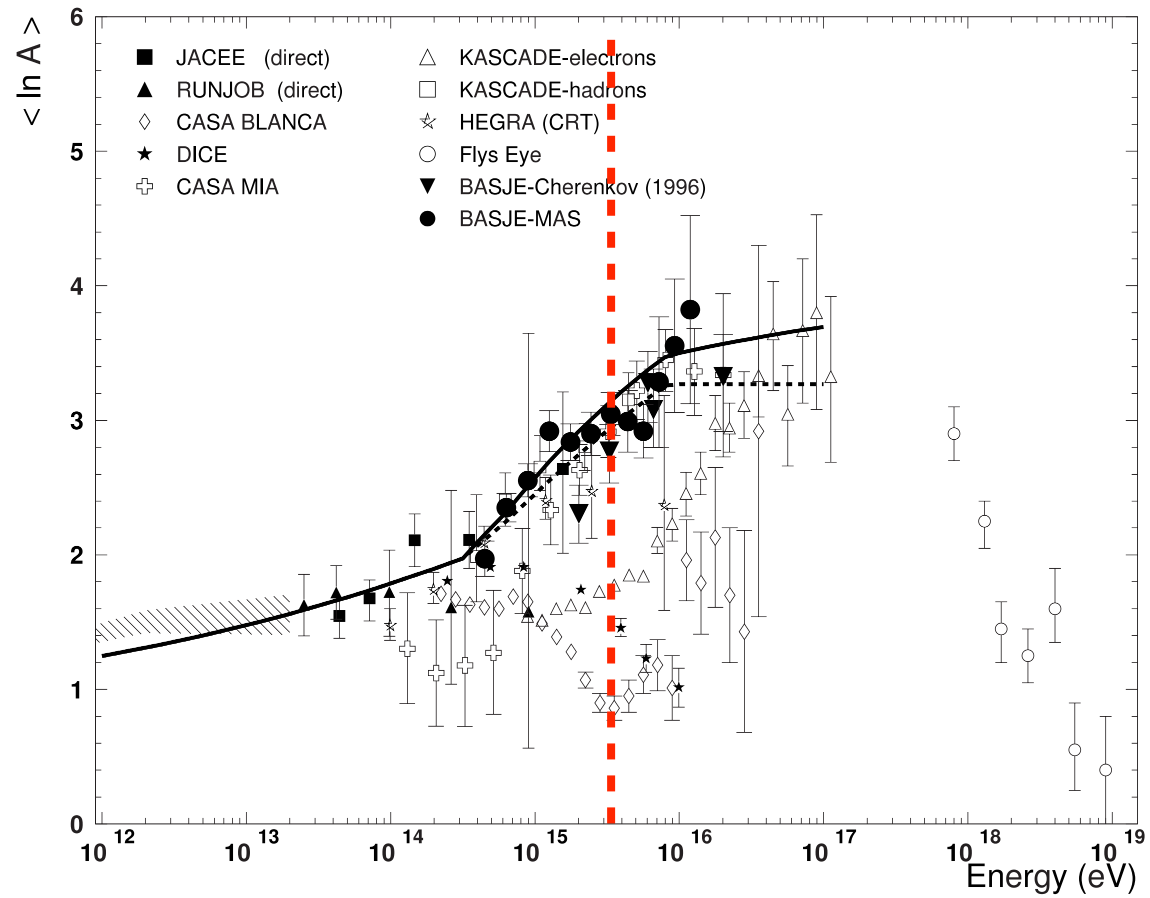

Finally, we conclude that the actual model suggests that the dominant component above 10^{15} eV is heavy and that the $\langle \ln A \rangle$ increases with the energy to about 3.5 at 10^{16} eV.

Measurement of CR energy spectrum with ARGO-YBJ

- Measurement of the CR energy spectrum (all-particle and light component) in the energy range TeV - 20 PeV by ARGO-YBJ with *different 'eyes'*
  - *'Digital readout'* (based on *strip multiplicity*) below 300 TeV
  - '*Analog readout'* (based on the *shower core density*) up to 20 PeV
  - '*Hybrid*' measurement with a Wide Field of view Cherenkov Telescope 200 TeV - few PeV

- Working at high altitude (4300 m asl):
  1. p and Fe produce showers with similar size
  2. Small fluctuations: shower maximum
  3. Low energy threshold: absolute energy scale calibration with the Moon Shadow technique and overposition with direct measurements

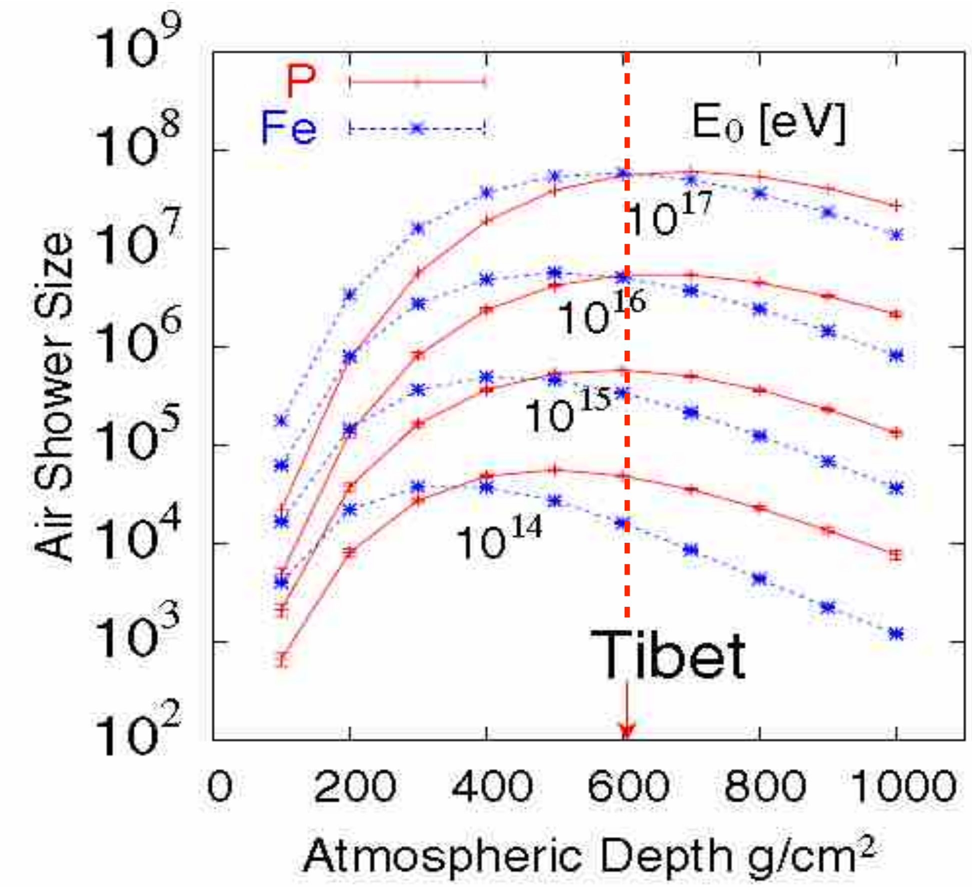

>4000 m asl ➡ *the 'right' altitude to study the knee*

All-particle energy spectrum by ARGO-YBJ

ARGO-YBJ reports evidence for the all-particle knee at the expected energy

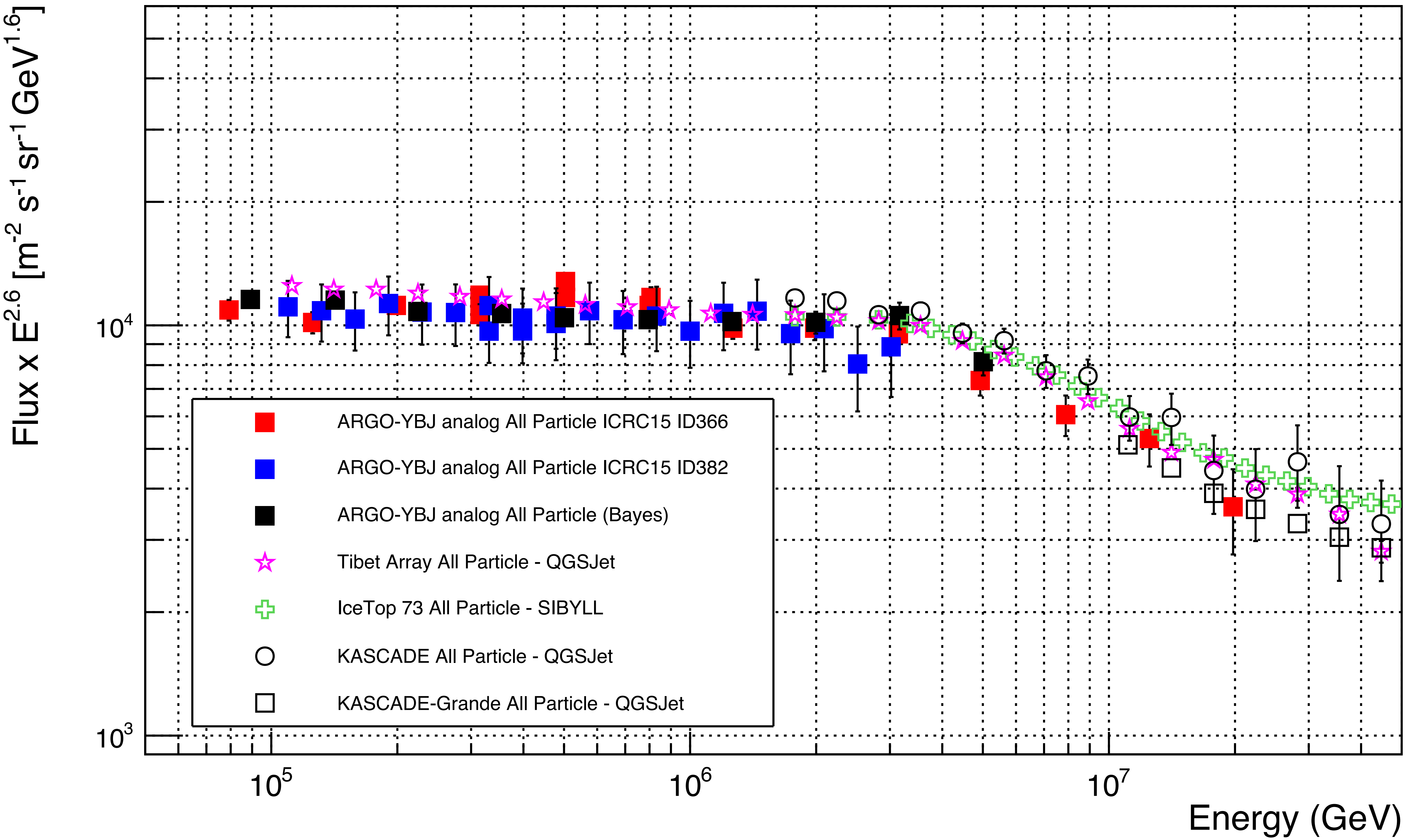

All-particle energy spectrum by ARGO-YBJ

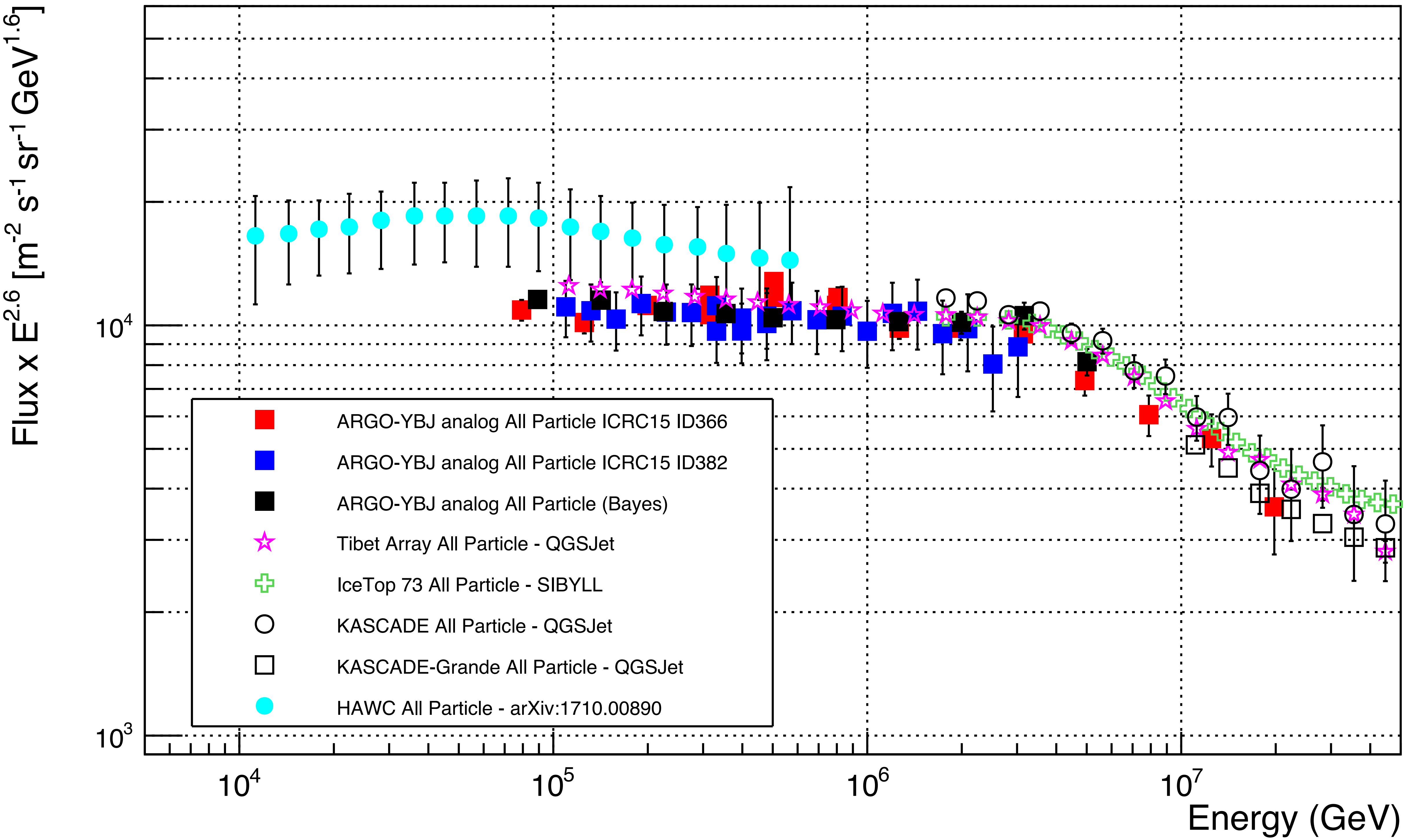

Selection of light (p+He) component

- Selection of (p+He)-induced showers: **NOT** by means of an unfolding procedure after the measurement of electronic and muonic sizes, but on an event-by-event basis exploiting showers topology, i.e. the lateral distribution of charged secondary particles.
- Energy reconstruction is based on the N_p^{8m} parameter: the *number of particle within 8 m from the shower core position.*

This truncated size is

- well correlated with primary energy
- not biased by finite detector effects
- weakly affected by shower fluctuations

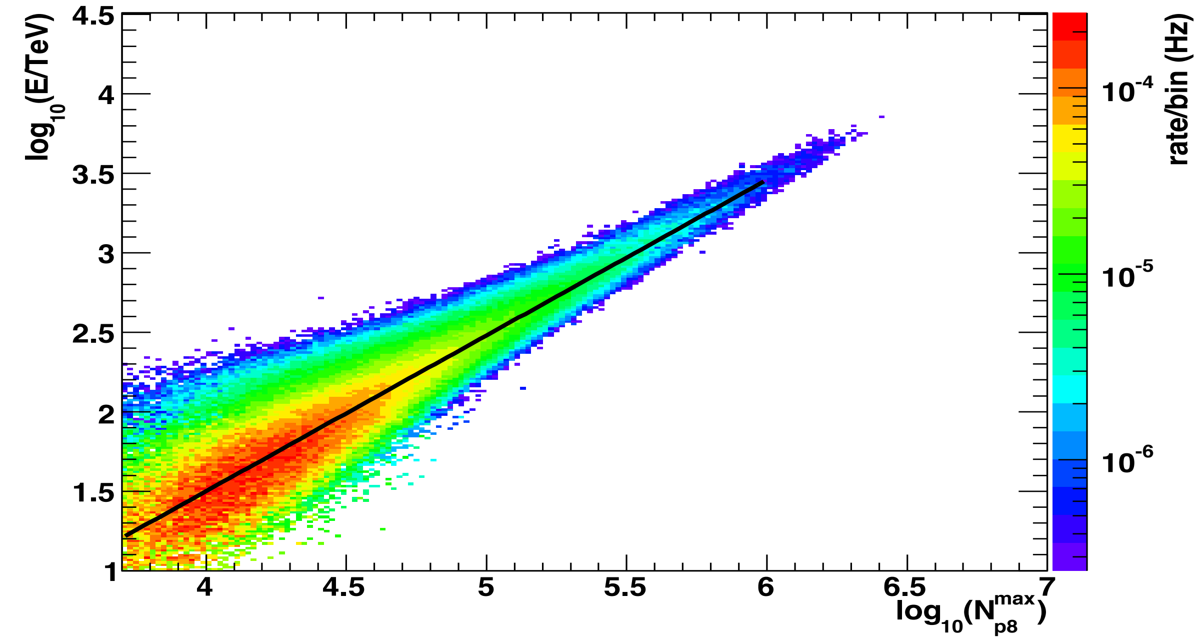

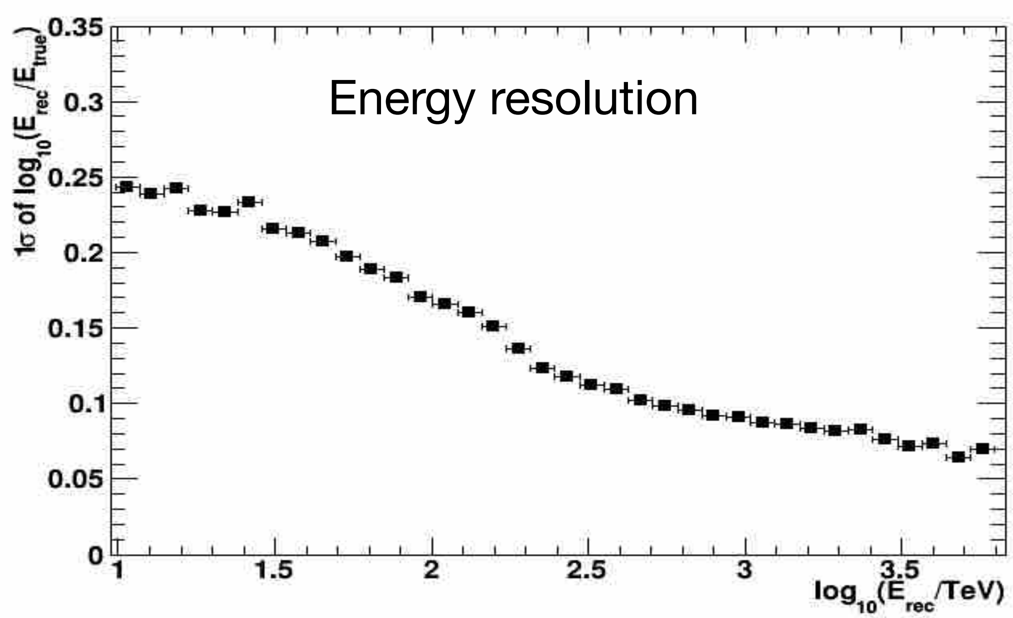

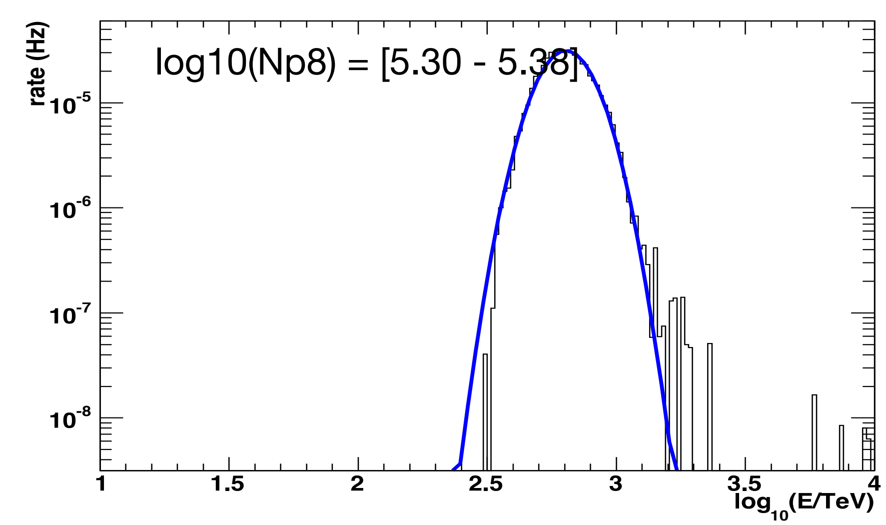

Lateral distribution

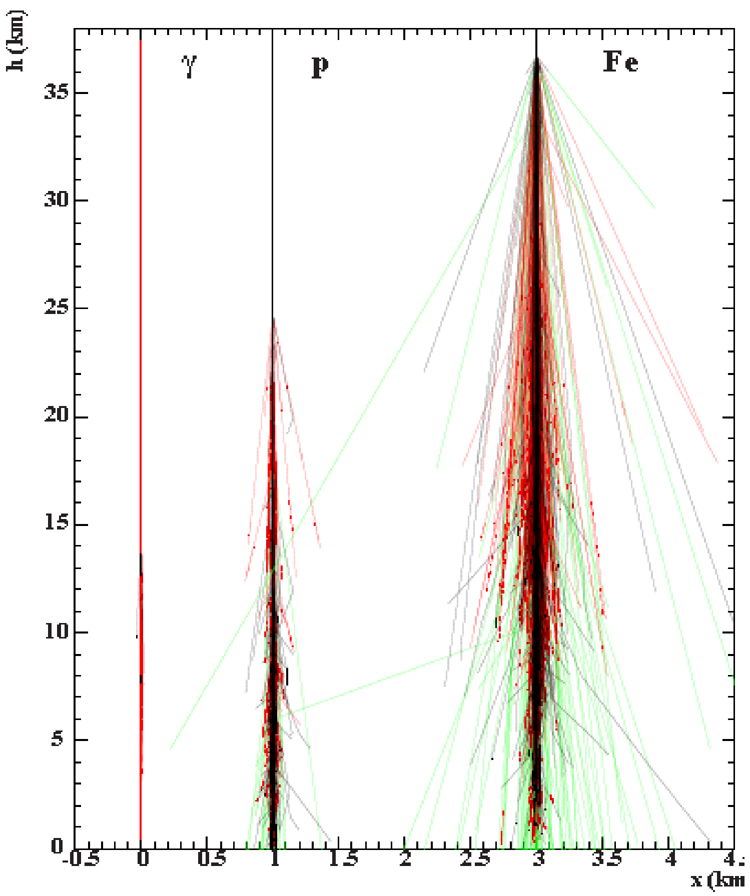

Fe showers develop higher in atmosphere than protons → Fe lateral distribution is slightly broader compared to p-showers

Increasing the mass A:

Larger deflection angles → flatter lateral distributions of secondary particles

J. Matthews, Astrop. Phys. 22 (2005) 387
J. Linsley, 15th ICRC, 12 (1977) 89.

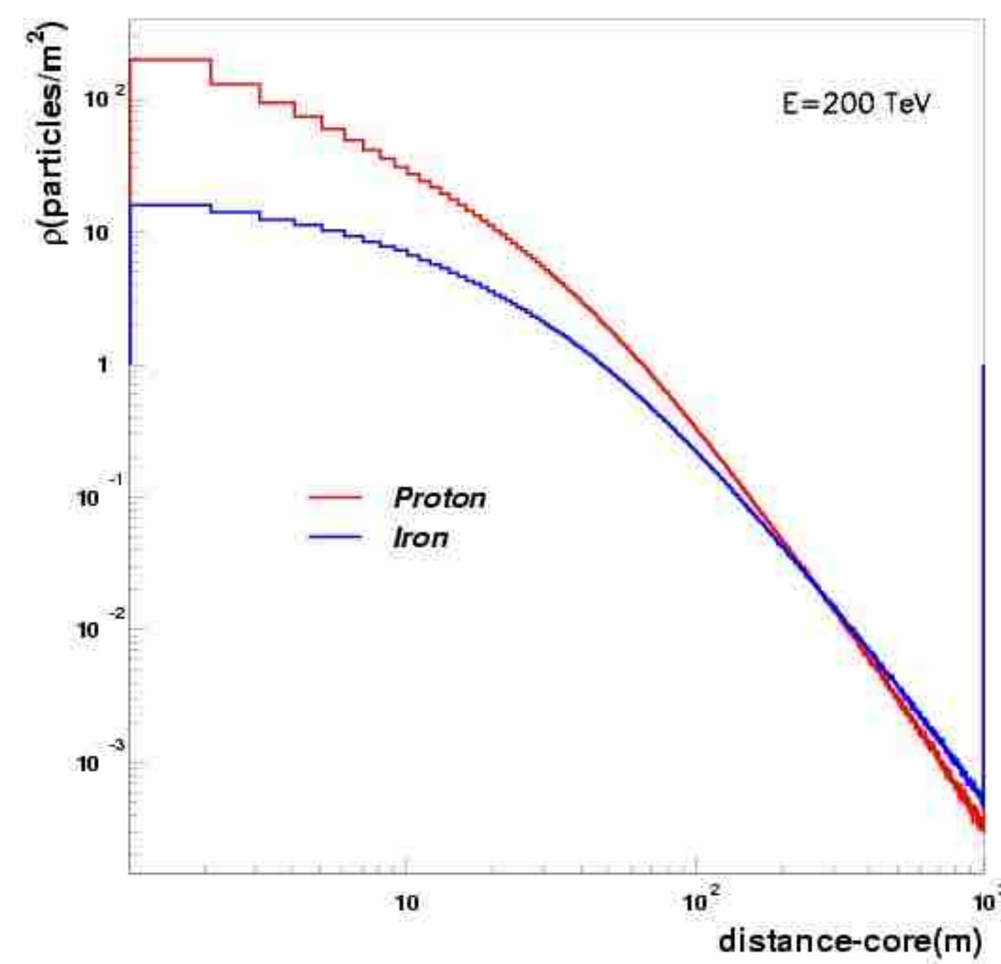

The showers can be classified in terms of the density ratio at two distances from the shower core

$$\rho(25\text{-}35\text{m}) / \rho(0\text{-}10\text{m})$$

The light-component spectrum (2.5 - 300 TeV)

Measurement of the light-component (p+He) CR spectrum in the energy region (2.5 – 300) TeV via a Bayesian unfolding procedure

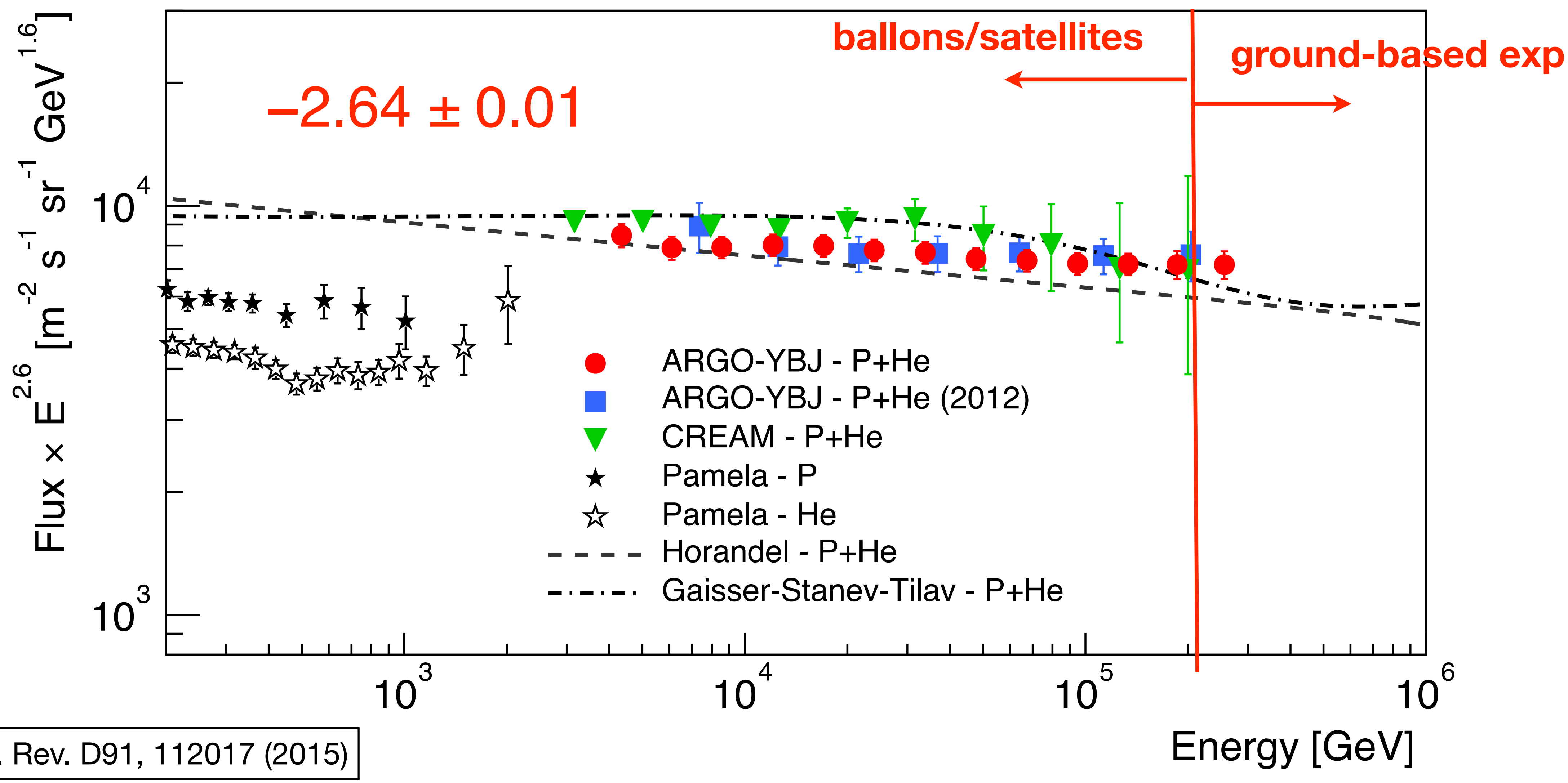

Phys. Rev. D91, 112017 (2015)

Direct and ground-based measurements overlap for a wide energy range thus making possible the cross-calibration of the experiments.

Stability of the CR flux measurement

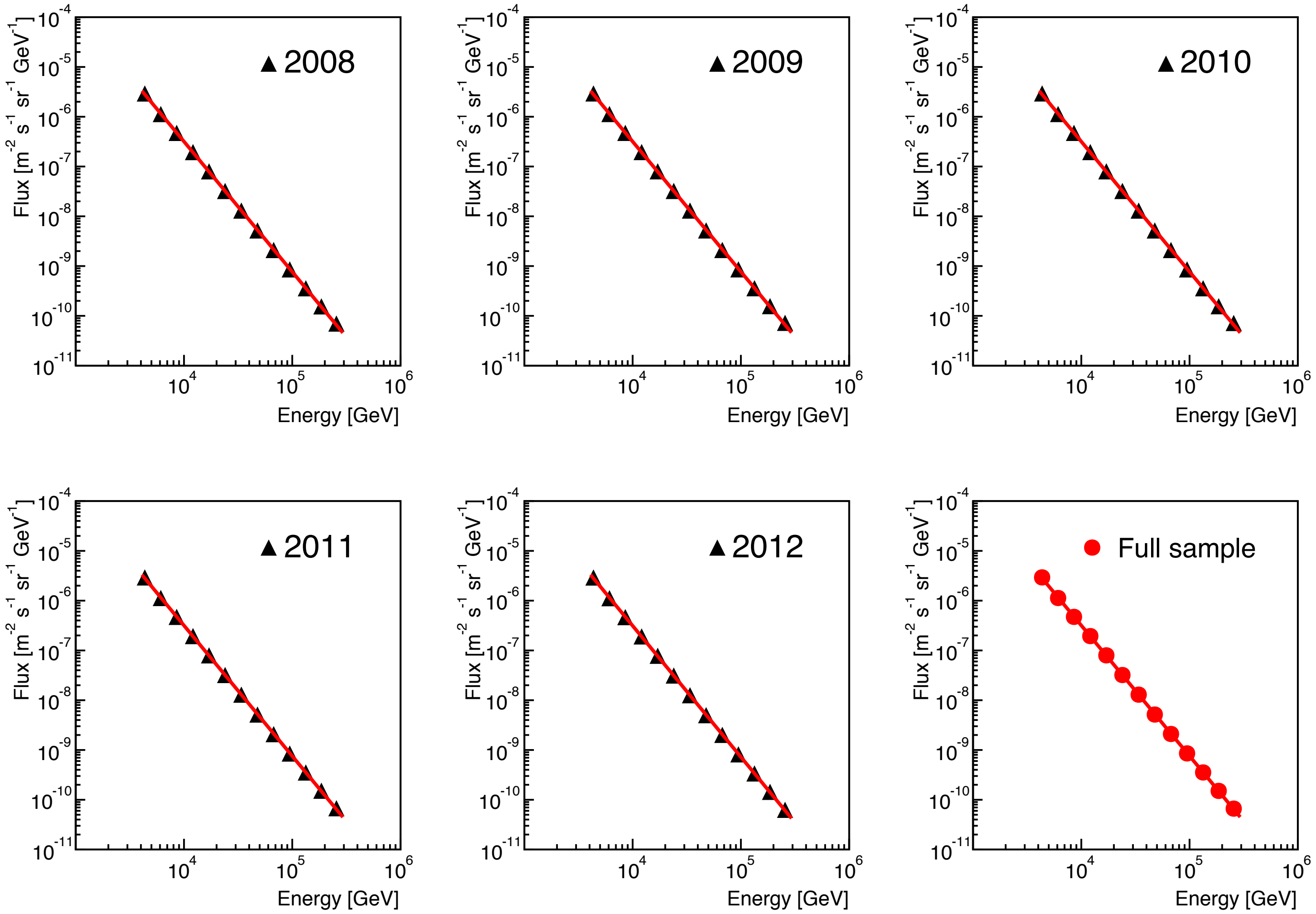

Phys. Rev. D91, 112017 (2015)

Year	Events	Gamma
2008*	7.5×10^{7}	2.61 ± 0.04
2008	5.57×10^{10}	2.63 ± 0.01
2009	5.65×10^{10}	2.63 ± 0.01
2010	5.56×10^{10}	2.63 ± 0.01
2011	5.64×10^{10}	2.64 ± 0.01
2012	5.69×10^{10}	2.65 ± 0.01
Full sample	2.81×10^{11}	2.64 ± 0.01

TABLE I. Proton plus helium flux measured at 5.0×10^{4} GeV.

Year	Flux $\pm$ tot. error [m^{-2} s^{-1} sr^{-1} GeV^{-1}]
2008	$(4.53 \pm 0.28) \times 10^{-9}$
2009	$(4.54 \pm 0.28) \times 10^{-9}$
2010	$(4.54 \pm 0.28) \times 10^{-9}$
2011	$(4.50 \pm 0.27) \times 10^{-9}$
2012	$(4.36 \pm 0.27) \times 10^{-9}$

p+He flux difference at 5% level

Hadronic Interaction Models

Corsika v 6980 + Fluka + EGS4
- QGSJET II.03
- SIBYLL 2.1
- EPOS 1.99

Phys. Rev. D91, 112017 (2015)

Not muons but lateral distribution ➜ topology

Ratio beetwen multiplicity distributions obtained with different models

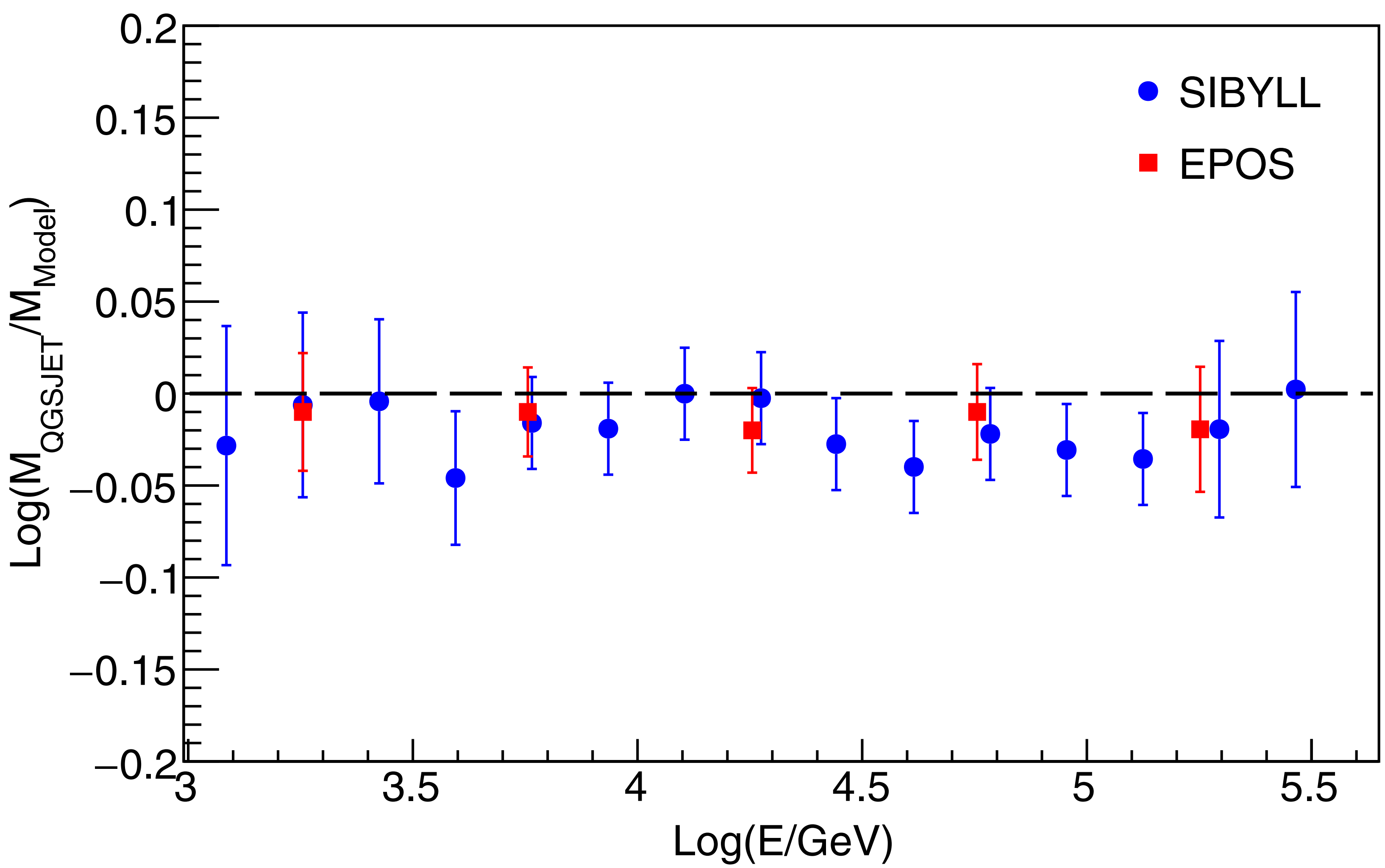

The light-component spectrum (0.3 - 5 PeV)

The high segmentation of the read-out allows to access the LDF down to the shower core.
Discrimination Light/Heavy based on the measurement of the LDF at different distances from the core

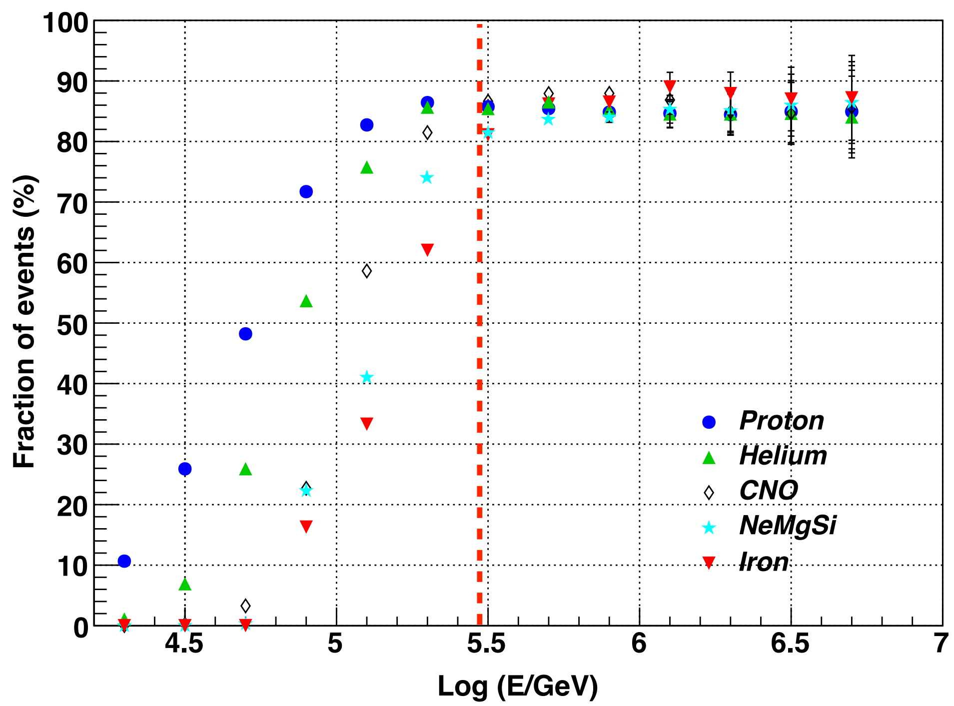

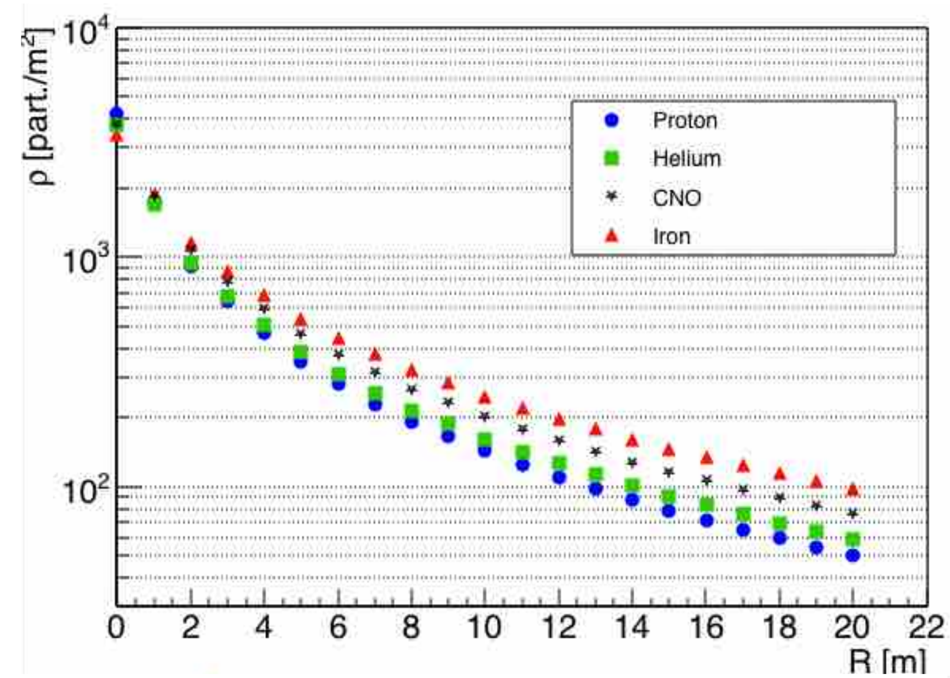

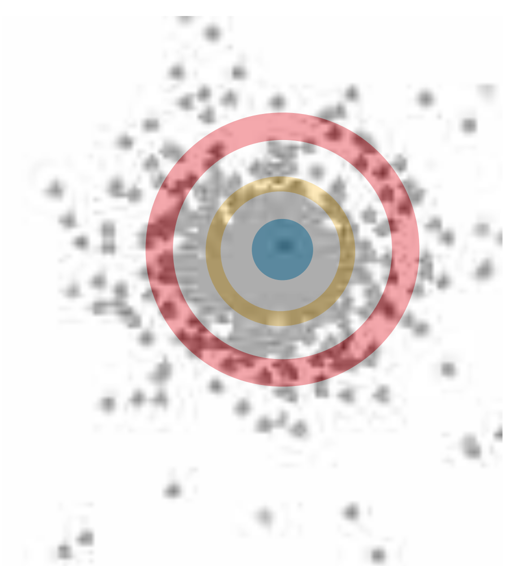

$$\beta_5 = \rho_5/\rho_0$$

$$\beta_{10} = \rho_{10}/\rho_0$$

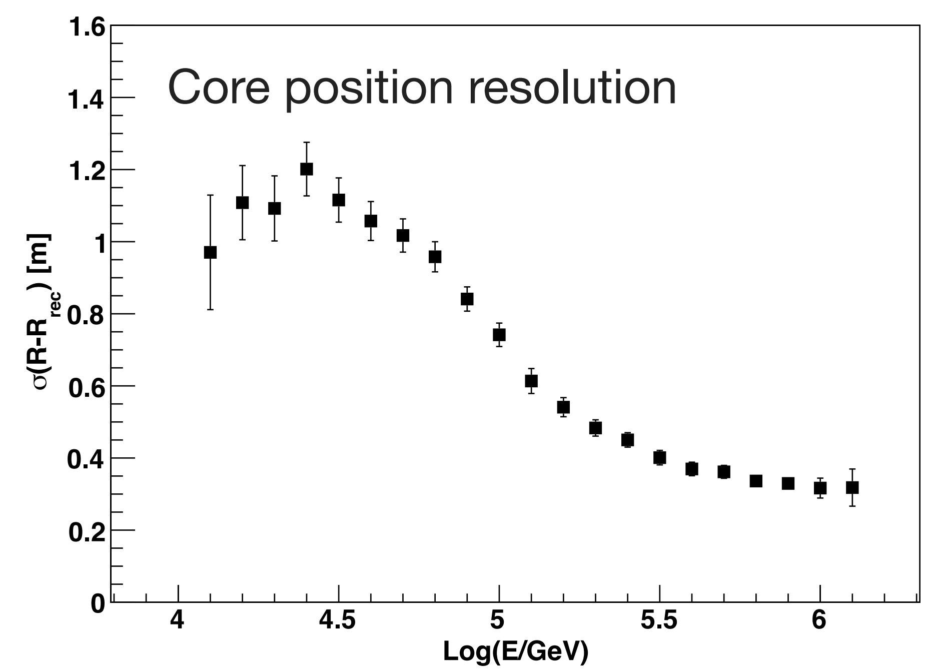

Light/Heavy discrimination

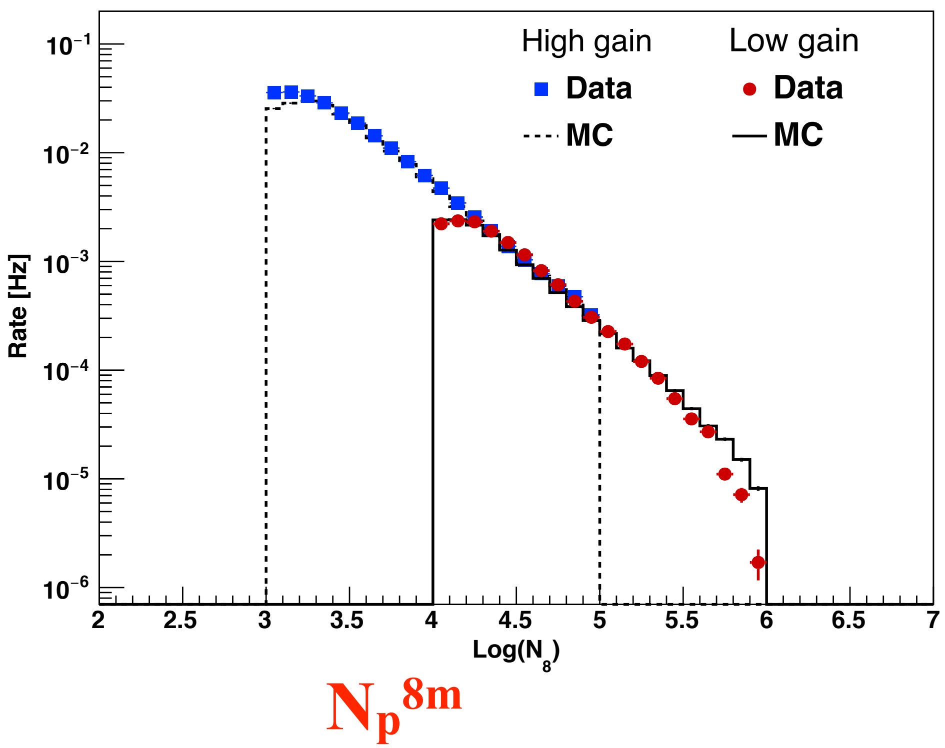

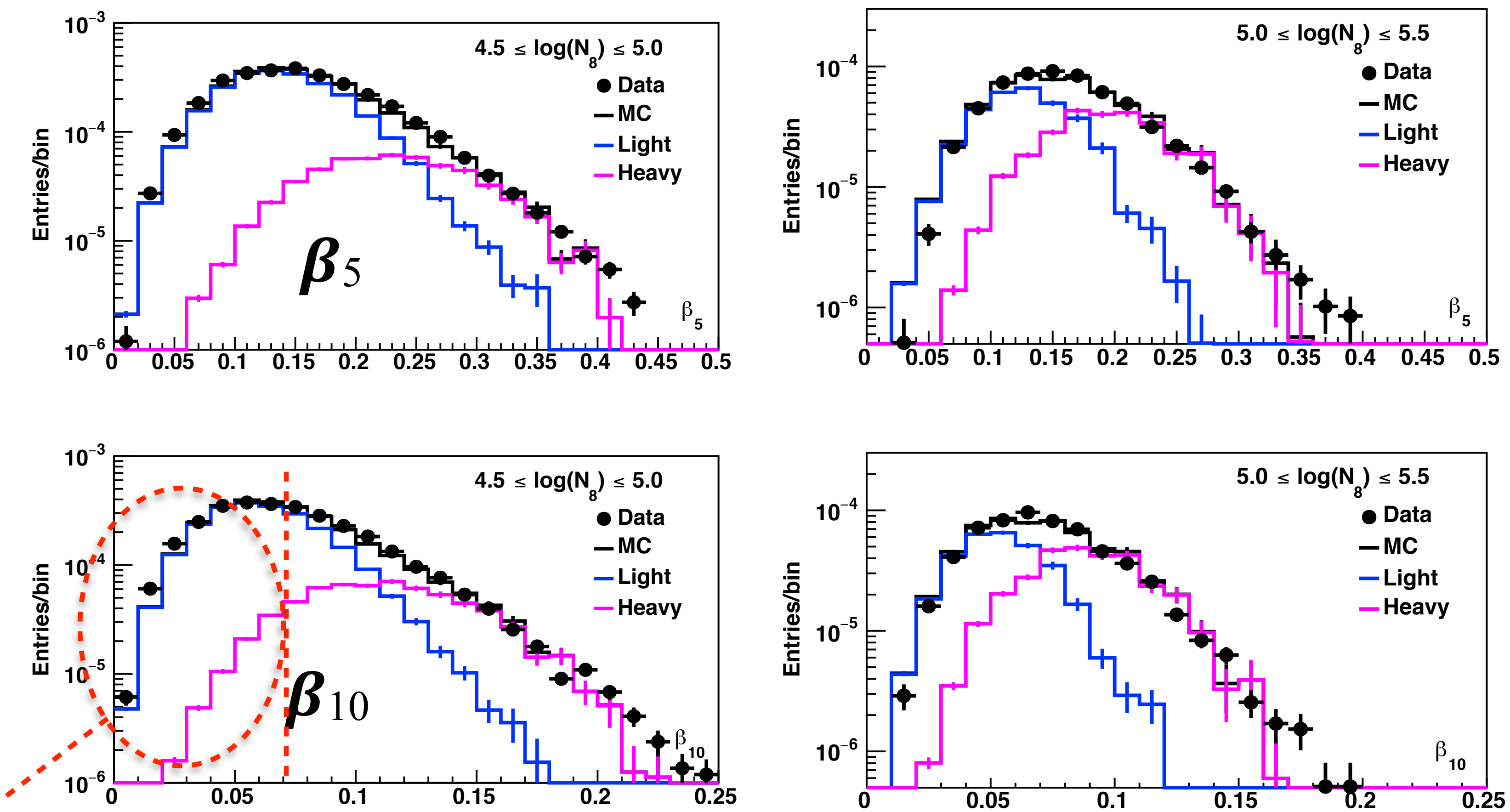

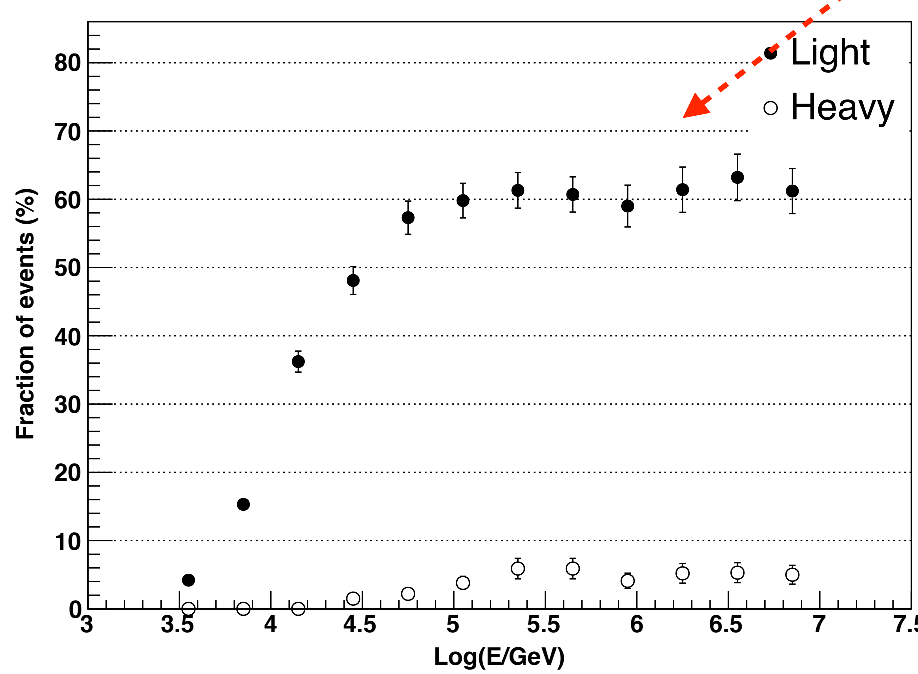

Fraction of events in the Light-selected sample only:
above ≈100 TeV ≈60% of all Light and ≈5% of all Heavy are selected

Wide Field of View Cherenkov Telescopes

One of the main component of LHAASO is the array of Wide Field of View Cherenkov Telescopes WFCTA.

The goal: measurement of the CR energy spectrum and composition in the range 10^{13} - 10^{18} eV

Why Cherenkov telescopes at high altitude ?

High altitude

(1) Measure EASs near maximum development points to reduce fluctuations.

(2) Use an unbiased trigger threshold for heavy components of primaries.

(3) Low energy theshold and wide energy range ($10^{13} \rightarrow 10^{18}$ eV).

Cherenkov signal

(4) Measure the electromagnetic component which is less dependent on hadronic interaction models than the muon component.

(5) Good separation capability between the different masses.

(6) Good energy resolution (<20%).

Chin. Phys. C 38, 045001 (2014)
Phys. Rev. D 92, 092005 (2015)

ARGO-YBJ + WFCTA

A prototype of the future LHAASO telescopes has been operated in combination with ARGO-YBJ

- 4.7 m^2 spherical mirror composed of 20 hexagon-shaped segments
- 256 PMTs (16 × 16 array)
- 40 mm Photonis hexagonal PMTs (XP3062/FL)
- pixel size 1°
- FOV: 14° × 14°
- Elevation angle: 60°

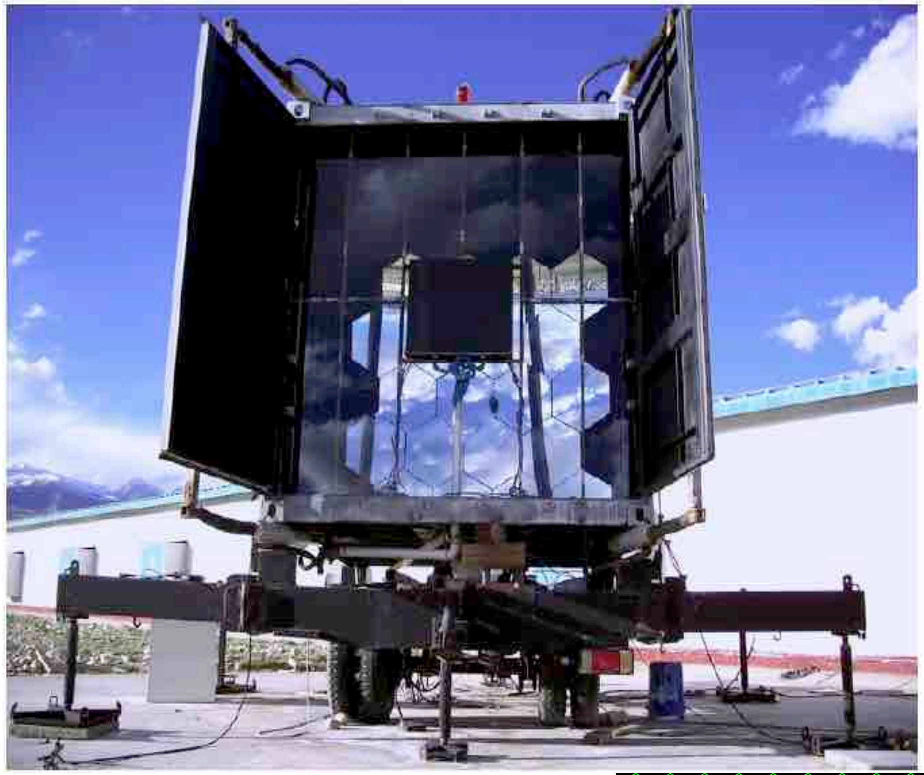

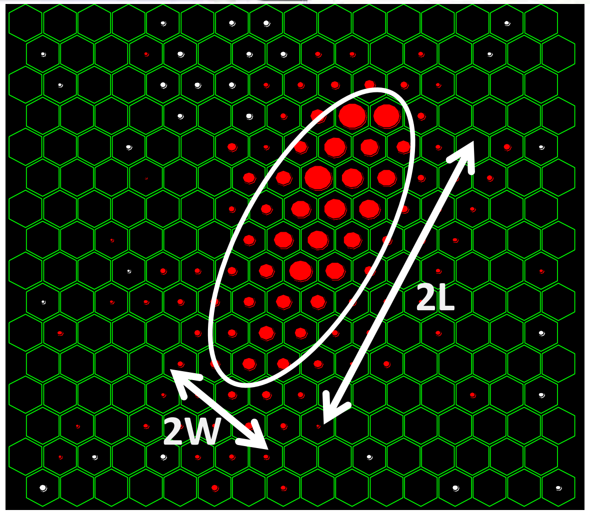

❖ *ARGO-YBJ:* core reconstruction & lateral distribution in the core region

→ mass sensitive

❖ *Cherenkov telescope:* longitudinal information

Hillas parameters → mass sensitive

- angular resolution: 0.2°
- shower core position resolution: 2 m

Phys. Rev. D 92, 092005 (2015)

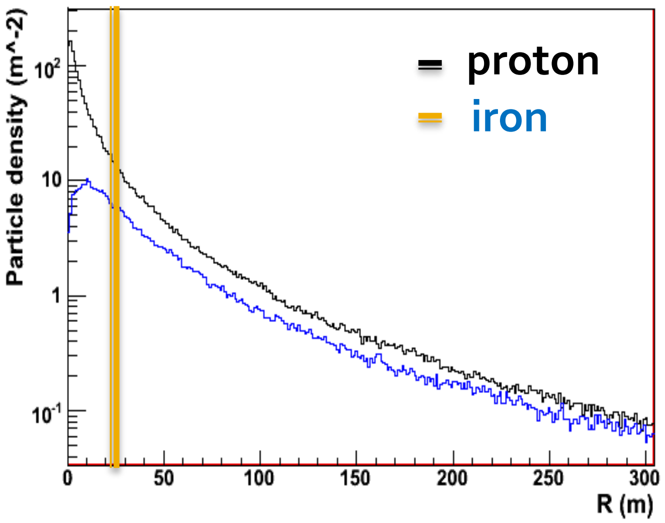

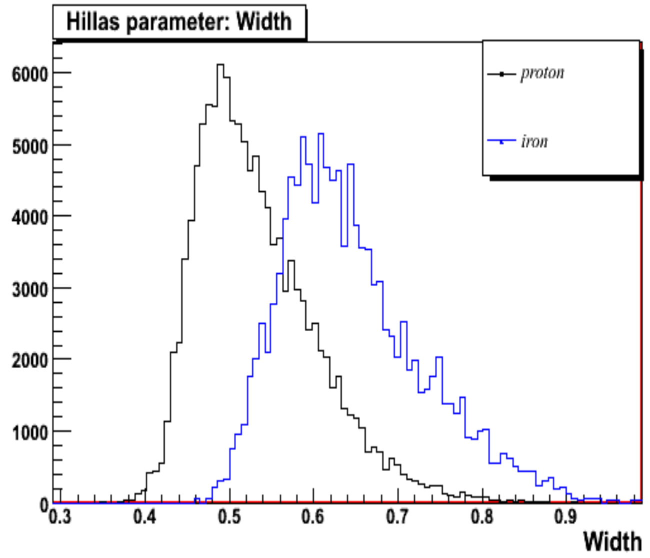

Light component (p + He) selection - (1)

According to MC, the largest number of particles N_{max} recorded by a RPC in an given shower is a useful parameter to measure the particle density in the shower core region, i.e. within 3 m from the core position.

N_{max} is a parameter useful to select different primary masses

$N_{max} \propto E_{rec}^{1.44}$, where E_{rec} is the shower primary energy reconstructed using the Cherenkov telescope.

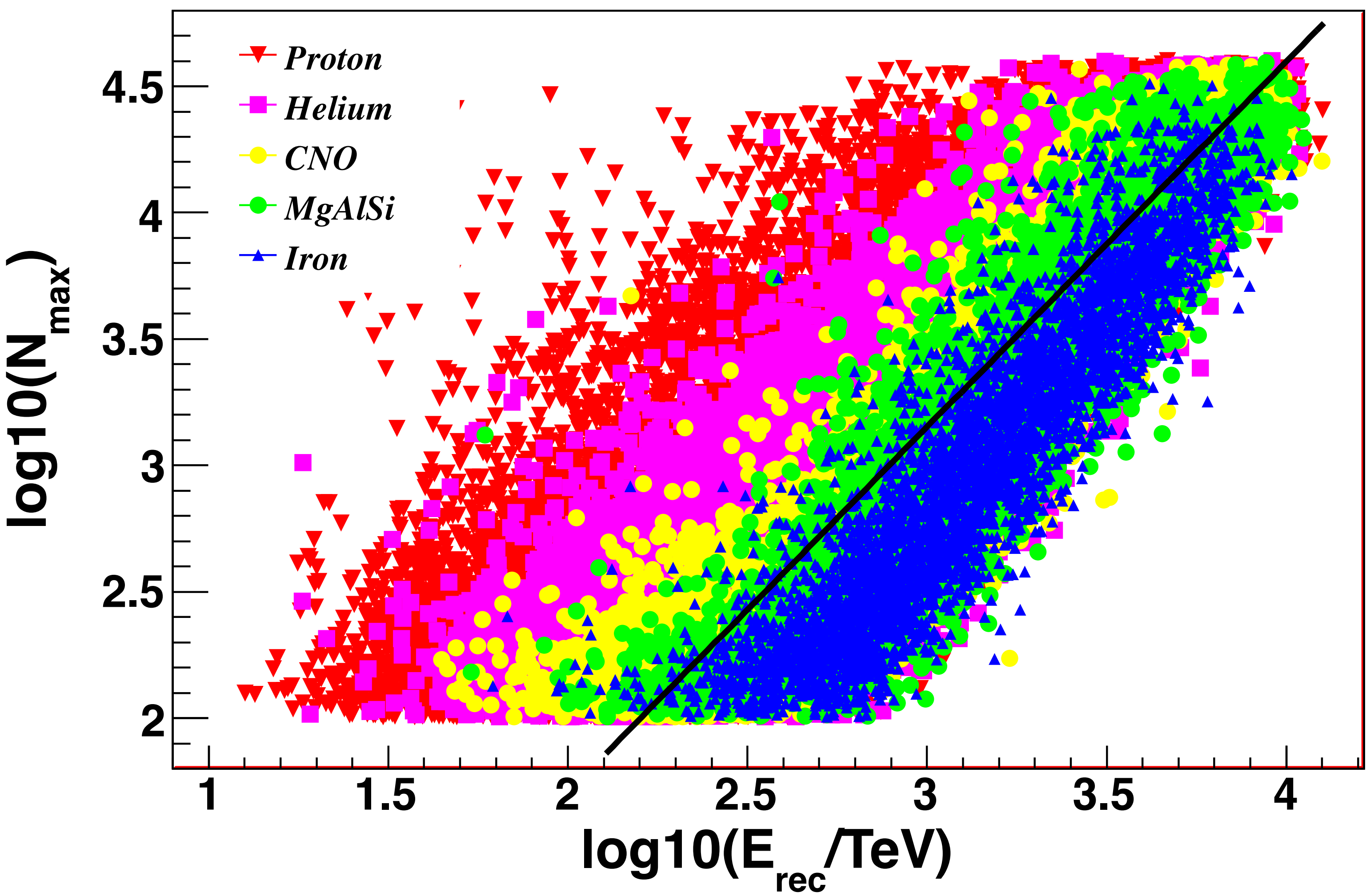

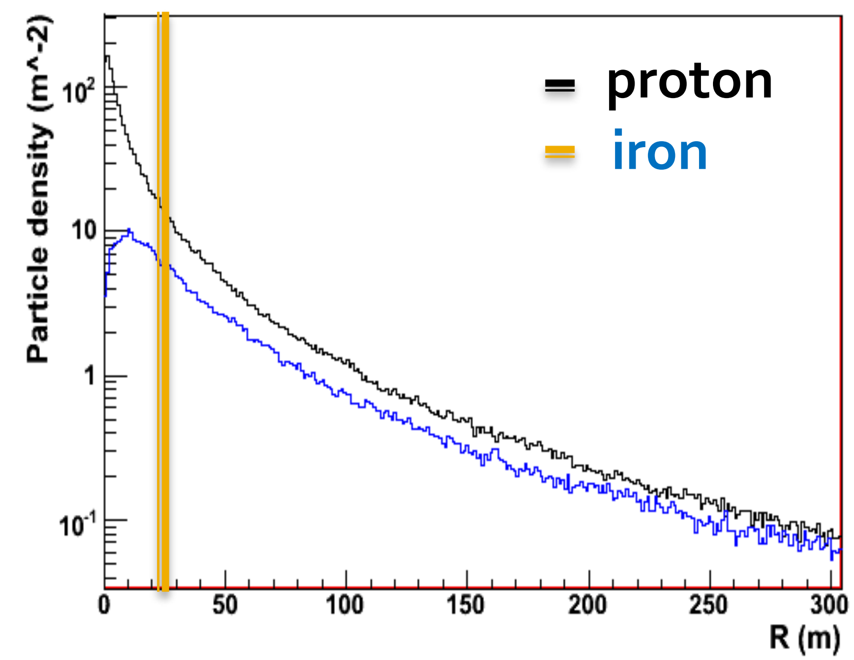

We can define a new parameter
to reduce the energy dependence

$$p_L = log_{10}(N_{max}) - 1.44 \cdot log_{10}(E_{rec}/TeV)$$

Chin. Phys. C 38, 045001 (2014)

Light component (p + He) selection - (2)

According to MC, the ratio between the length and the width (L/W) of the Cherenkov image is another good estimator of the primary mass.

Elongation of the shower image proportional to impact parameter L/W ~ 0.09 (R_p / 10m).

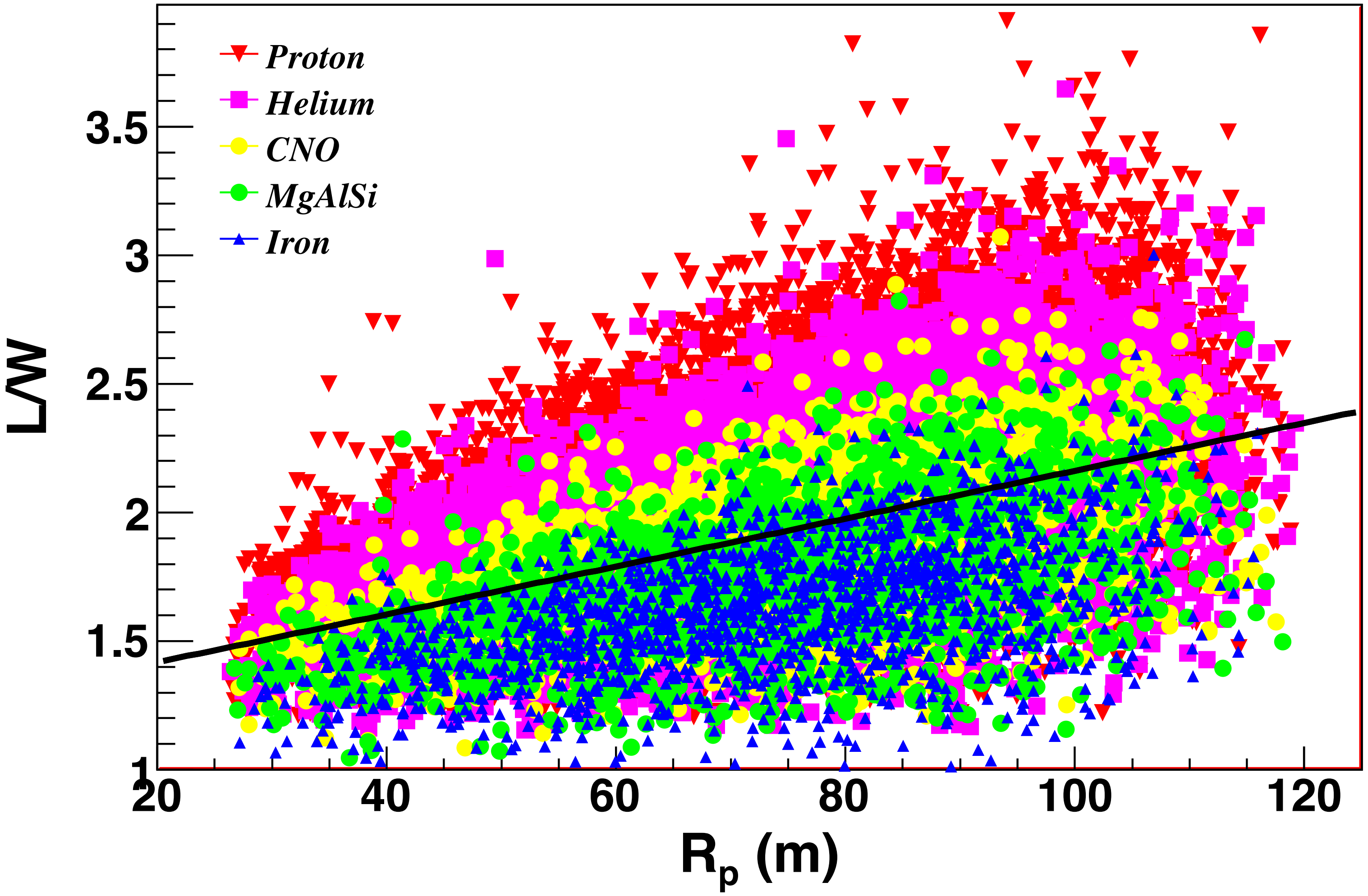

Typical Cherenkov footprint

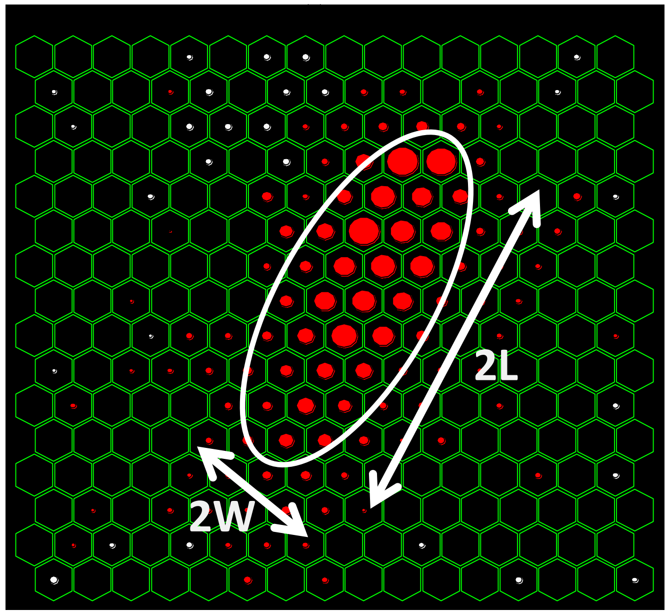

The shower impact parameter R_p is calculated with 2 m resolution exploiting the ARGO-YBJ characteristics.

We define a new parameter to reduce the R_p and energy dependence

$$p_C = L/W - 0.0091(R_p/1\,m) - 0.14 \cdot log_{10}(E_{rec}/TeV)$$

Chin. Phys. C 38, 045001 (2014)

Light component (p + He) selection

- Contamination of heavier component ≈10 %
- Energy resolution: ~25% constant with energy
- Uncertainty : ~25% on flux

$$p_L = log_{10}(N_{max}) - 1.44 \cdot log_{10}(E_{rec}/TeV)$$

$$p_C = L/W - 0.0091(R_p/1\,m) - 0.14 \cdot log_{10}(E_{rec}/TeV)$$

Events for which $p_L \leq -4.53$ and $p_C \leq 0.78$ are rejected

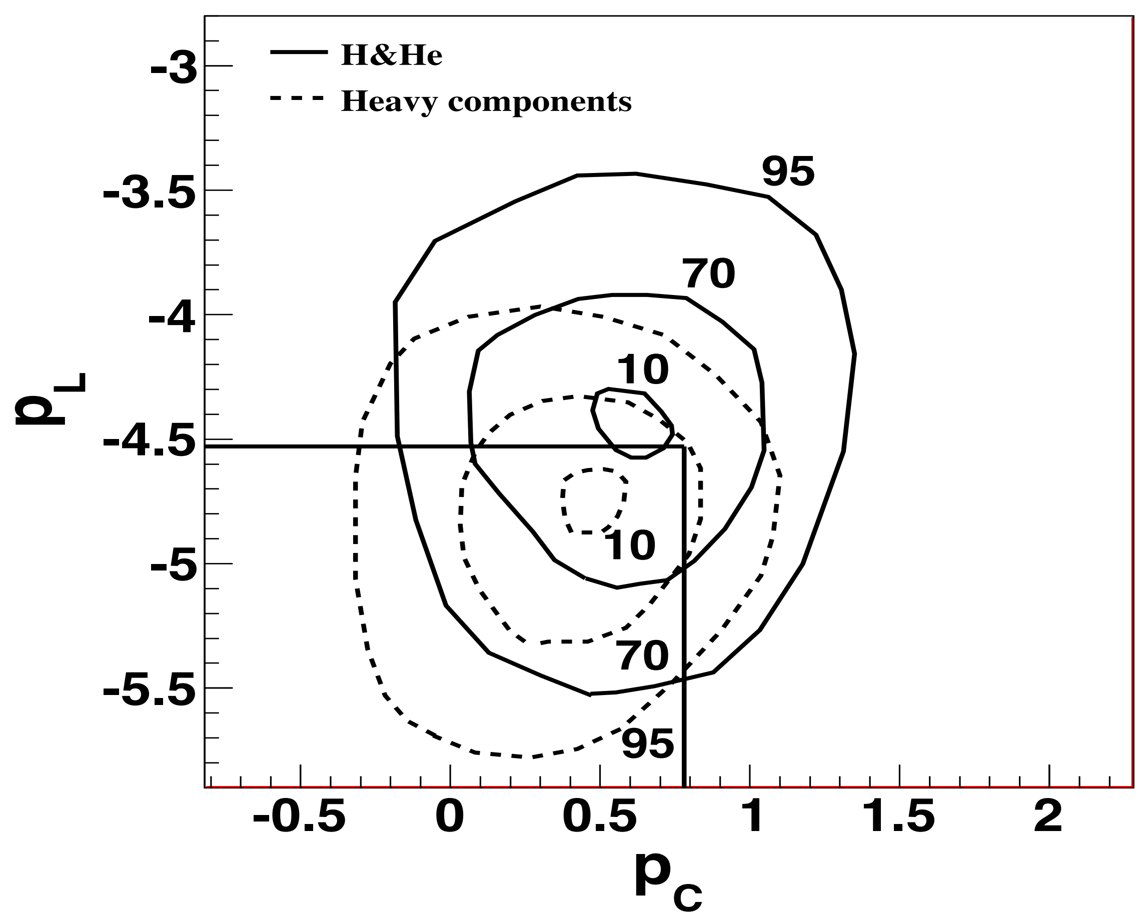

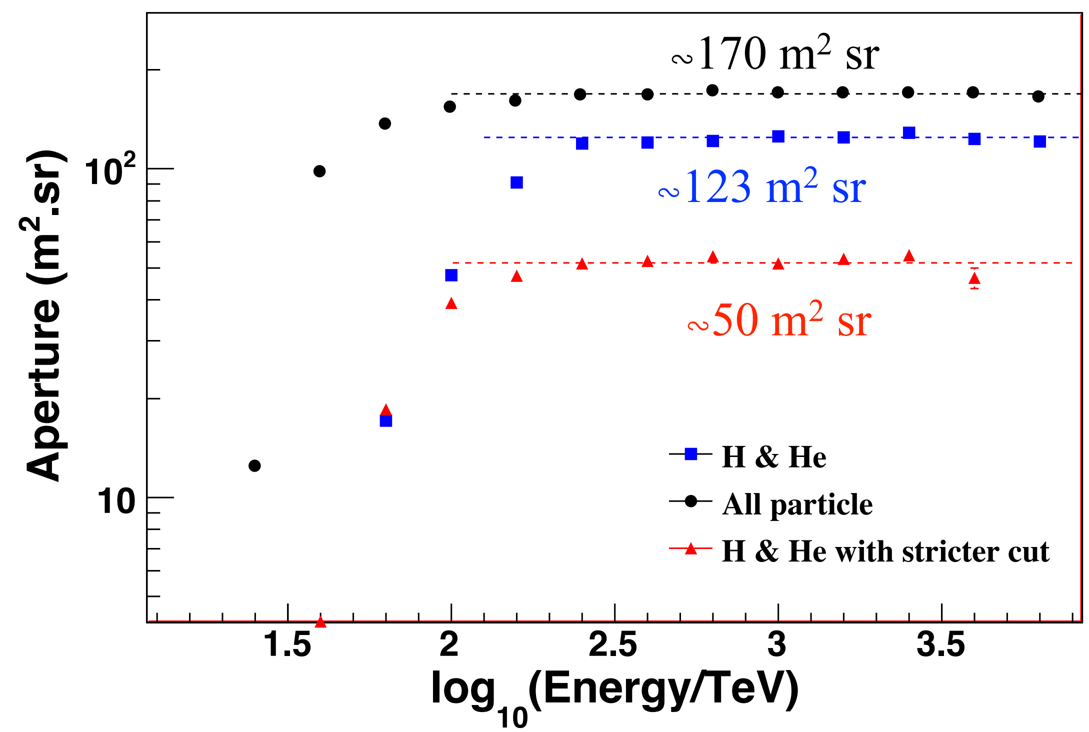

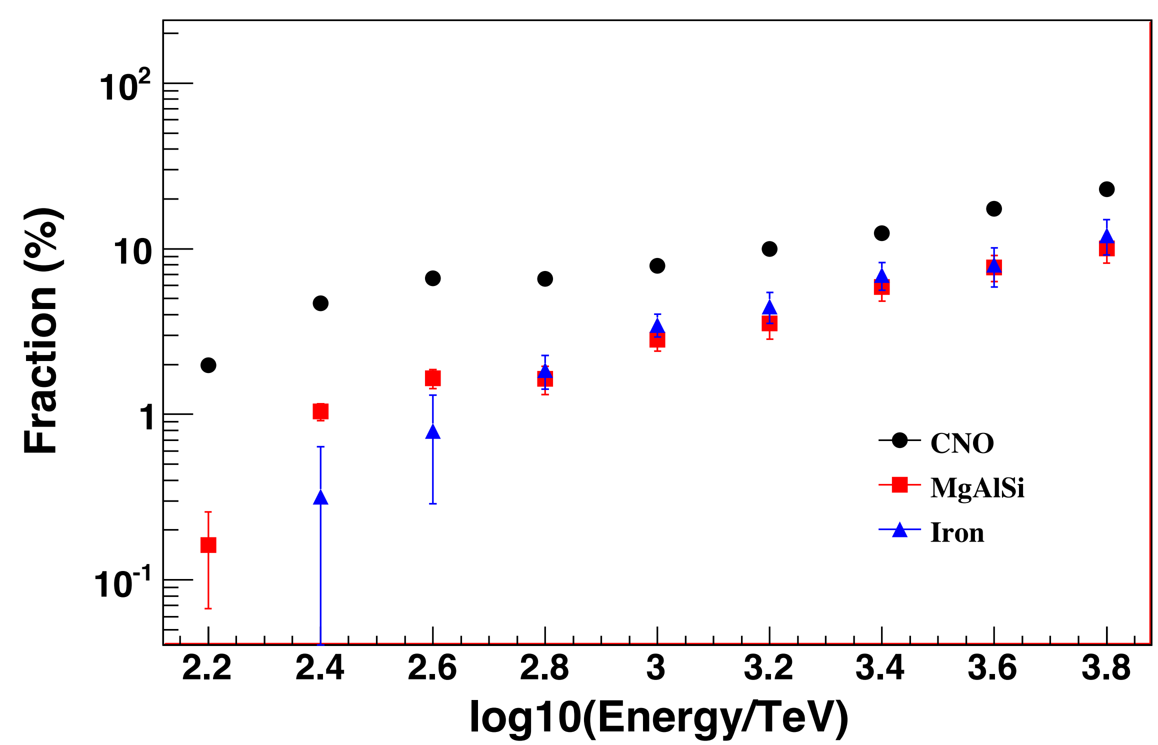

Light component spectrum (3 TeV - 5 PeV) by ARGO-YBJ

ARGO-YBJ reports evidence for a proton knee starting at about 700 TeV

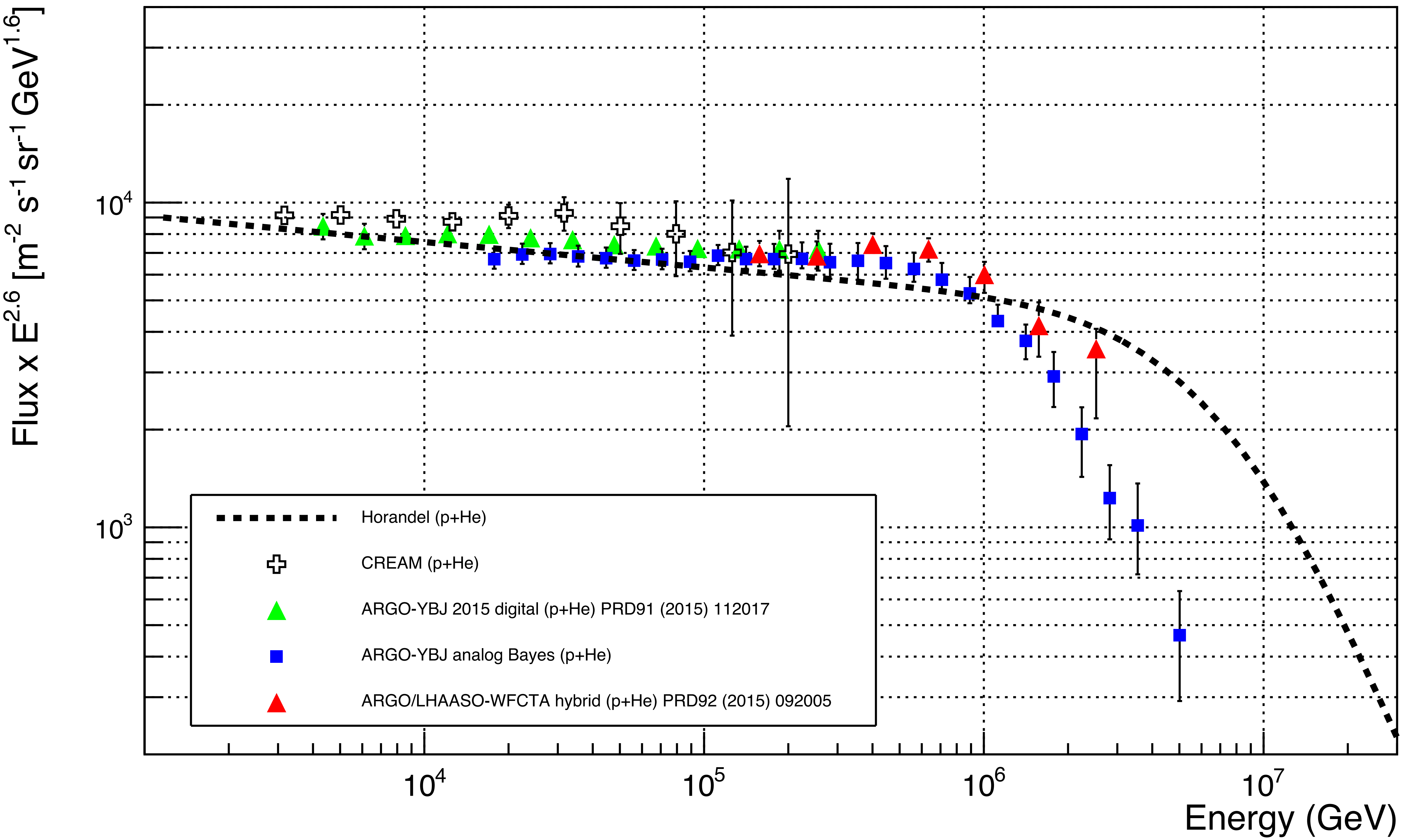

The overall picture

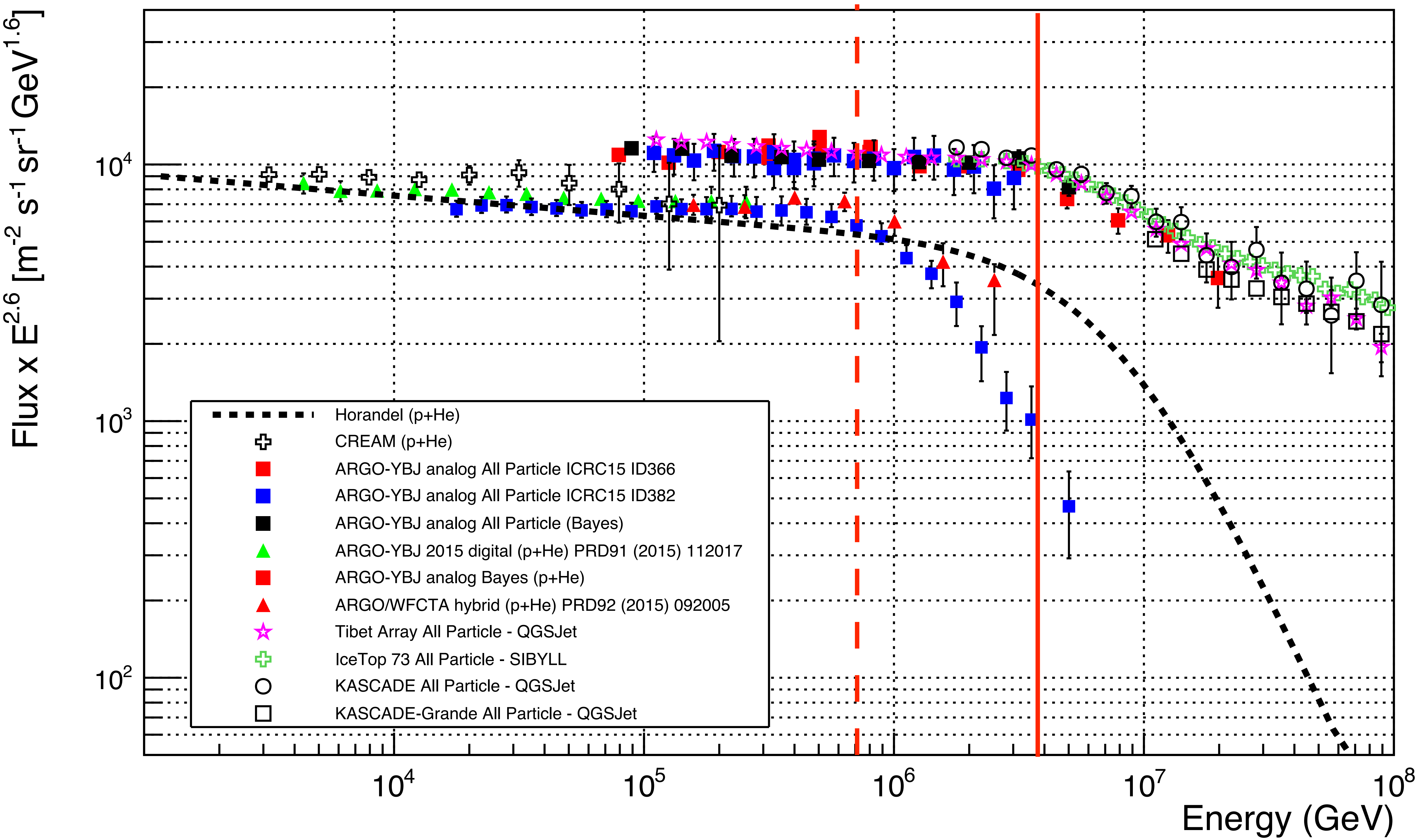

A comment

Is not surprising that decades after the experimental discovery of the knee experimental results are still conflicting and there are still uncertainties on its interpretation.

This is the first time that we are actually probing this region with direct measurements on one side, and *the first time that we are studying EAS very close to the shower maximum (high altitude), and its core, with full coverage arrays.*

The proton spectrum is distinctly softer than that of Helium (and possibly other heavy elements) at all energies (Pamela,CREAM, AMS02).

"The harder He spectrum has the interesting consequence that by the time one gets to the knee energies it dominates hydrogen in the all-particle energy spectrum (though not in energy per nucleon or rigidity).

Thus the knee in the all-particle spectrum at 3×10^{15} eV is actually predominantly a Helium and CNO knee, and it is possible that the proton spectrum cuts off significantly before this as has been suggested by the Tibet ARGO-YBJ experiment".

Drury arXiv:1708.08858

Cosmic Ray diffusive propagation and anisotropy

CR anisotropy as fingerprint for their origin and propagation

Distribution of nearby SNRs in the Galaxy

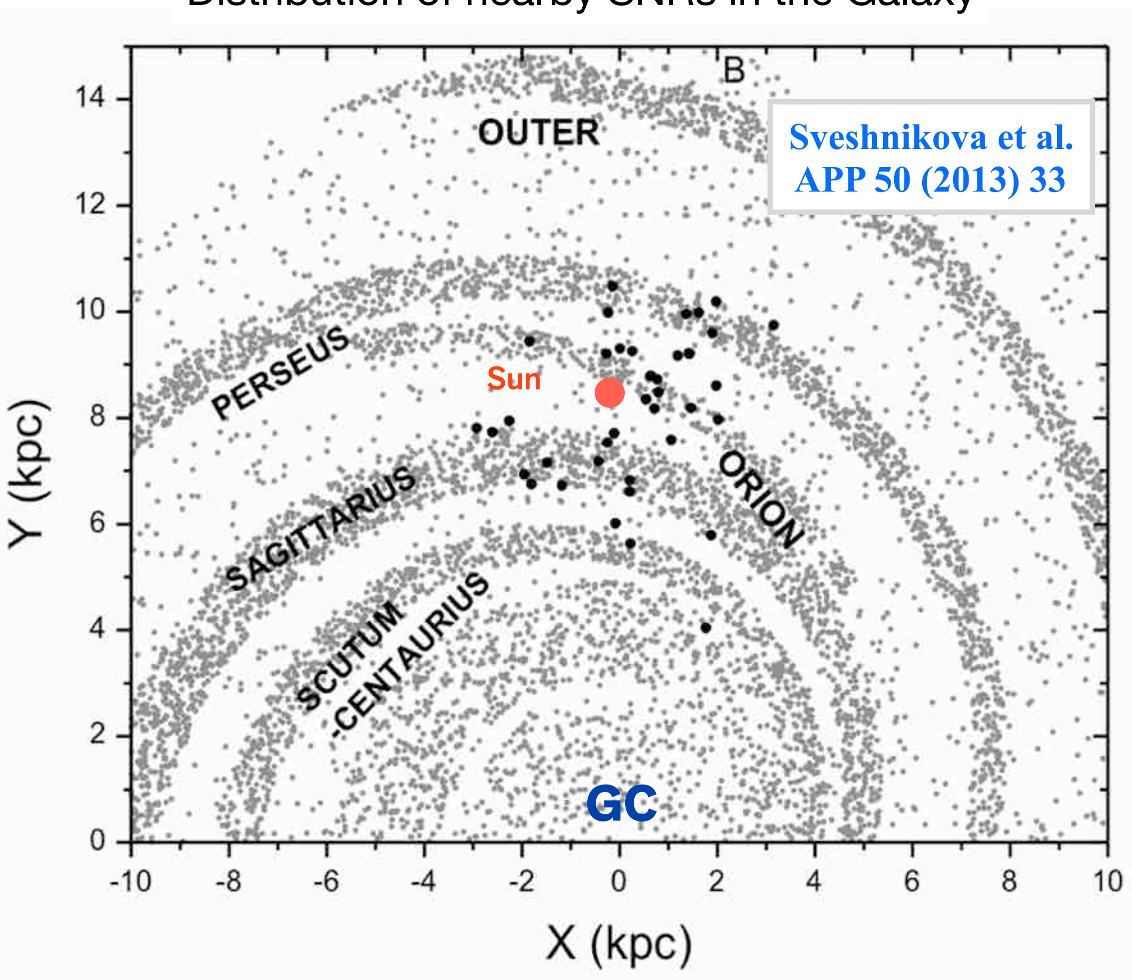

Galactic Cosmic Rays

- Accelerated in SNRs
- Propagate diffusively

Consequences for anisotropy

- CR density gradients are visible as anisotropy
- Anisotropy amplitude $\lesssim 10^{-2}$
- Amplitude increases with energy
- Dipole shape
- Phase pointing towards the most significant sources

A weak anisotropy is expected from the diffusion and/or drift of GCRs in GMF.

Generally speaking, the dipole component of the anisotropy is believed to be a tracer of the CR source distribution, with the largest contribution from the nearest ones.

M. Ahlers & P. Mertsch, arXiv:1612.01873

Large scale anisotropy by ARGO-YBJ

2 years data: 2008 - 2009, during minimum of solar activity

ApJ 809 (2015) 90

E ≈1 TeV, 3.6×10^{10} events in the declination band -10° < δ < +70°

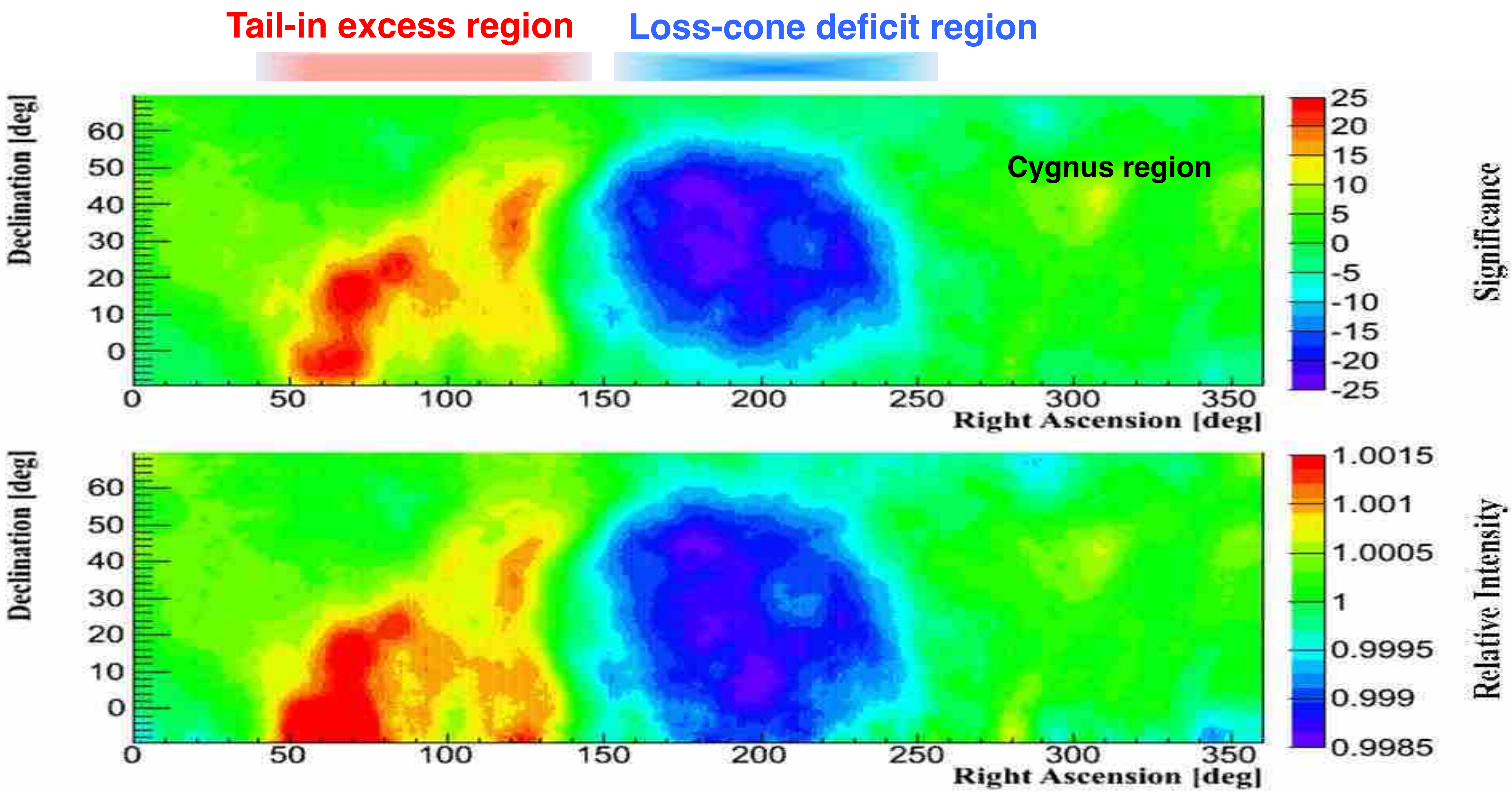

What this observation tell us ?

- *“Tail in”* and *“loss cone”* regions are observed with high stat. significance (> 20 s.d.)
- Anisotropy regions observed in the Cygnus region (13 s.d. level)
- R.A. profile of anisotropy can be described with 2 harmonics

$$I = 1 + A_1 cos[2\pi(x-\phi_1)/360] + A_2 cos[2\pi(x-\phi_2)/180]$$

$A_1 = 6.8\times10^{-4}$, $\Phi_1 = 39.1°$
$A_2 = 4.9\times10^{-4}$, $\Phi_2 = 100.9°$

- The LSA cannot be described by a simple dipole.
- Data rule out the hypotesis of the sidereal Compton-Getting effect (orbital motion of the solar system aroud the Galactic Center) be the dominant anisotropy component.

→ CRs corotate with GMF

ApJ 809 (2015) 90

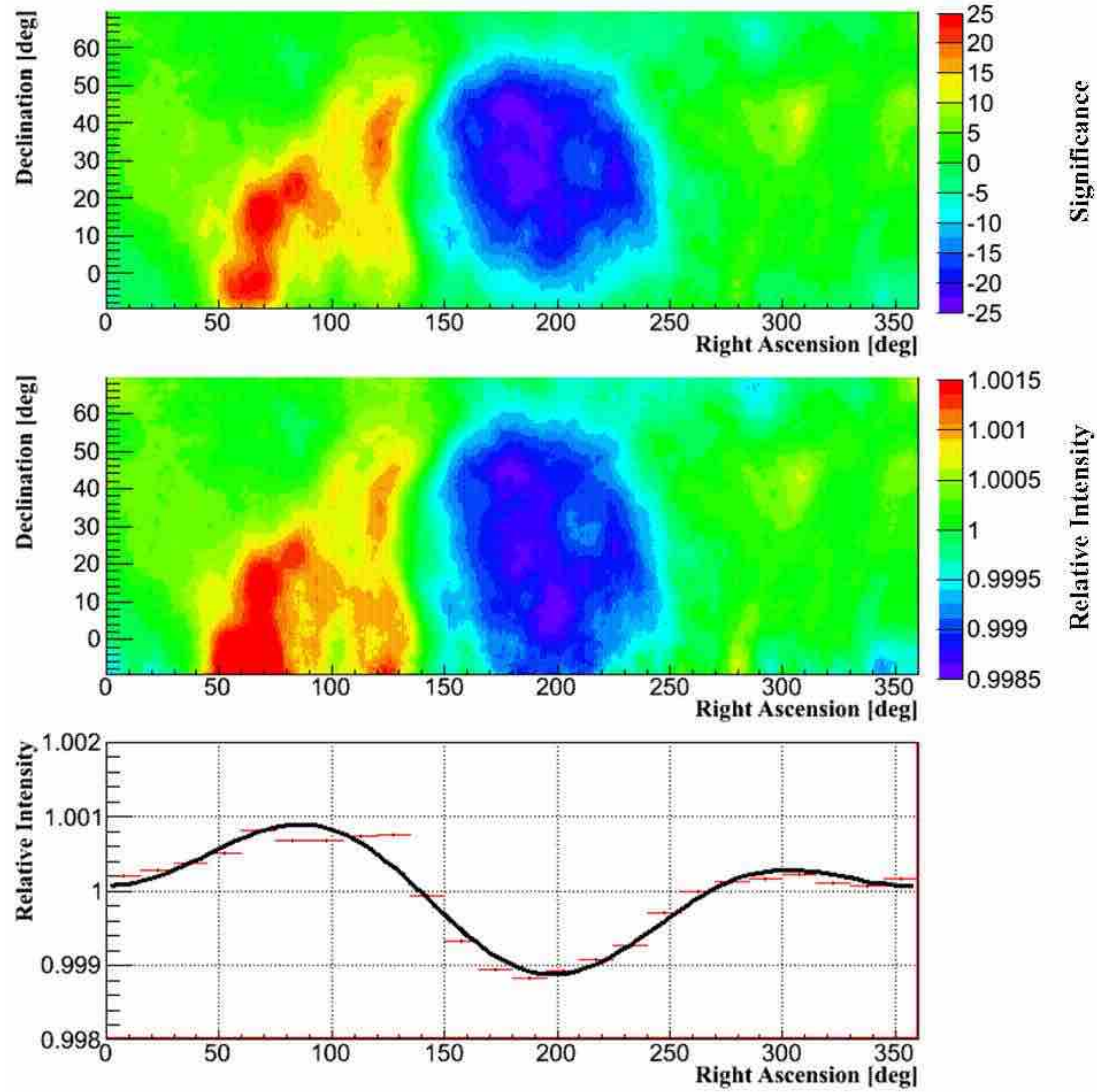

Galactic CG expectations:

$A_{CG} = 3.5\times10^{-3}$, much larger than observations
maximum in the direction of the Galactic Center (R.A.=315° and δ=0°)
minimum at R.A.=135° and δ=0°

Anisotropy vs energy

First measurement with an EAS array in an energy region so far investigated only by underground muon detectors.

Structures with complex morphologies are visible in all the maps, changing shape with energy.

The tail-in broad structure appears to dissolve to smaller angular scale spots with increasing energy.

ApJ 809 (2015) 90

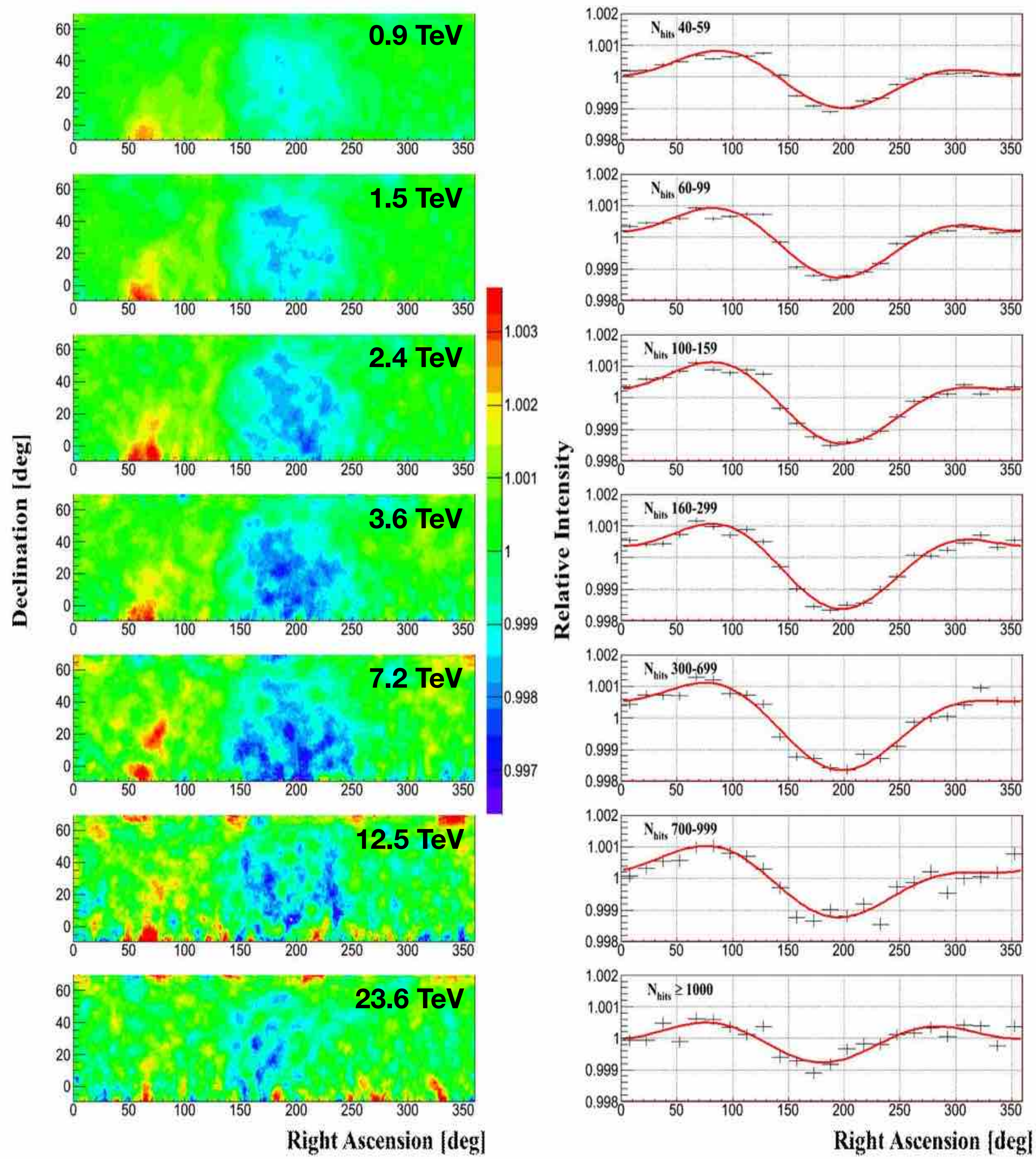

High energies (>100 TeV) with ARGO—YBJ

At 185 TeV dramatic change of anisotropy !

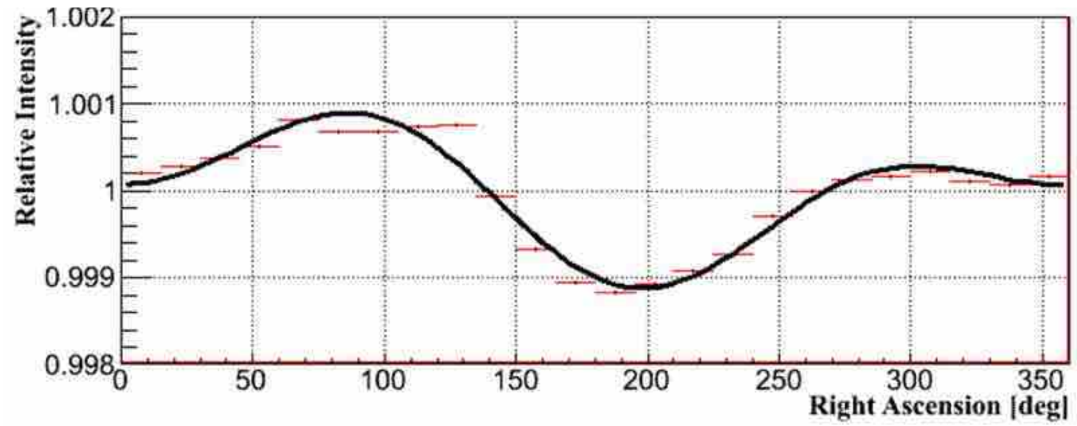

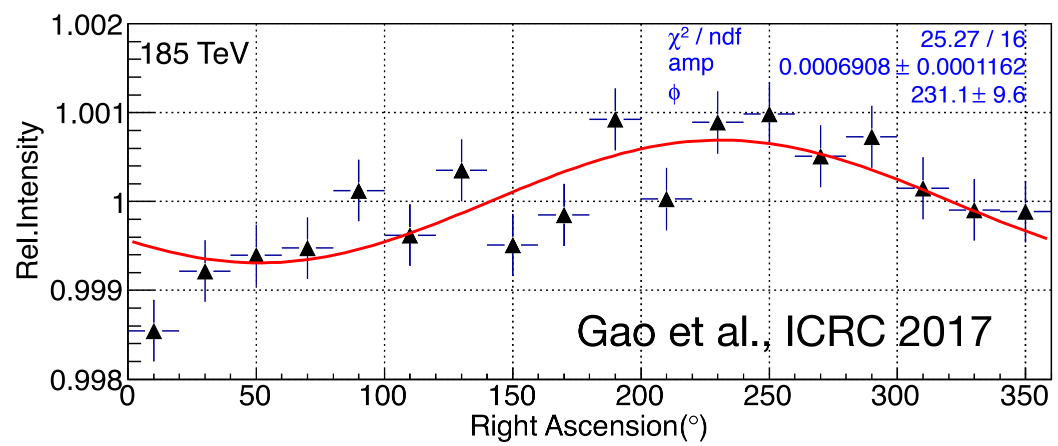

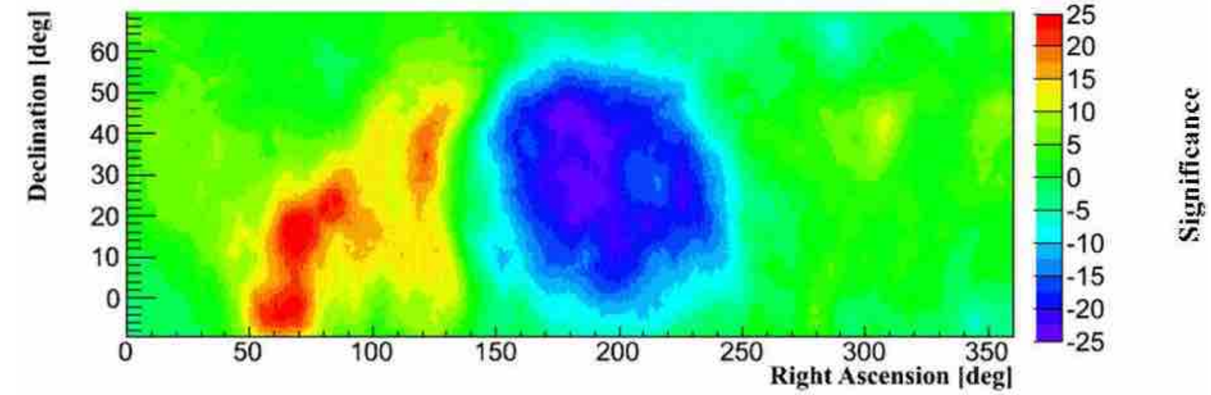

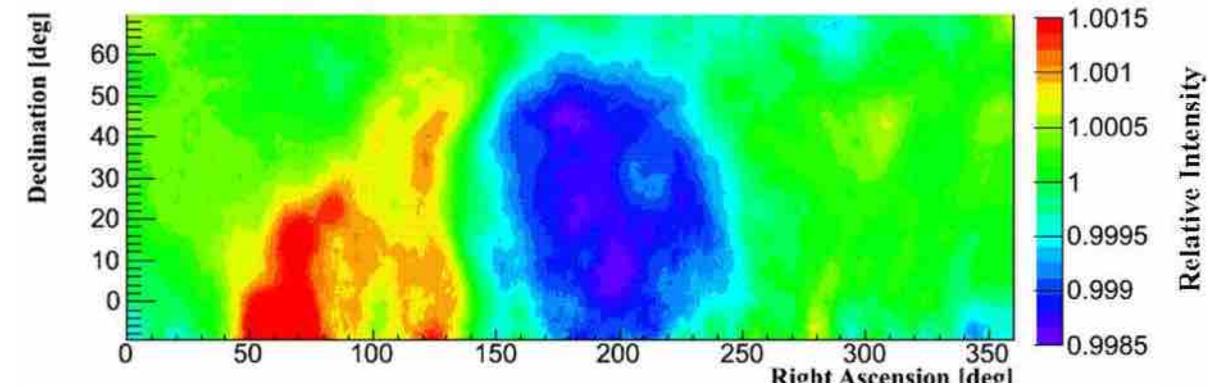

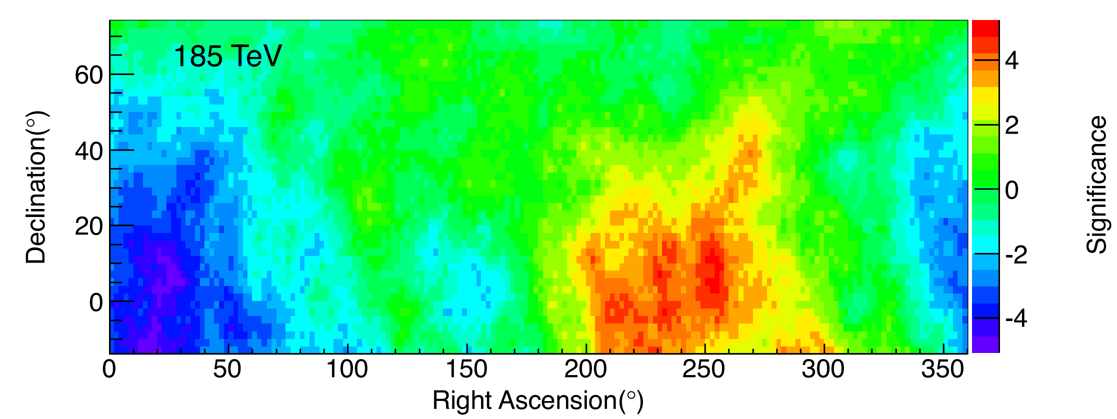

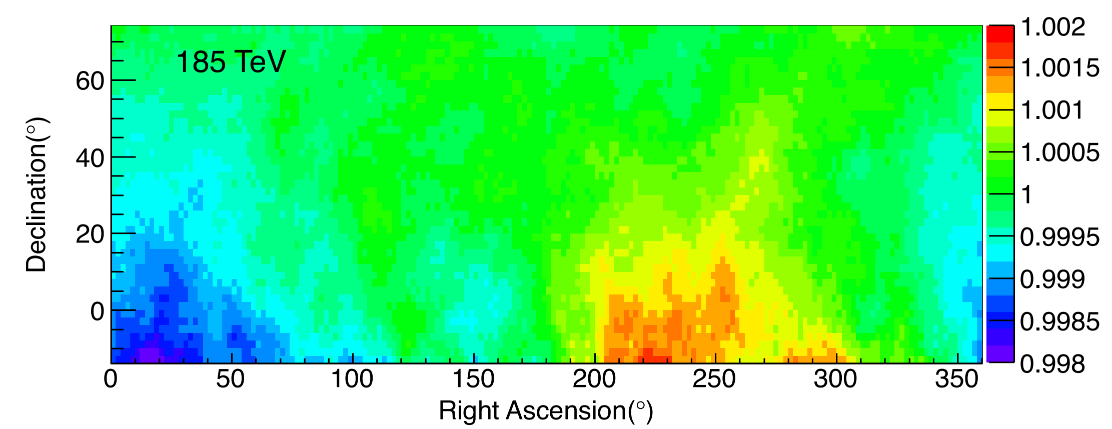

excess region: $\alpha \approx 240^{o}$
deficit region: $\alpha \approx 70^{o}$

consistent with IceCube/IceTop and Tibet ASγ results

Amplitude and Phase of the first harmonic

dipole component as a tracer
of the CR source distribution

- Extremely small amplitude: 10^{-4} — 10^{-3}
- Slow increase of A_1 with increasing energy to a maximum around 10 TeV.
- Slow fall of A_1 to a minimum at about 100 TeV.
- Evidence of increasing A above 100 TeV.
- Phase nearly constant around 0 hrs.
- Dramatic change of phase above 100 TeV.

The variation of the amplitude with energy seems to be difficult to interpret in terms of the conventional GCR diffusion model in the Galaxy.

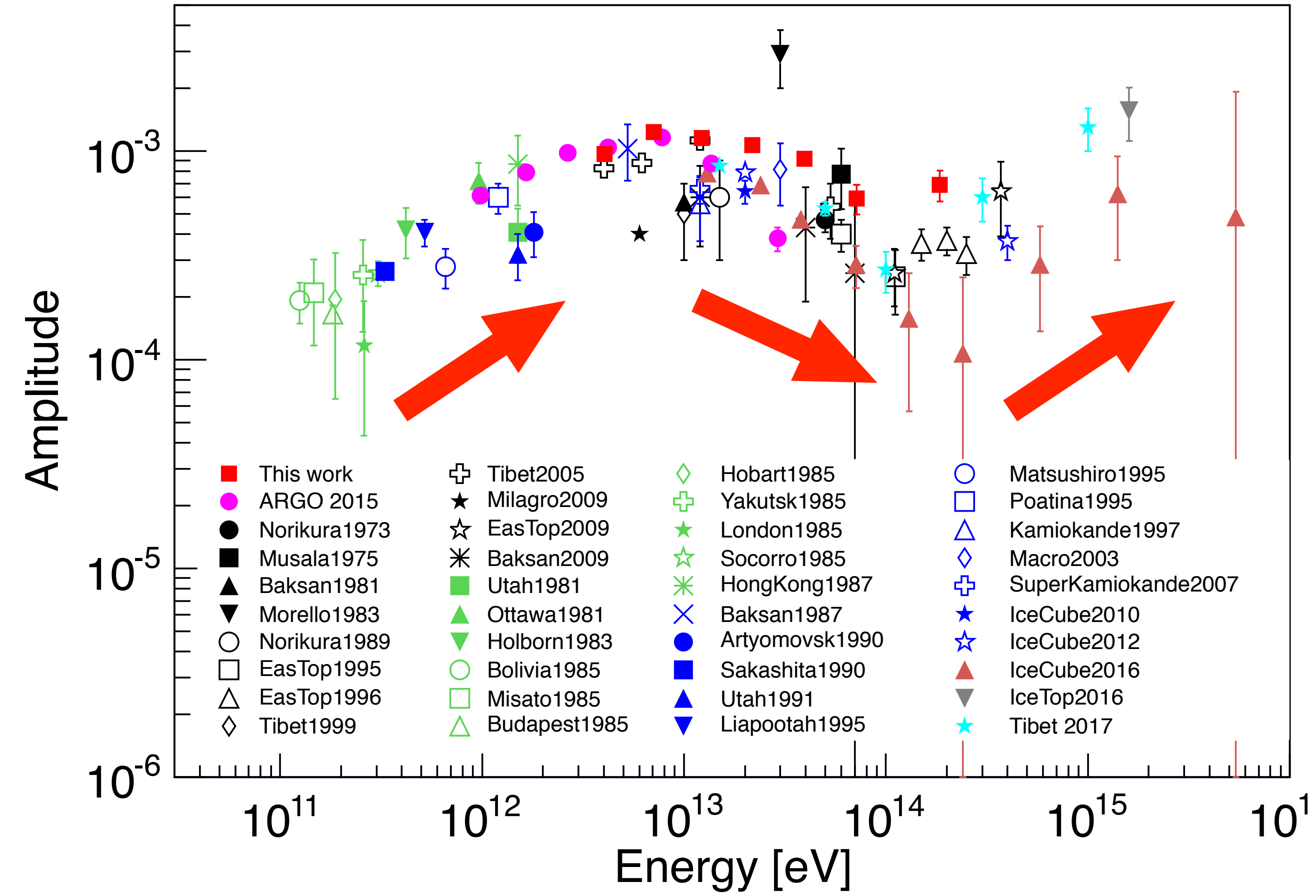

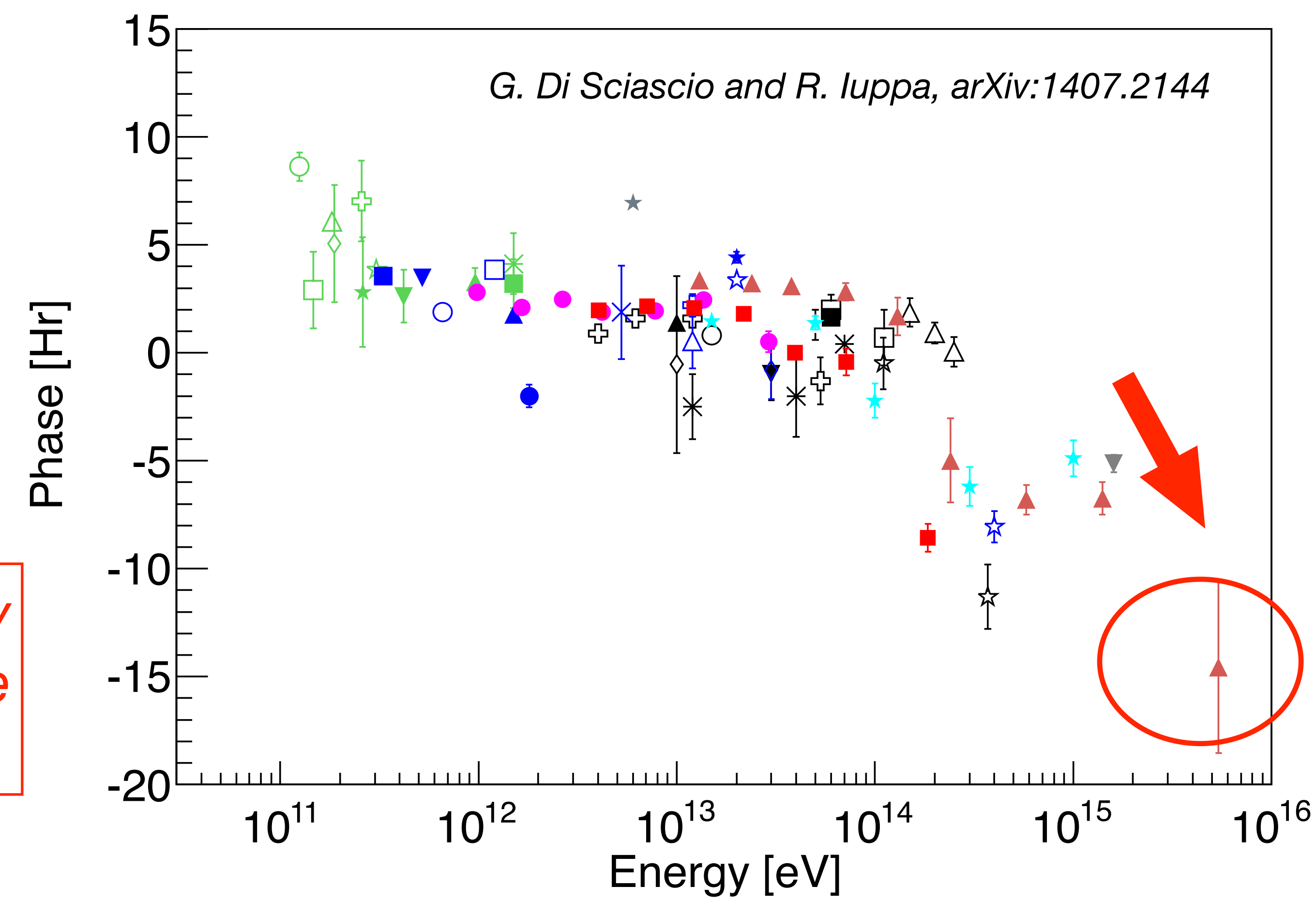

Medium/Small Scale Anisotropy

Data: November 8, 2007 - May 20, 2012
≈ 3.70×10^{11} events

dec. region δ ~ -20°÷ 80°

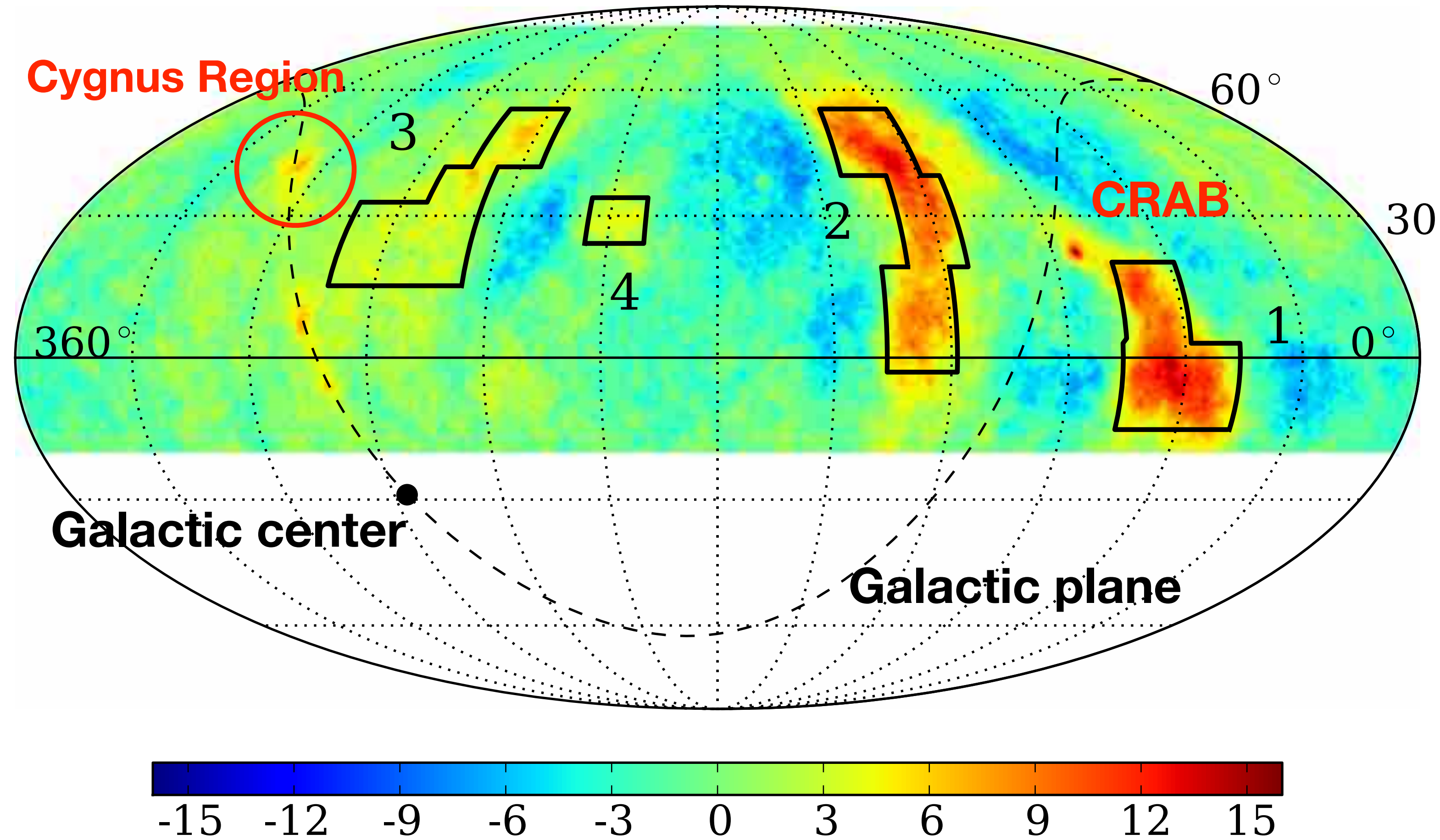

Map smoothed with the detected PSF for CRs, obtained with the Moon Shadow analysis

Proton median energy ≈ 1 TeV

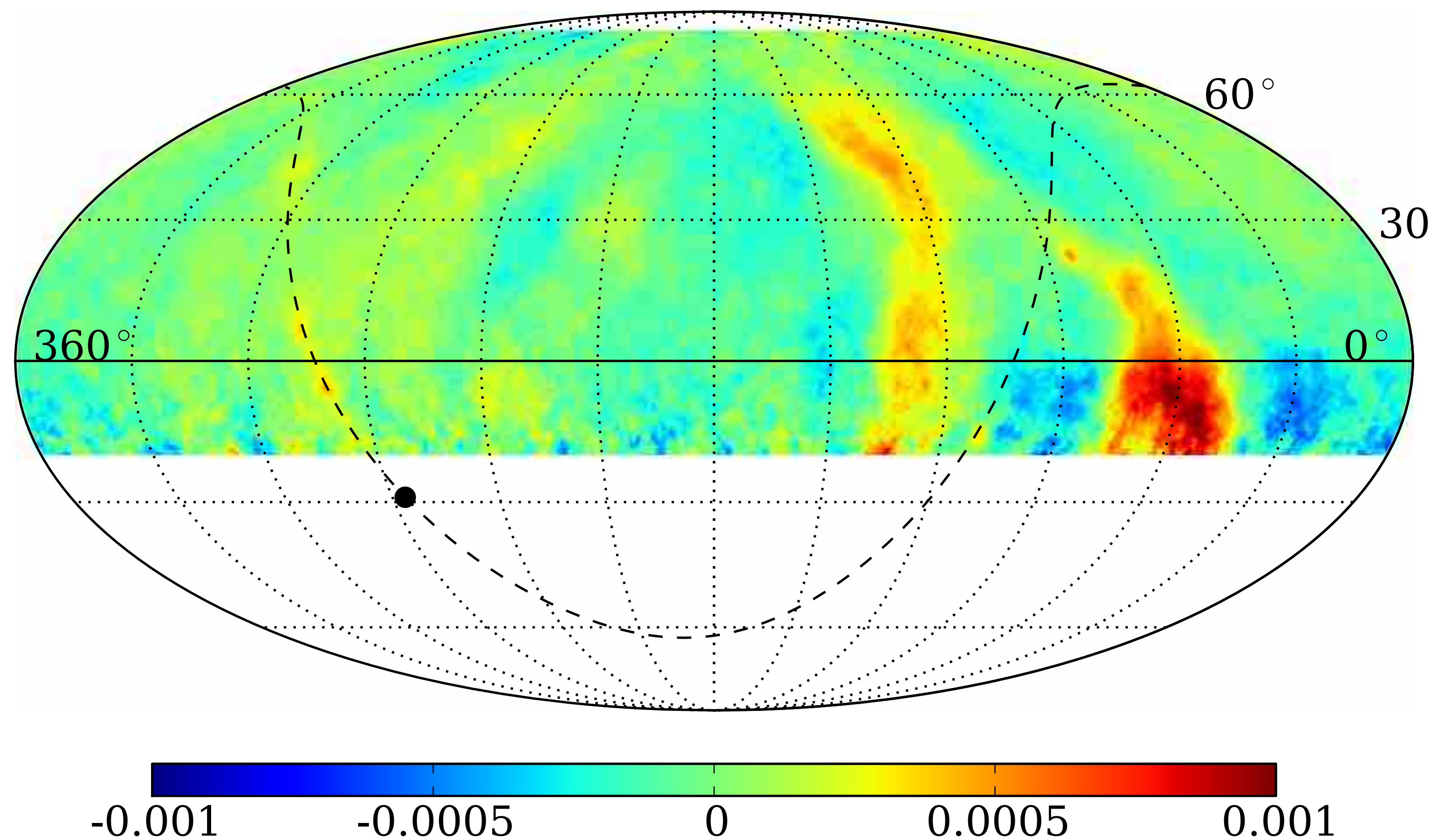

CRs excess ≈ 0.1 %
with significance up to 15 s.d.

Phys. Rev. D 88 (2013) 082001

ApJ 809 (2015) 90

Conclusions

- ❑ With ARGO-YBJ for the first time direct-indirect measurements of the CR spectrum overlaps for more than one energy decade, thus providing a solid anchorage to the CR measurements at higher energies.
- ❑ Clear observation of the proton knee at ≈ 700 GeV with different analises.

- ★ Large Scale Anisotropy was measured with high accuracy in the range 1 - 200 TeV.
  The dramatic change of the phenomenology above 100 TeV is confirmed.

- ★ New TeV small/medium scale anisotropy regions have been observed for the first time in the Northern hemisphere.

★ New generation EAS arrays (LHAASO in China) open up new possibilities for more complex observations that go beyond mapping of the arrival direction distribution as a function of the energy, allowing the measurement of energy spectrum and composition in distinct regions of the sky.

Solar activity

The Sun goes through an 11-year activity cycle shown by sunspots number. At each solar max the Sun flips its magnetic field polarity (A>0, A<0) showing a periodicity of 22 years.

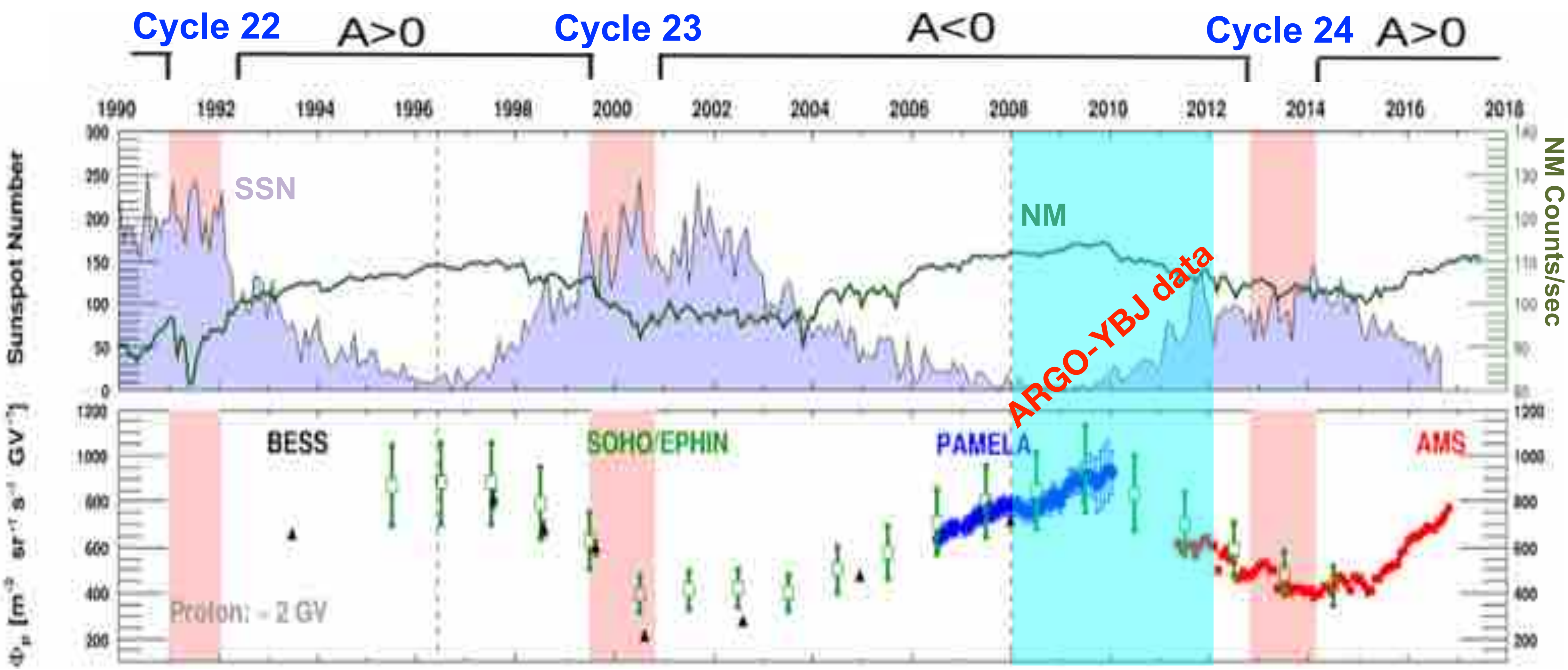

The flux of GCRs is anti-correlated with the intensity of the solar activity.

LHAASO layout

- 1.3 km^2 array, including 5195 scintillator detectors 1 m^2 each, with 15 m spacing.
- An overlapping 1 km^2 array of 1171, underground water Cherenkov tanks 36 m^2 each, with 30 m spacing, for muon detection (total sensitive area ≈ 42,000 m^2).

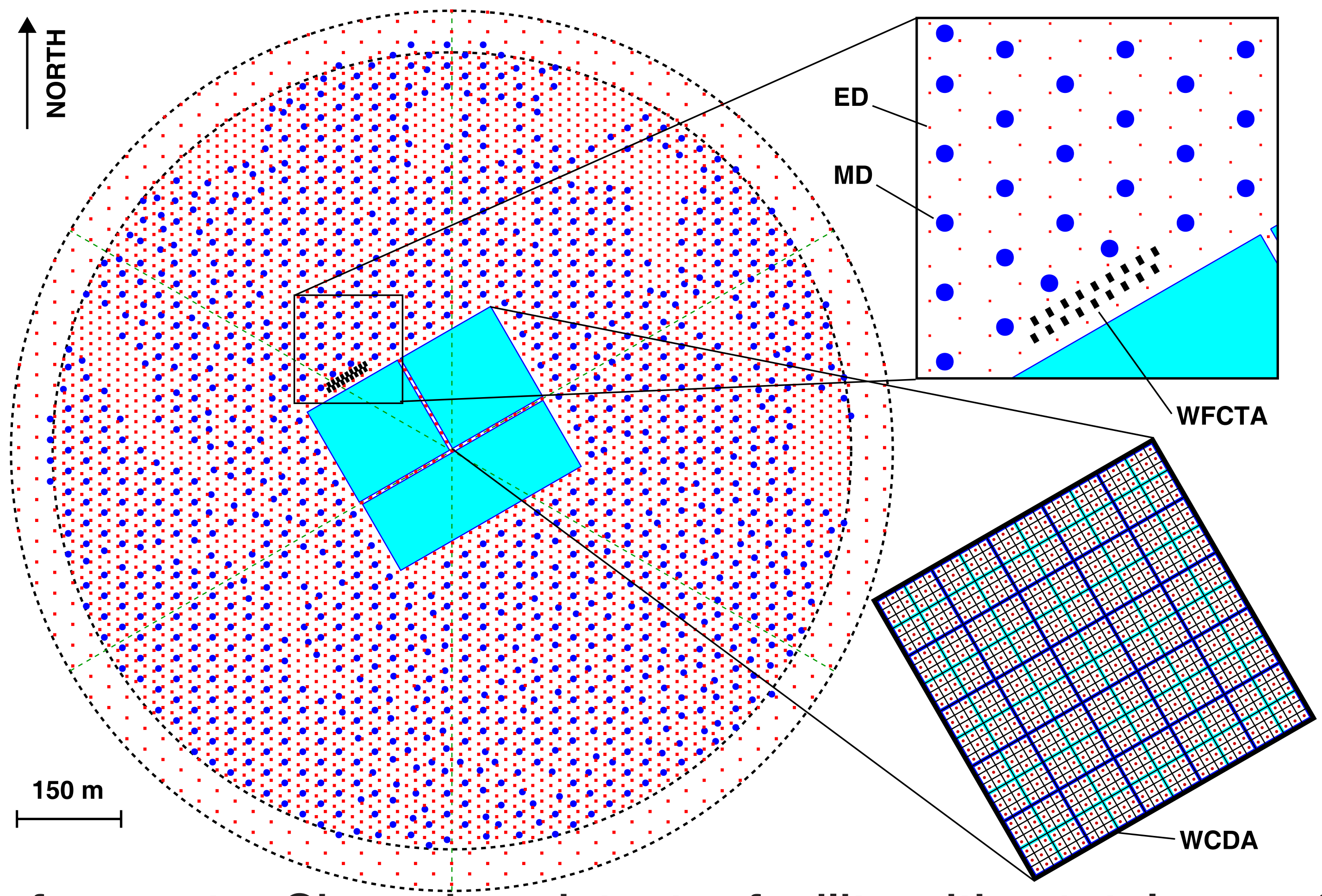

- A close-packed, surface water Cherenkov detector facility with a total area of 80,000 m^2.
- 18 wide field-of-view air Cherenkov (and fluorescence) telescopes.
- Neutron detectors

The LHAASO site

The experiment is located at 4400 m asl (600 g/cm^2) in the Haizishan (Lakes' Mountain) site, Sichuan province

Coordinates: 29° 21' 31'' N, 100° 08' 15'' E

700 km to Chengdu
50 km to Daocheng City (3700 m asl, guest house)
10 km to the highest airport in the world

Status of the experiment

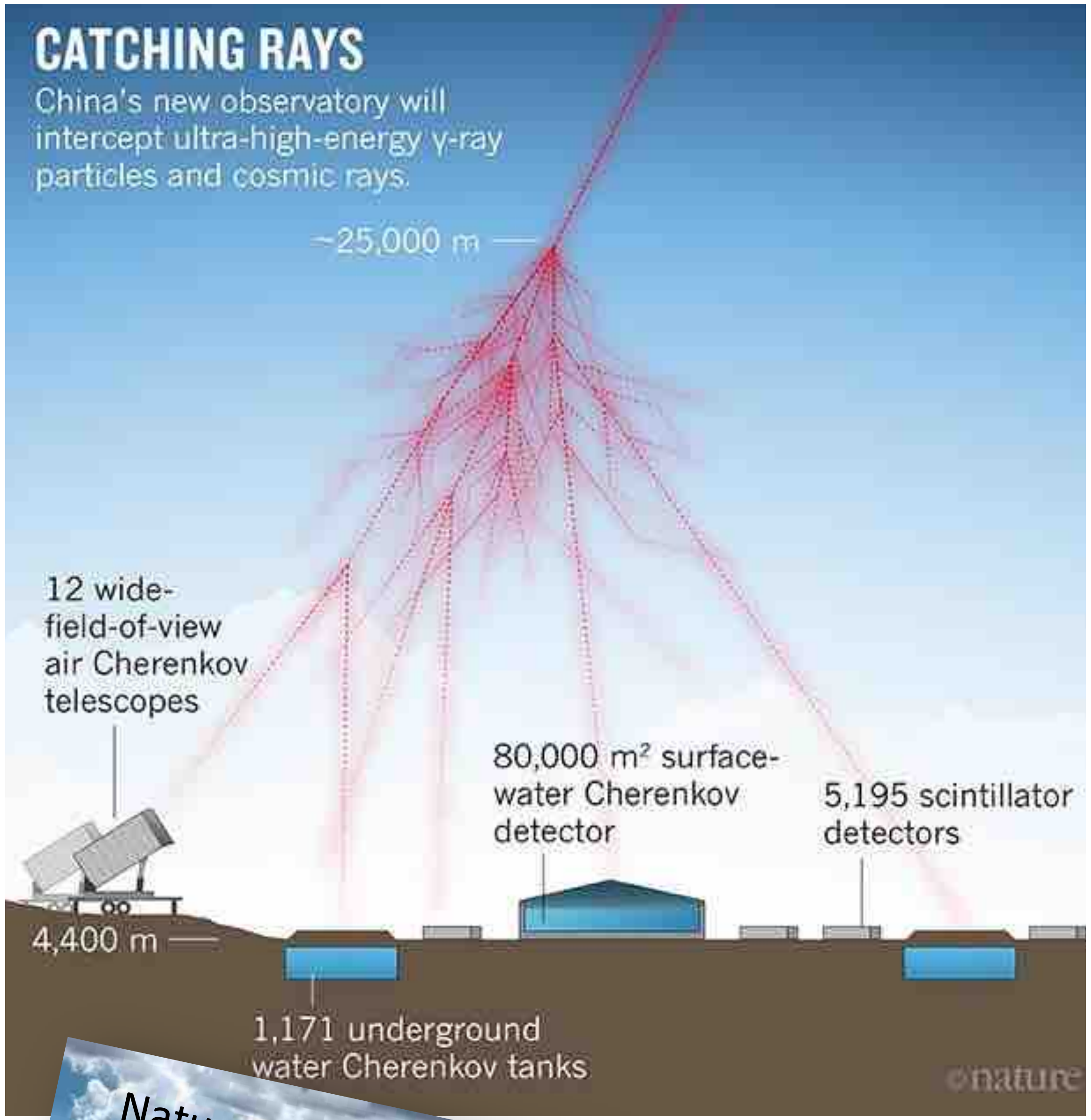

★ The first pond (HAWC-like) will be completed by the end of 2017 and instrumented in 2018.

★ 1/4 of the experiment in commissioning by the end of 2018 (sensitivity better than HAWC):

- 6 WFCTA telescopes
- 22,500 m^2 water Cherenkov detector
- ≈200 muon detectors

★ Completion of the installation in 2021.

LHAASO vs other EAS arrays

Experiment	Altitude (m)	e.m. Sensitive Area (m^2)	Instrumented Area (m^2)	Coverage
LHAASO	4410	5.2×10^3	1.3×10^6	4×10^{-3}
TIBET ASγ	4300	380	3.7×10^4	10^{-2}
IceTop	2835	4.2×10^2	10^6	4×10^{-4}
ARGO-YBJ	4300	6700	11,000	0.93 (central carpet)
KASCADE	110	5×10^2	4×10^4	1.2×10^{-2}
KASCADE-Grande	110	370	5×10^5	7×10^{-4}
CASA-MIA	1450	1.6×10^3	2.3×10^5	7×10^{-3}

		μ Sensitive Area (m^2)	Instrumented Area (m^2)	Coverage
LHAASO (✦)	4410	4.2×10^4	10^6	4.4×10^{-2}
TIBET ASγ	4300	4.5×10^3	3.7×10^4	1.2×10^{-1}
KASCADE	110	6×10^2	4×10^4	1.5×10^{-2}
CASA-MIA	1450	2.5×10^3	2.3×10^5	1.1×10^{-2}

- ✓ LHAASO will operate with a coverage similar to KASCADE (about %) over a much larger effective area.
- ✓ The detection area of muon detectors is about 70 times larger than KASCADE (coverage 5%) !
- ✓ Redundancy: different detectors to study hadronic models dependence

(✦) Muon detector area: 4.2×10^4 m^2 + 8×10^4 m^2 (WCDA)

Intrinsic linearity: test at the BTF facility

Linearity of the RPC @ BTF in INFN Frascati Lab:

- *electrons (or positrons)*
- *E = 25-750 MeV (0.5% resolution)*
- *<N>=1÷10^8particles/pulse*
- *10 ns pulses, 1-49 Hz*
- *beam spot uniform on 3×5 cm*

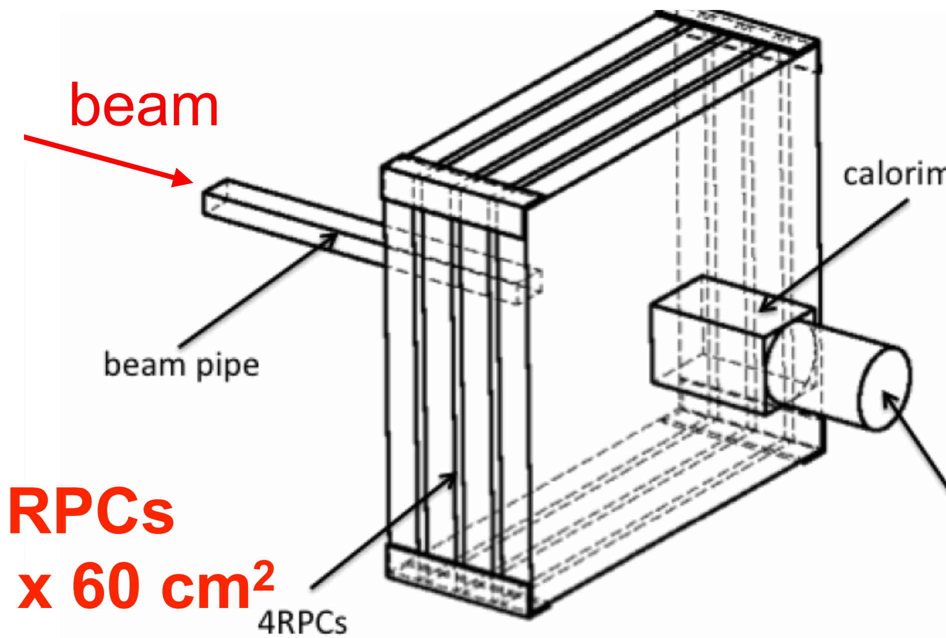

4 RPCs
60 x 60 cm²

Calorimeter: lead glass block from OPAL, PMT a Hamamatsu R2238.

Good overlap between 4 scales with the maximum density of the showers spanning over three decades

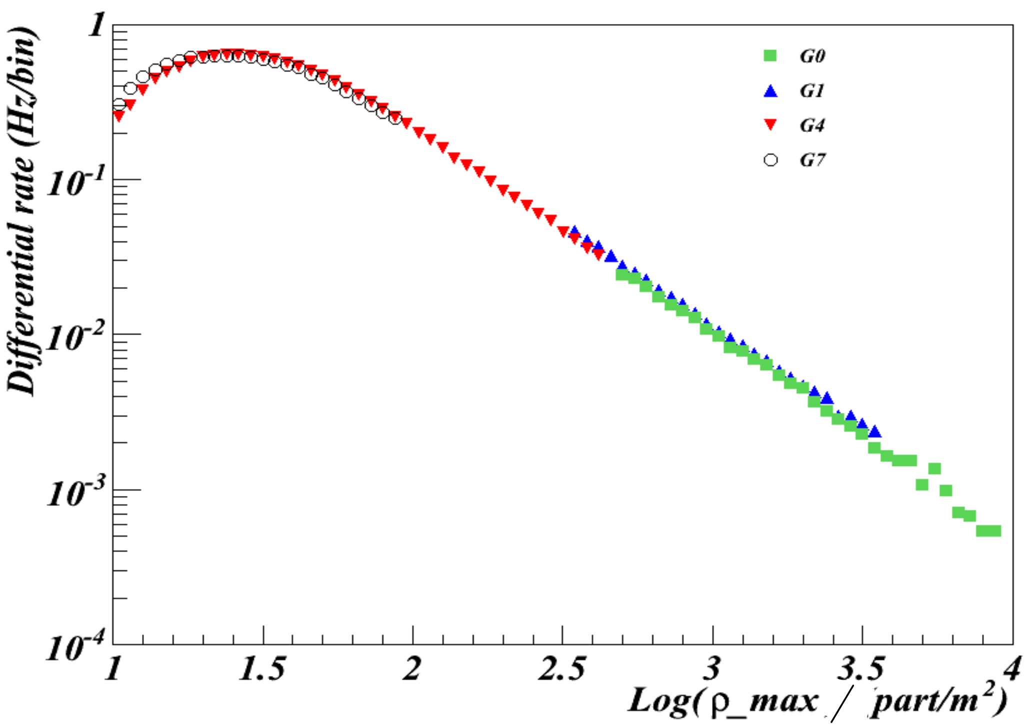

Astrop. Phys. 67 (2015) 47

The RPC signal vs the calorimeter signal

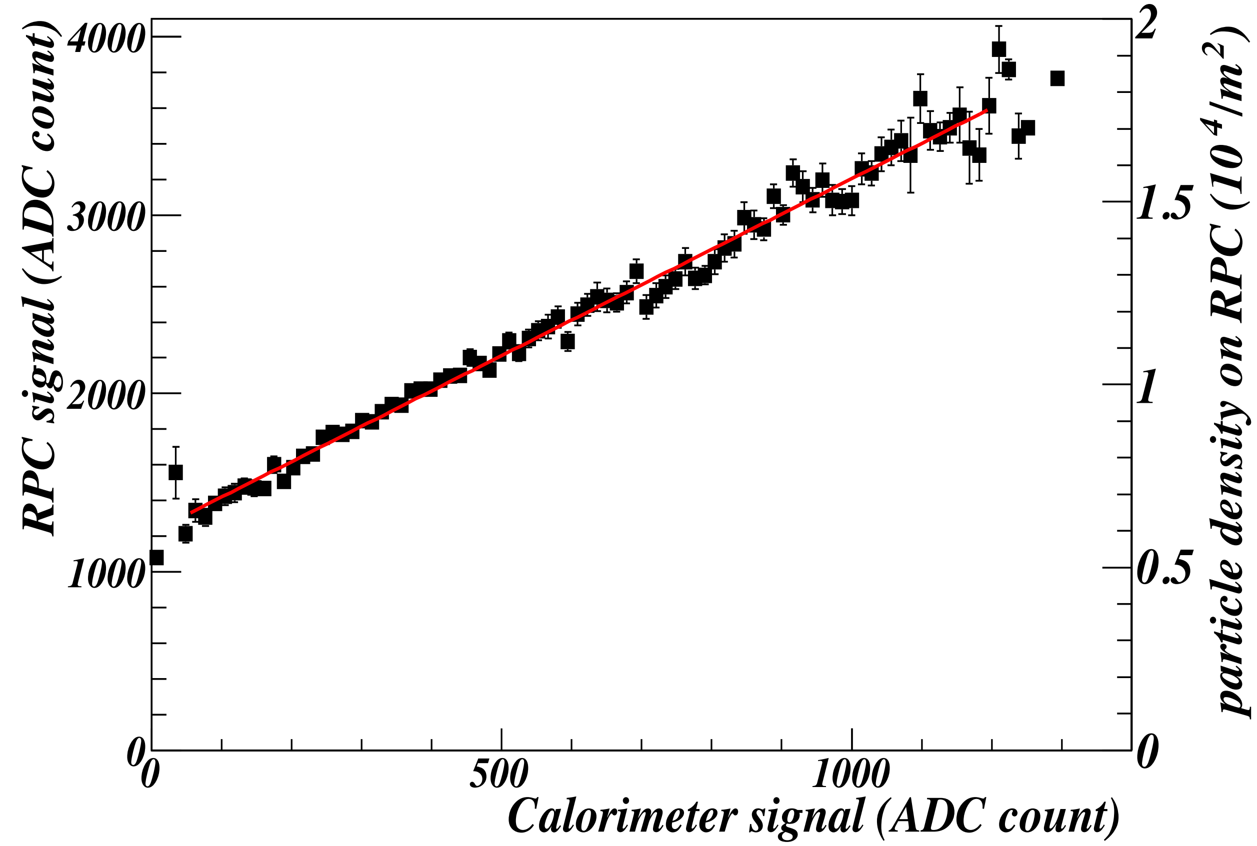

➔ Linearity up to ≈ 2 · 10^4 particle/m²

HAWC all-particle spectrum

arXiv:1710.00890

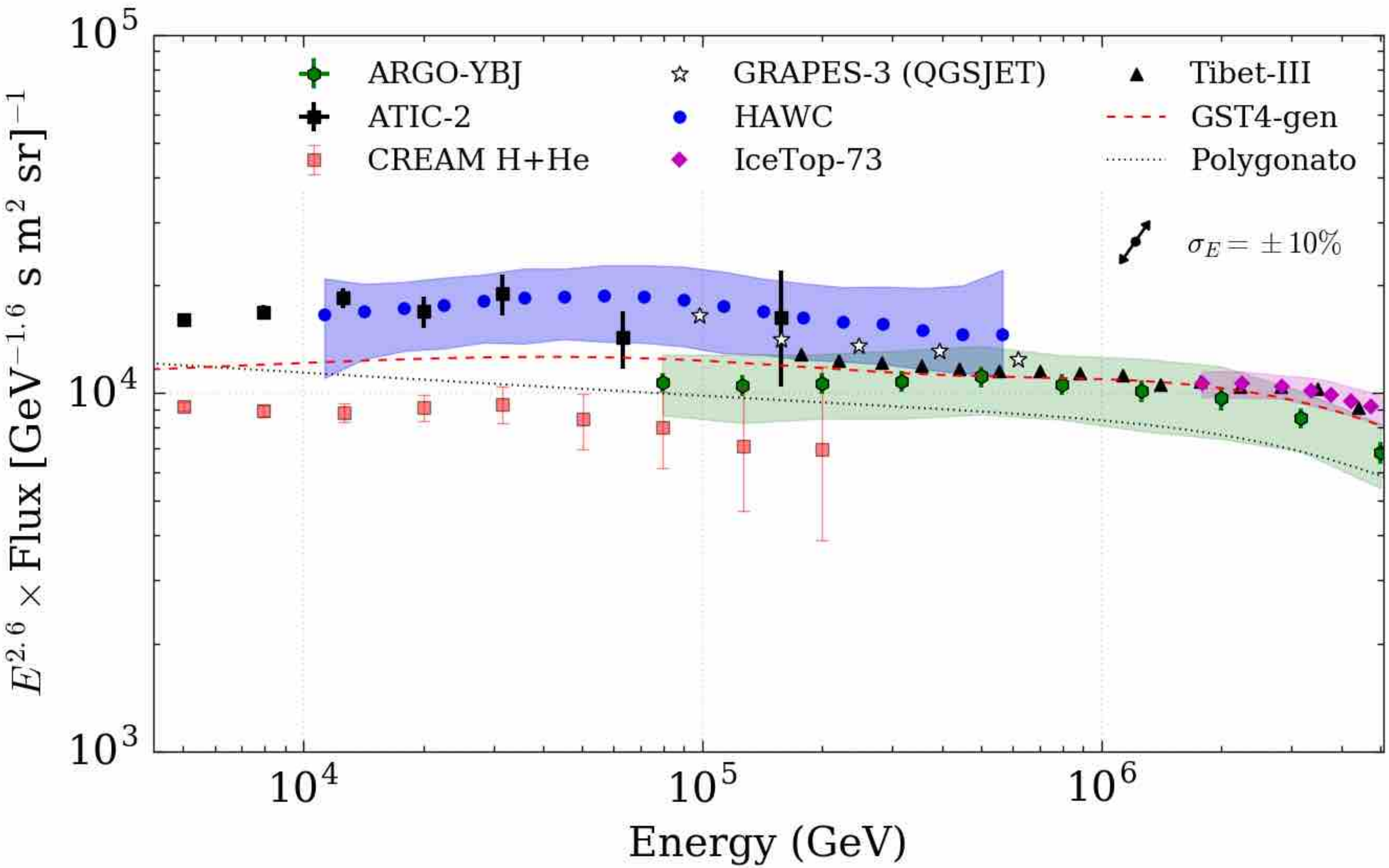

Comparison with other experiments

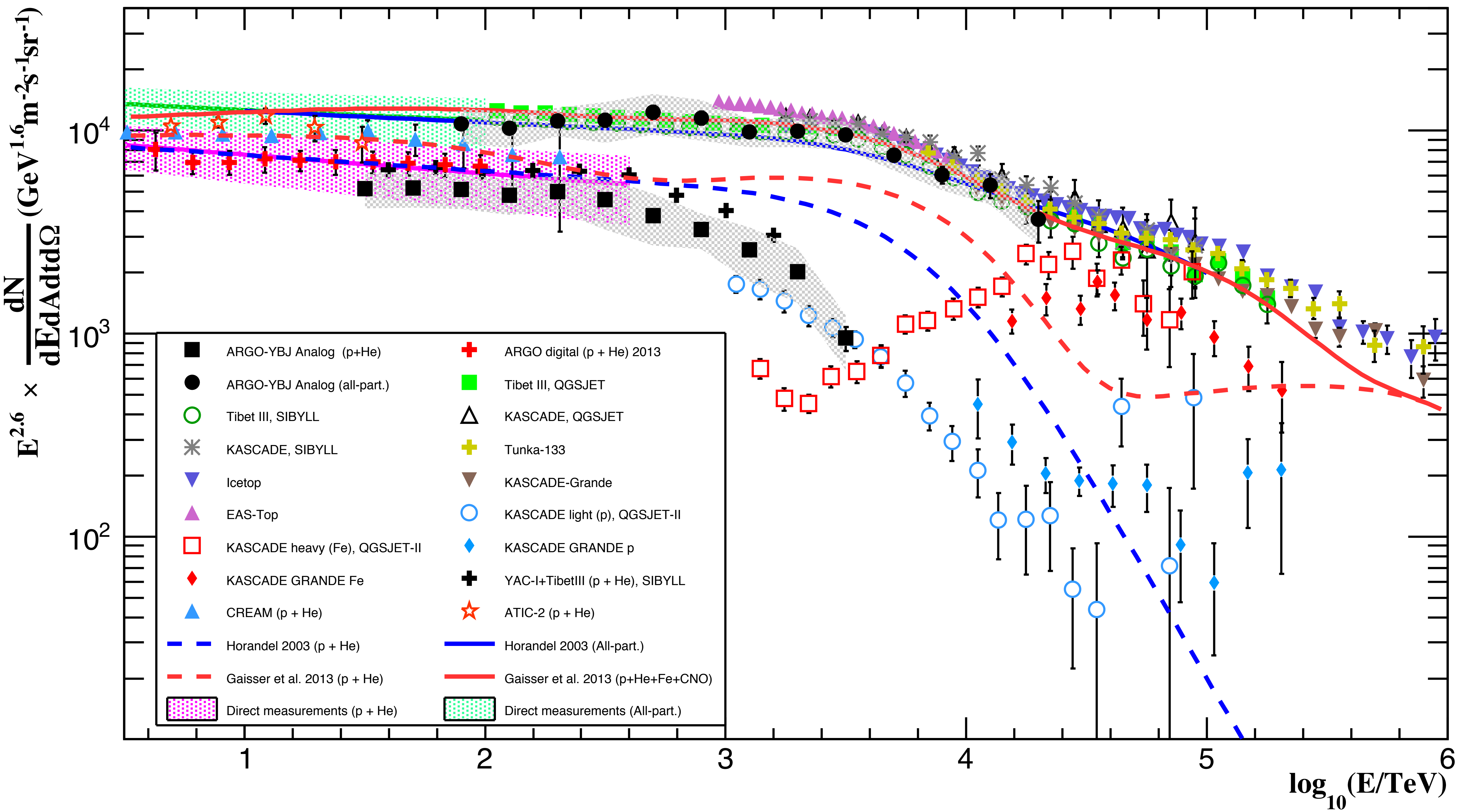

CR spectrum and atmospheric neutrinos

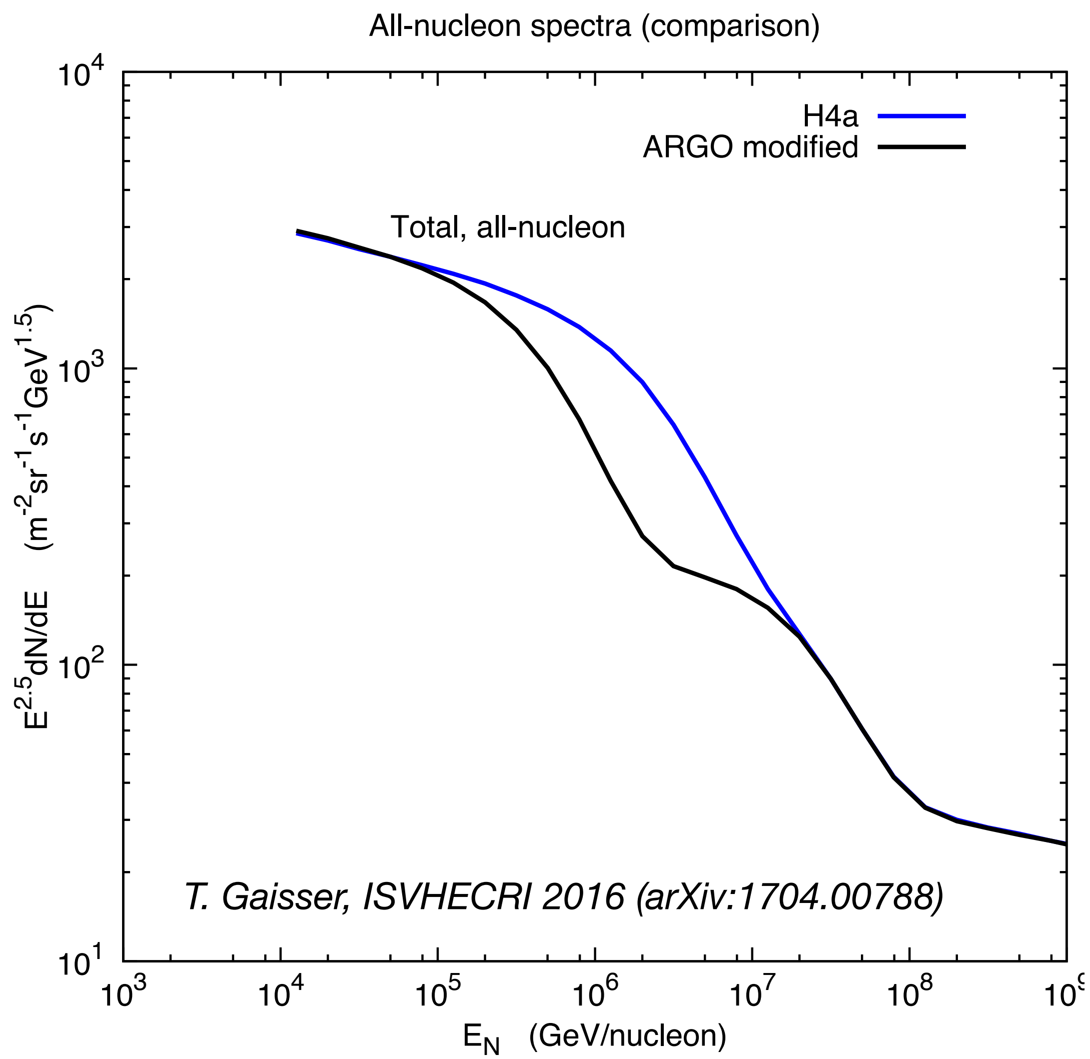

The spectrum of nucleons for the H4a model compared with a modified version in which the cutoff rigidities for p and He are reduced to 700 GeV and the all-particle spectrum is restored by increasing the contribution of the CNO and Fe groups.

A practical aspect of the energy of the proton knee is its implication for the atmospheric neutrino flux at high energy.

Calculation of *the flux of atmospheric neutrinos depends on the spectrum of nucleons as a function of energy per nucleon,* which is dominated by protons and helium.

If the proton and helium components steepen at 700 GeV, then there should be a compensating increase in heavier nuclei to keep the all-particle spectrum constant.

The sketch illustrates the effect, which would likely be a *suppression of the flux of nucleons in a range around a PeV that arises if the all-particle spectrum is dominated by heavy nuclei in this region.*

This in turn would significantly reduce the flux of muons and muon-neutrinos around 100 TeV.

x-check: the anti-sidereal time distribution

The investigation of the systematic uncertainties is very important for a weak intensity detection.

The standard check is the study of time distribution in the anti-sidereal time:
an artificial time which has 364.25 cycles per year

1 day less than the number of days in a year of solar time, and 2 days less than the number of sidereal days.

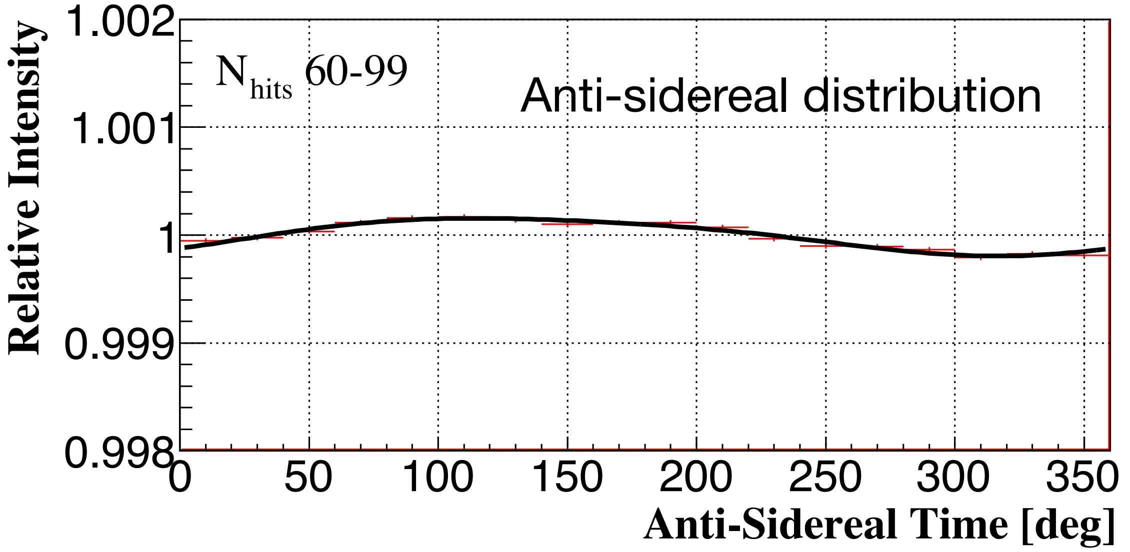

In principle, the harmonic analysis in anti-sidereal time should find no anisotropy at all, since no physical phenomena exist with such a periodicity.

However, if some effect in solar time affects the sidereal distribution, it will also affect the anti-sidereal one.

The anti-sidereal result can be used to estimate such systematics and, if needed, to correct them.

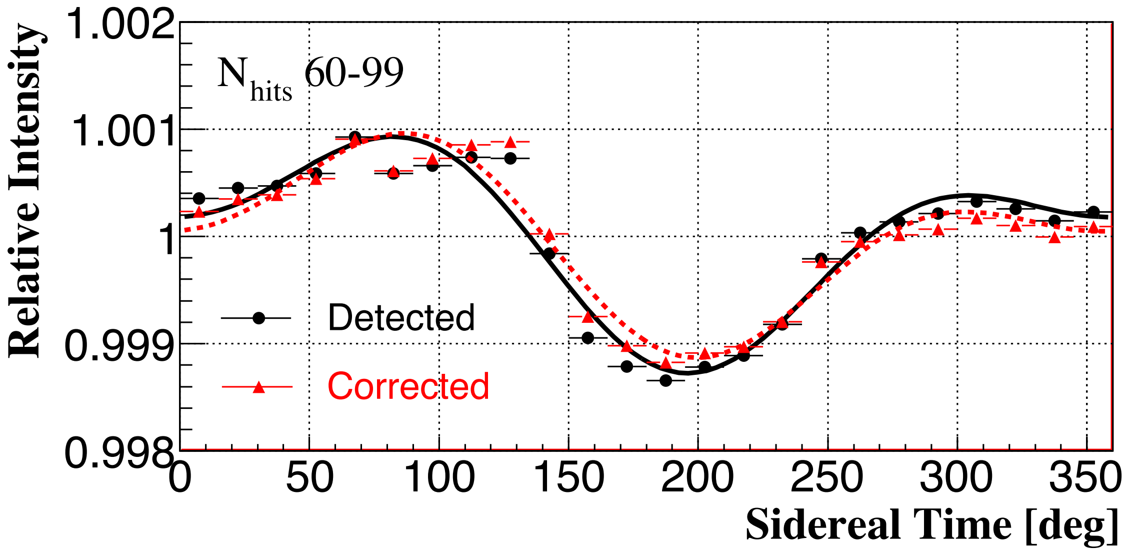

Anti-sidereal amplitude: more than a factor 10 smaller than the sidereal one.

The curves before and after the correction are very close, showing that the influence of seasonal and diurnal variations is negligible during the observation period.

x-check: the East-West method

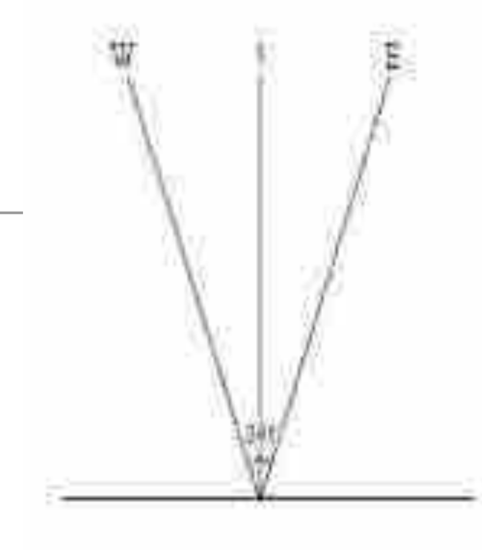

Based on counting rate differences between East and West directions, allowing to remove variations of atmospheric origin.

It is based on a “differential” approach: at the moment t vertical North-South plane divide the sky into two sectors East-ward and West-ward.

Most of systematics affecting the detector operation or bias influencing the analysis of the events are equal for both sectors. The idea is that considering the difference of counts from two directions makes them cancelling each other and result is true differential wave.

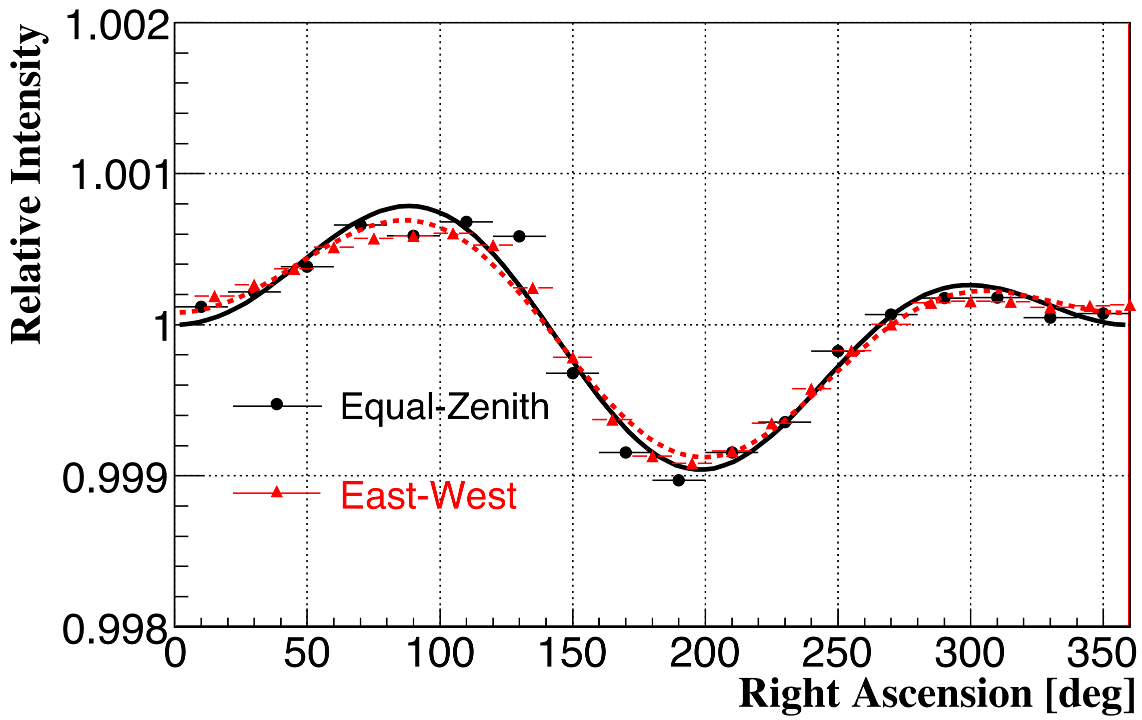

The East-West method is an ‘old’ method used when experiments were not able to collect enough statistics to study the distribution of CR arrival direction both in right ascension and declination.

Due to the deep differences between the equi-zenith and the East-West method, both in the approach and in data-handling, the comparison among them provides a good estimation of systematic uncertainties.

No significant differences were found among the distributions

The Compton-Getting effect

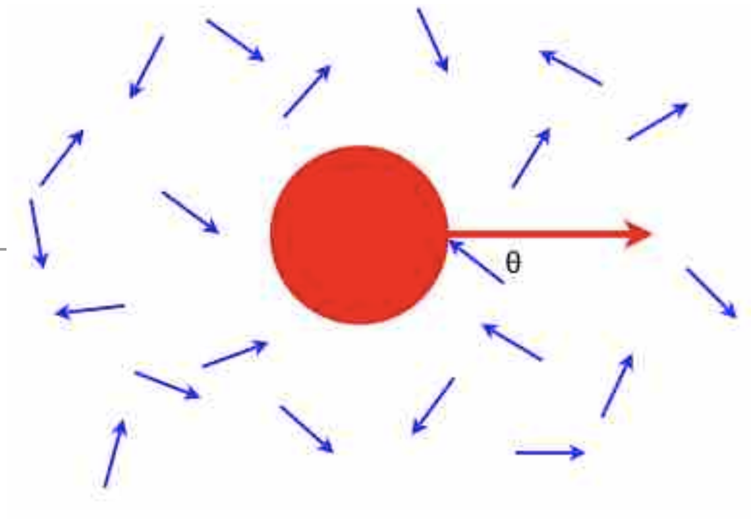

★ Expected CR anisotropy due to Earth's orbital motion around the Sun: when an observer (CR detector) moves through a gas which is isotropic in the rest frame (CR "gas"), he sees a current of particles from the direction opposite to that of its own motion.

Compton, A. H., & Getting, I. A. 1935, PhRv, 47, 817

A benchmark for the reliability of the detector and the analysis method. In fact, all the features (period, amplitude and phase) of the signal are predictable without uncertainty, due to the exquisitely kinetic nature of the effect.

$$\frac{\Delta I}{\langle I \rangle} = (\gamma + 2)\frac{v}{c}\cos\vartheta$$

I = CR intensity
γ = power-law index of CR spectrum (2.7)
v = detector velocity ≈ 30 km/s
θ = angle between detector motion and CR arrival direction

A detector on the Earth moving around the Sun scans various directions in space while the Earth spins. Maximum at 6 hr solar time (when the detector is sensitive to a direction parallel to the Earth's orbit)

$$\frac{\Delta I}{\langle I \rangle}(\exp): \ 0.047\%$$

$$\varphi(\exp): \ 6hr$$

The first clear observation of the SCG effect with an EAS array was reported by EAS-TOP (LNGS) in 1996 at about 10^{14} eV.

Compton-Getting effect by ARGO-YBJ

$N_{hits} > 500$ ➡ ≈14 TeV

to avoid solar effects on low energy CRs

Solar CG effect observed with a maximum intensity $(3.64 \pm 0.36) \times 10^{-4}$ at 6.67±0.37 hr solar time

Solare Time (UT)
2008 – 2009 data

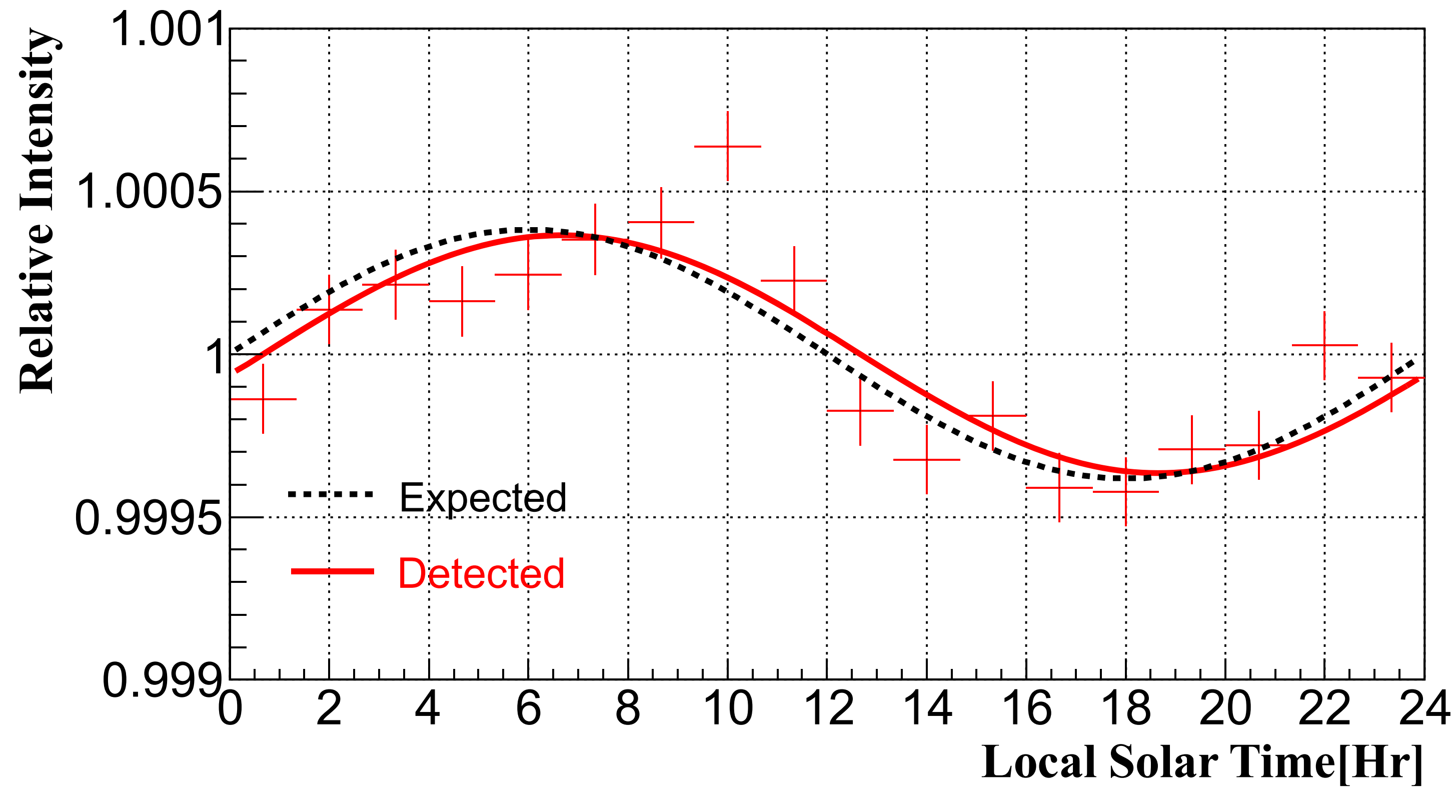

Figure 6. Projection of the event distribution in solar time for $N_{\rm hits} > 500$. The dotted line represents the expected Compton–Getting modulation. The abscissa bars present the width of bins and the ordinate errors are statistical.

MSA vs energy

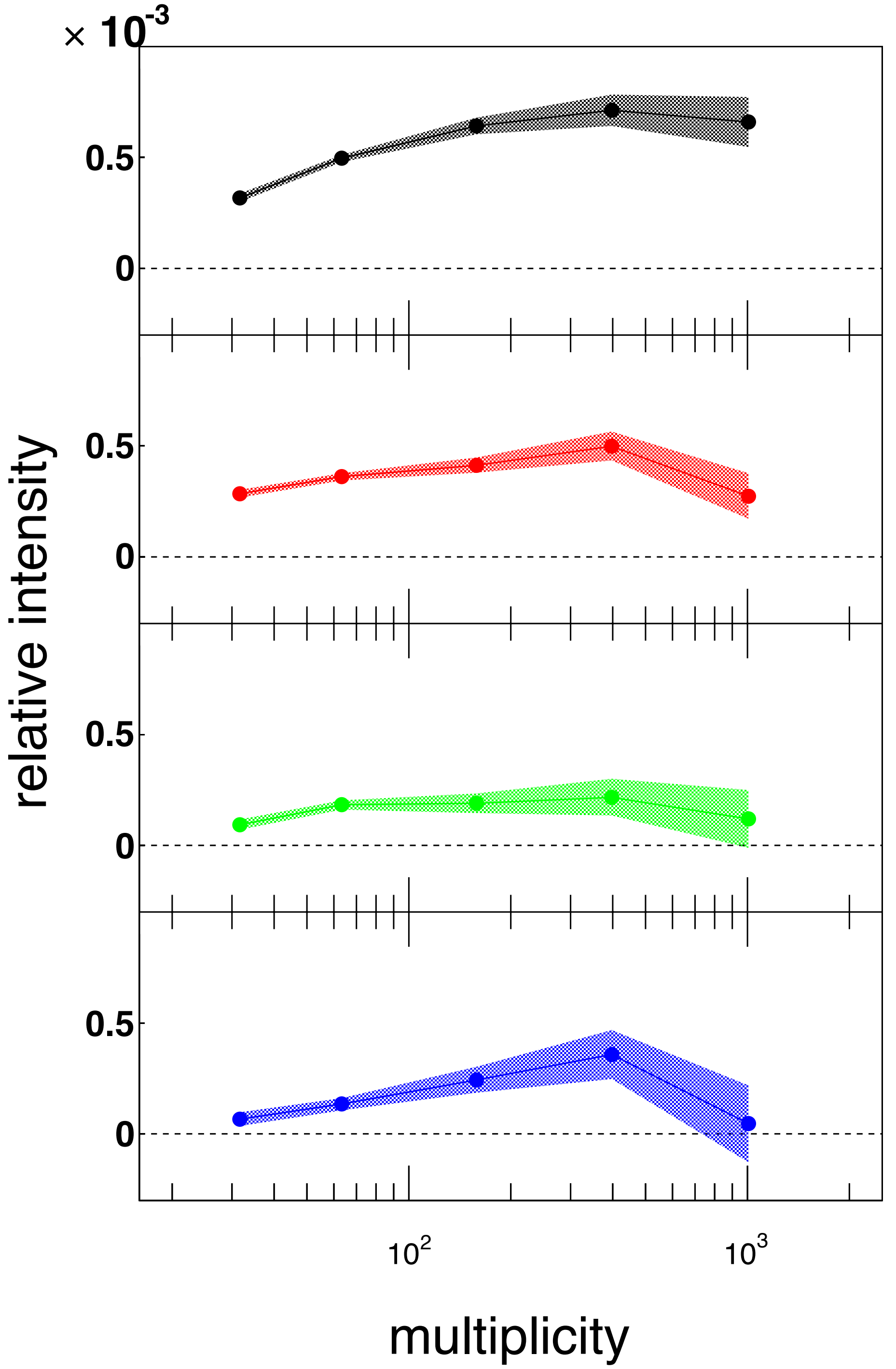

The size spectra look quite harder than the CR isotropic flux

Strip-multiplicity interval	number of events		E_p^{50} [TeV]
25 – 40	1.1409×10^{11}	(38%)	0.66
40 – 100	1.4317×10^{11}	(48%)	1.4
100 – 250	3.088×10^{10}	(10%)	3.5
250 – 630	8.86×10^{9}	(3%)	7.3
more than 630	3.52×10^{9}	(1%)	20

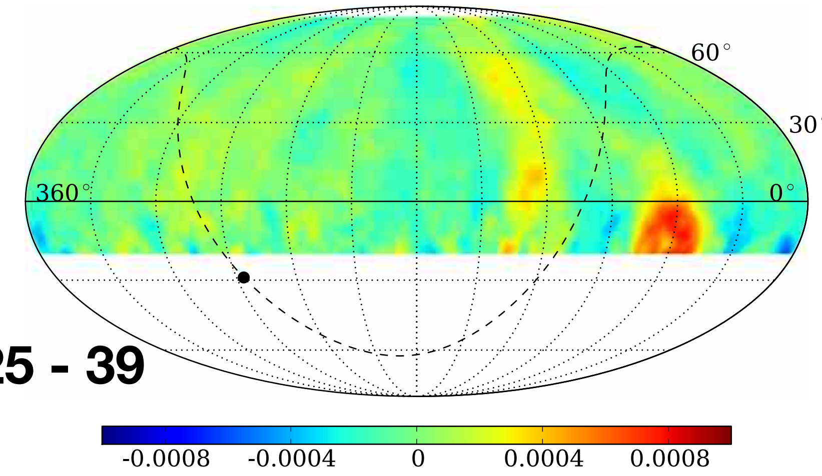

N = 25 - 39

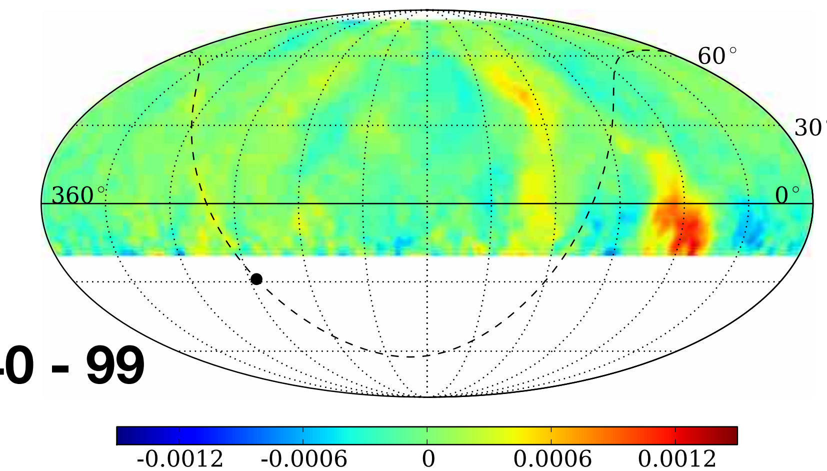

40 - 99

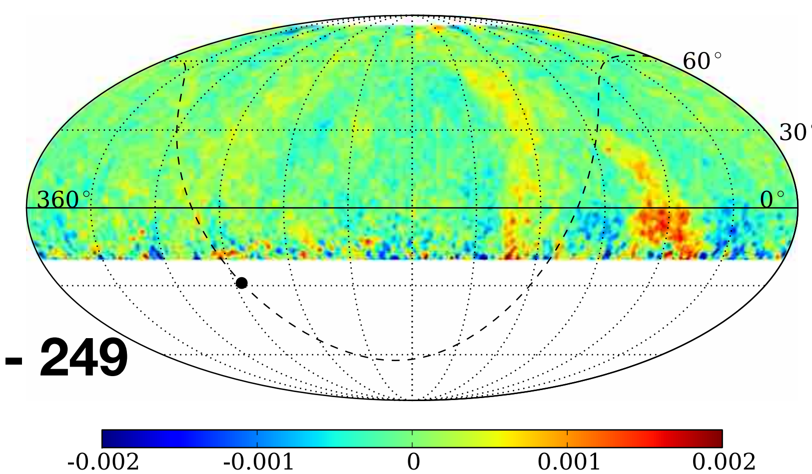

100 - 249

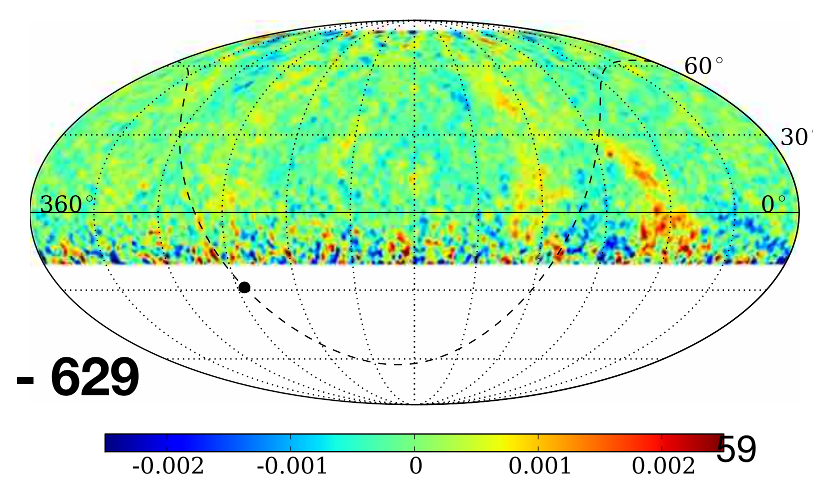

250 - 629

Temporal variation of MSA by ARGO-YBJ

Magnetic fields of the heliosphere may have an influence on the anisotropy. Therefore, is important to probe the local interstellar space surrounding the heliosphere and the magnetic structure of the heliosphere.

The study of temporal variation of CR anisotropy is a useful tool to investigate the effects of solar activities.

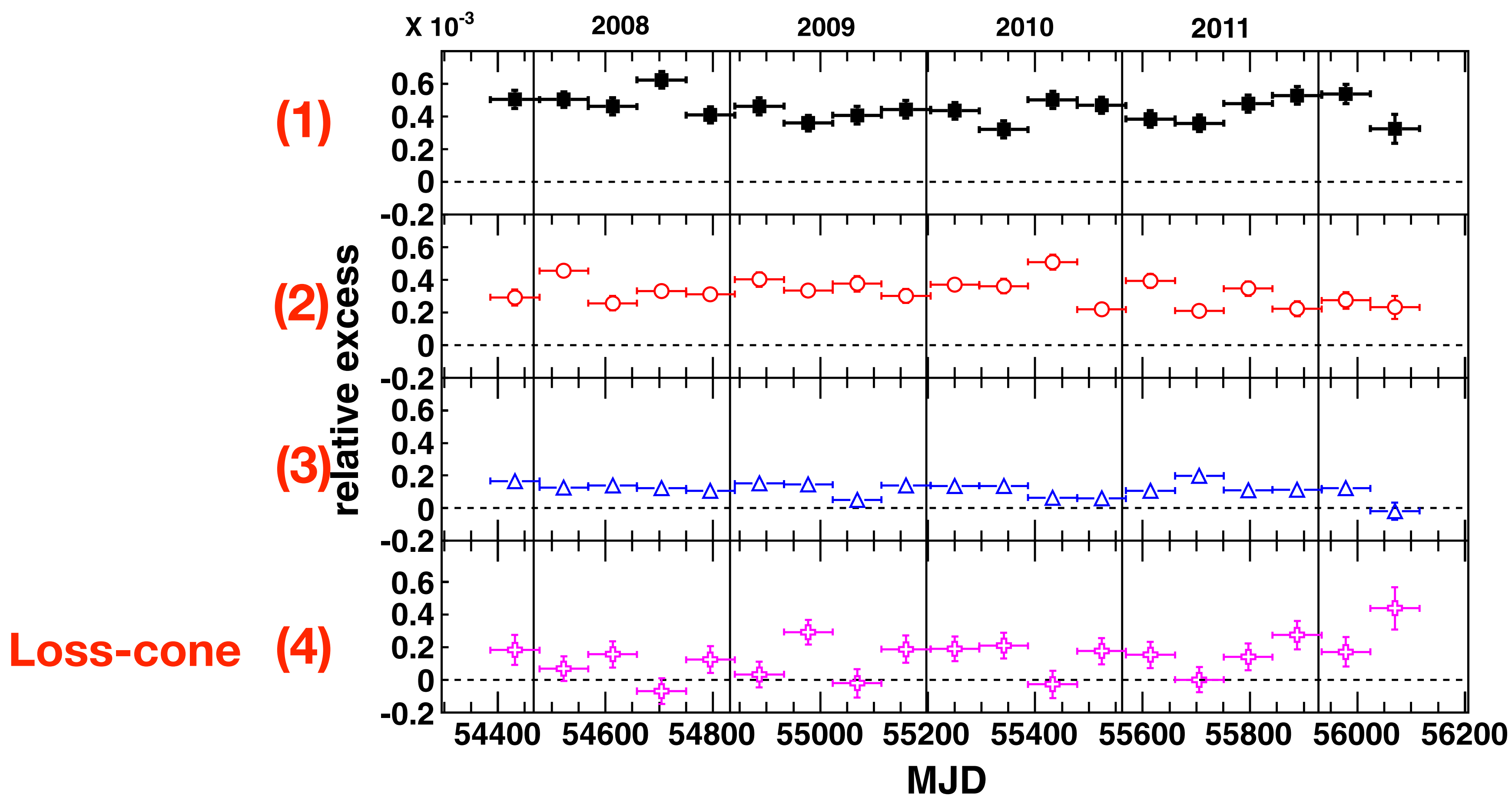

The time-bin width is 3 months

There is no evidence either of a seasonal variation or of constant increasing or decreasing trend of the emission.

Region 1

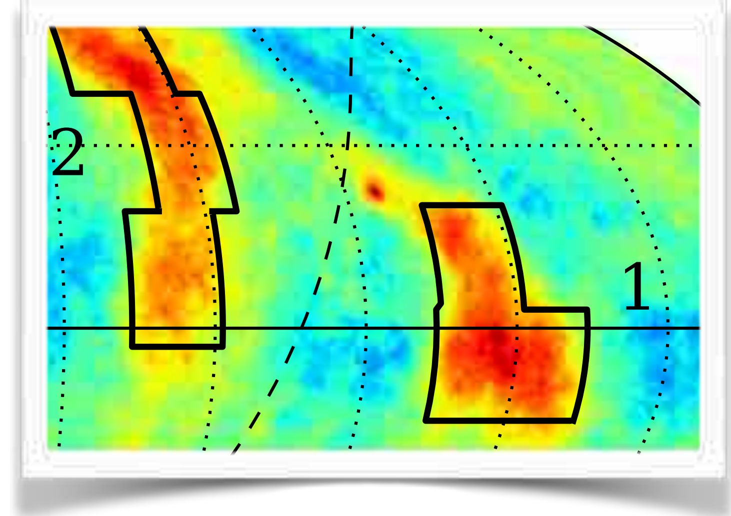

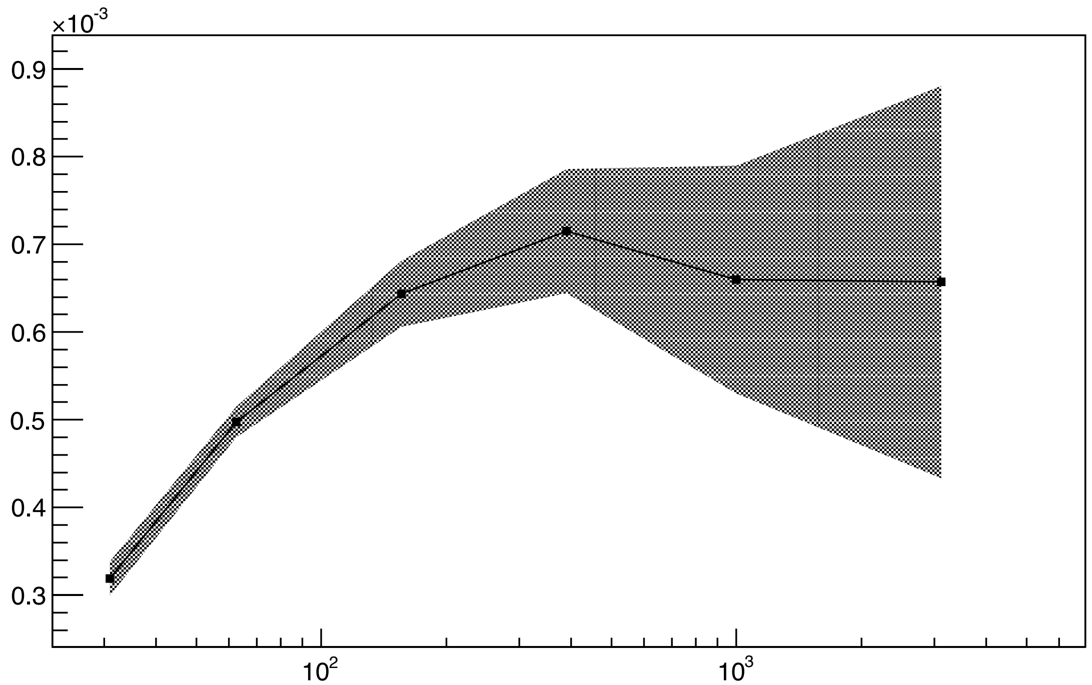

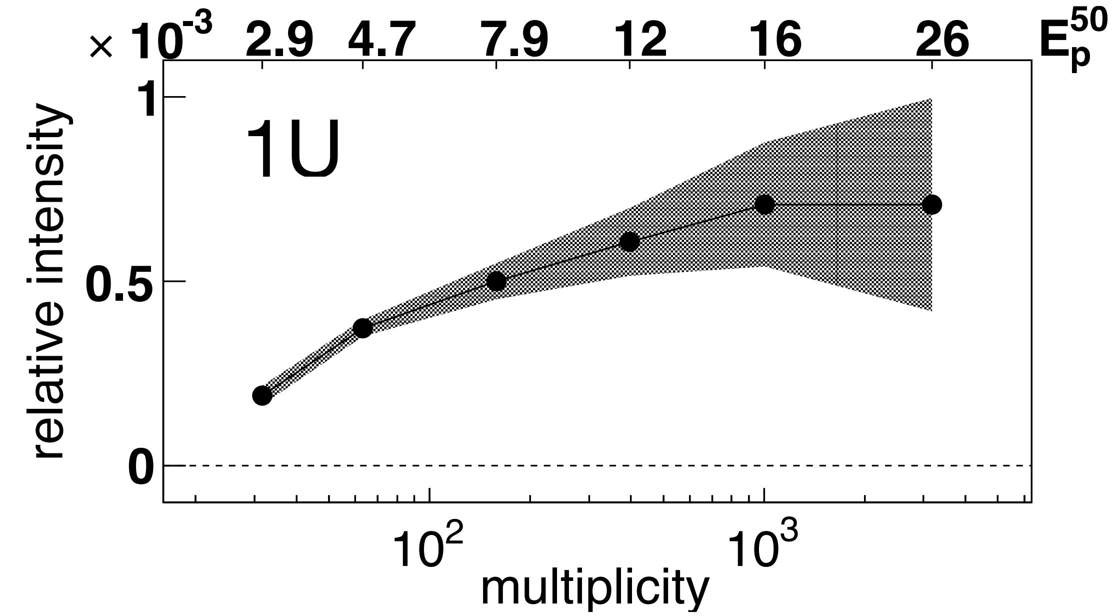

For the region 1L a cut-off around 15-20 TeV can be noticed, compatible with that observed by Milagro in the region “A”.

The statistics at high multiplicity is very poor and does not allow to establish whether the cut-off continues at higher energy or not.

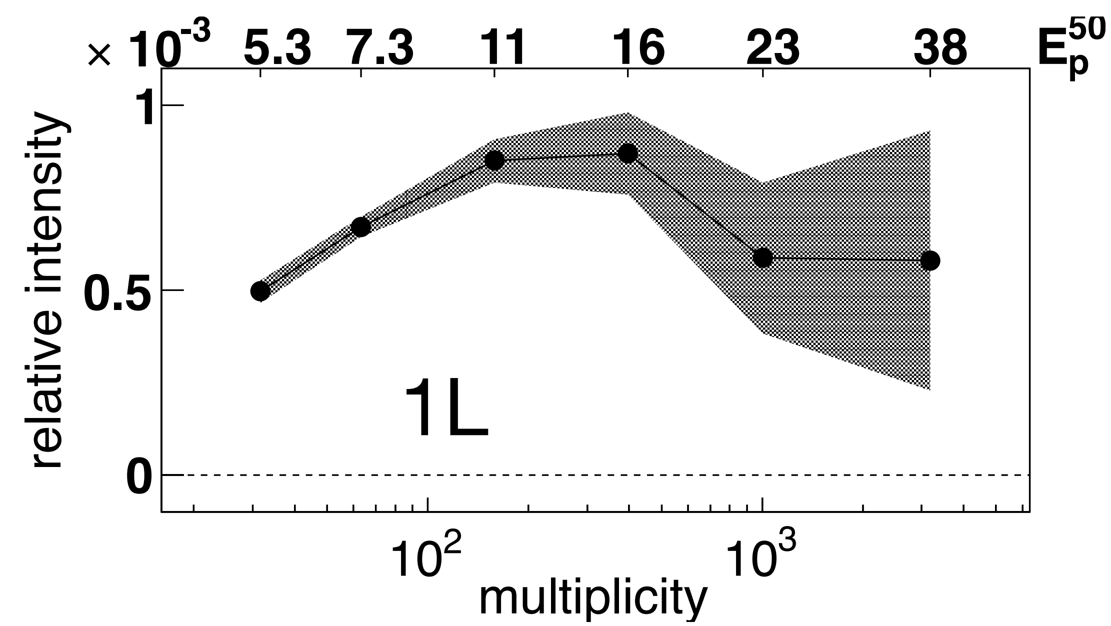

Conversely, for region 1U a constantly increasing trend is obtained up to 26 TeV, what marks a possible difference between the sub-regions.